UC Berkeley
UC Berkeley Electronic Theses and Dissertations

Title
The Role of Sirtuins in the Molecular Topography of Silenced Chromatin

Permalink
https://escholarship.org/uc/item/4zm832v6

Author
Thurtle, Deborah Mary

Publication Date
2014

Peer reviewed|Thesis/dissertation

eScholarship.org Powered by the California Digital Library
University of California

The Role of Sirtuins in the Molecular Topography of Silenced Chromatin

by

Deborah Mary Thurtle

A dissertation submitted in partial satisfaction of the

requirements for the degree of

Doctor of Philosophy

in

Molecular and Cell Biology

in the

Graduate Division

of the

University of California, Berkeley

Committee in charge:

Professor Jasper Rine, Chair
Professor Barbara Meyer
Professor Douglas Koshland
Professor Daniel Zilberman

Spring 2014

Abstract

The Role of Sirtuins in the Molecular Topography of Silenced Chromatin

by

Deborah Mary Thurtle

Doctor of Philosophy in Molecular and Cell Biology

University of California, Berkeley

Professor Jasper Rine, Chair

Heterochromatin is key to the appropriate regulation of cell identity. *Saccharomyces cerevisiae* silent mating loci, *HML* and *HMR*, provide a simple, yet elegant model for the regional control of transcriptional repression and its contribution to cell identity. Yeast can be of mating type **a** or α as is dependent on the alleles at the actively transcribed *MAT* locus. However, additional copies of the α and **a** genes are present elsewhere in the genome to facilitate mating-type switching. Interestingly, even though *HML* and *HMR* have the exact same promoters as when the genes are at the *MAT* locus, the genes are not expressed. This promoter-independent repression is due to the Silence Information Regulator (Sir) proteins. Current models of yeast silencing posit that Sir proteins are recruited by transcription factors to *HML* and *HMR*. Sir2, whose catalytic activity is necessary for silencing and is the founding member of the sirtuin enzymatic class, deacetylates the neighboring nucleosome creating a high-affinity binding site for the Sir complex. Iterative rounds of this deacetylation results in spreading of Sir proteins across the silenced locus, which is key to silencing. Through a similar mechanism, the Sir-protein complex is also important for silencing telomeres.

This nucleation and spreading model for silencing makes testable prediction of silencing. For example, if iterative rounds of deacetylation by Sir2 are necessary for silencing, then a Sir complex would occupy each nucleosome at silenced loci. Additionally, this model only attributes Sir-protein association to *HML*, *HMR* and telomeres and not elsewhere in the genome. Lastly, if Sir2's only known role is to deacetylate nucleosome tails then its catalytic activity should be bypassed by preemptively removing these histone acetylations.

To test these predictions of the silencing model I have definitively characterized the distribution of Sir proteins throughout the genome and explored the unaccounted role for Sir2's catalytic activity in silencing. By characterizing the distributions of Sir2, Sir3 and Sir4 at high-resolution I have revealed unappreciated nucleation sites for Sir proteins at *HML* and *HMR* and a possible higher-order structure critical to silencing. Characterization of Sir proteins across the genome revealed an unanticipated phenomenon of highly-expressed genes being vulnerable to non-specific ChIP enrichment. Lastly, I performed a forward genetic screen to restore silencing independent of Sir2 catalytic activity. This screen identified a non-sirtuin deacetylase as refractory to silencing and suggested the possible role of a non-histone deacetylase substrate as important for silencing. This dissertation work has refined the *Saccharomyces cerevisiae* silencing model, contributing to our understanding of regional repression across organisms.

Table of Contents

Chapter 1: An Introduction to Silent Chromatin in *Saccharomyces cerevisiae* 1
1.1 Yeast Mating Type as a Model for Chromatin Regulation of Cell Identity 1
1.2 Silencers and the Establishment of Silencing 1
1.3 The Sir Complex 2
1.4 The Nucleosome and Silencing: Modification and Positioning 4
1.5 The Nucleation and Spreading Model 5
1.6 Telomeric Silencing 7
1.7 Predictions and Untested Assumptions of Silencing in Yeast 9

Chapter 2: The Molecular Topography of Silenced Chromatin in *Saccharomyces cerevisiae* 11
2.1 Abstract 11
2.2 Introduction 11
2.3 Materials and Methods 13
2.4 Results 17
2.4.1 Sir Proteins Showed Heterogeneous Distribution at *HML* and *HMR* 17
2.4.2 H4K16 was Hypoacetylated Across Silent Mating-Type Loci 22
2.4.3 Sir Proteins Showed Discrete Enrichment at Natural Telomeres 22
2.4.4 Restricted Sir3 and Sir4 Enrichment in Cells Lacking Sir2 Catalytic Activity 25
2.4.5 Formaldehyde Crosslinking Captured a Unique Feature of Silenced Chromatin Architecture 27
2.4.6 The Chromatin Superstructure Appeared Specific to Silenced but not Repressed Genes 30
2.5 Discussion 34
2.5.1 Crosslinking Captured a Higher-order Chromatin Super Structure 34
2.5.2 The Contribution of the Chromatin Superstructure to Silencing 35
2.5.3 Nucleation and Sir-Protein Association at Silenced Chromatin 37
2.5.4 The Domains of Hypoacetylated H4K16 37
2.5.5 Chromatin Architecture Facilitating Regional Repression 38

Chapter 3: Highly expressed loci are vulnerable to misleading ChIP localization of multiple unrelated proteins 39
3.1 Abstract 39
3.2 Introduction 39
3.3 Materials and Methods 40
3.4 Results 44
3.4.1 Unrelated Proteins show Overlapping Enrichment in ChIP-Seq Datasets 44
3.4.2 The Hyper-ChIPable Regions Coincided with Highly Expressed Genes 47
3.4.3 Green Fluorescent Protein was Enriched at Highly-Expressed Loci by ChIP-Seq Analyses in an Expression-Dependent Manner 52
3.4.4 No-Tag Controls Did Not Eliminate Hyper-ChIPability 57
3.4.5 Utilizing GFP ChIP-Seq to Remove False Positive Targets 57

3.5 Discussion 60

Chapter 4: Mutation of a Non-Sirtuin Histone Deacetylase Restores Silencing Independent of Sir2 Catalytic activity 69
4.1 Abstract 69
4.2 Introduction 69
4.3 Materials and Methods 71
4.4 Results 78
4.4.1 A Screen Identified Five Supressors able to Silence Independently of Sir2 Catalytic Activity 78
4.4.2 Mutation of *RPD3* Restored Sir Silencing 80
4.4.3 Wild-type Sas2 Prevented *rpd3Δ* silencing restoration 82
4.4.4 Restoration of Silencing by *rpd3* was Dependent on Another Sirtuin Hst3 85
4.4.5 Silencing Restoration by Rpd3 mutant was Independent of known Histone Substrates 85
4.4.6 Many Non-Histone Acetylations were Dependent on Rpd3 and Hst3 88
4.5 Discussion 95
4.5.1 The Role of Rpd3 in Silencing 95
4.5.2 Hst3 Has a Unique Role in Silencing 95
4.5.3 The Importance of Non-Histone Acetylation Substrates 96
4.5.4 Silencing Independent of Sir2 Catalytic Activity 96

References 98

List of Figures

1.1 Chromosome III of *Saccharomyces cerevisiae* 3
1.2 The Nucleation and Spreading Model 6
1.3 Telomeres of *Saccharomyces cerevisiae* 8

2.1 Sir protein ChIP-seq of sonicated chromatin showed heterogeneous distribution at *HML* and *HMR* 18
2.2 Sir-proteins showed continuous, though quantitatively variable enrichment from *HML* to the left telomere of Chromosome III 19
2.3 Sir protein ChIP-seq at *HML* and *HMR* on cross-linked chromatin digested with MNase 21
2.4 H4K16 was hypoacetylated throughout *HML* and at *HMR* 23
2.5 Sir protein enrichment at telomeres was discrete 24
2.6 Sir3 and Sir4 enrichment in a strain lacking Sir2 catalytic activity revealed nucleation sites 26
2.7 H3 was differentially recovered in immunoprecipitates from native versus cross-linked chromatin 28
2.8 Nucleosome occupancy between crosslinked and native chromatin preparations varies dramatically at silenced regions 29
2.9 Increased cross-linking time shows similar H3 ChIP distribution 31
2.10 H3 can be recovered in cross-linked samples at loci of site-specific transcriptional repression 32

2.11 Nucleosome occupancy was very similar between native and cross-linked samples at loci of site-specific repression 33
2.12 A model for a silenced superstructure at *HMR* 36

3.1 Euchromatic enrichment of the Sir complex in ChIP-Seq datasets 45
3.2 Enrichment Due to High Read Coverage in the Immunoprecipitate 46
3.3 Confirmation of ChIP enrichment at highly expressed genes by ChIP-qPCR 48
3.4 Sir-enriched euchromatic loci are hyper-ChIPable 48
3.5 Sir3 levels correlate with ChIP-Seq signals for Ste12 and Cse4 49
3.6 Highly expressed loci are hyper-ChIPable 50
3.7 Pol II levels correlate with ChIP-Seq signals for Sir2, Sir3, Sir4, and Cse4 51
3.8 tRNA proximity correlates with ChIP-Seq signals for Sir2, Sir3, Sir4, Cse4, and Ste12 53
3.9 Sir proteins are enriched across the entire Open Reading Frame 54
3.10 Confirmation of GFP hyper-ChIPability 55
3.11 ChIP-Seq of nuclear-localized GFP shows hyper-ChIPability 56
3.12 Hyper-ChIPability is present but variable in no-tag and no-GFP ChIP-Seq 58
3.13 GFP and Sir ChIP-Seq levels are correlated only in euchromatin 59
3.14 Using GFP ChIP-Seq to improve ChIP localization analysis 61

4.1 A forward genetic screen identified suppressors of Sir2's catalytic activity 79
4.2 Mutation of *RPD3* and *SIN3* restored silencing 81
4.3 The *rpd3* mutant restored Sir-based silencing 83
4.4 Restoration of silencing by *rpd3Δ* depends on *sas2Δ* 84
4.5 Silencing by the *rpd3* mutant was dependent on Hst3 86
4.6 Silencing by *rpd3Δ* was independent of known histone acetylation 87

List of Tables

2.1 Yeast strains used in chapter 2 14
2.2 Number of reads mapped for each experiment in chapter 2 16

3.1 Yeast strains used in chapter 3 41
3.2 Number of reads mapped for each experiment in chapter 3 43
3.3 The 238 Sir-enriched Euchromatic loci 63

4.1 Yeast strains used in chapter 4 72
4.2 Plasmids used in chapter 4 75
4.3 Number of reads mapped for each experiment in chapter 4 77
4.4 Primers used for qPCR in chapter 4 77
4.5 Acetylations dependent on Rpd3 89
4.6 Acetylations dependent on Hst3 92

Acknowledgements

None of this work could have been possible without the support of my mentor, Jasper Rine. Over the past six years he has supported both as a person and as a scientist, providing me the most challenging and nurturing environment that allowed me to grow into the scientist I am today. I will cherish his mentorship and hope to reflect the same respect to those that I mentor in the future.

I would have not made it through the past six years without the crazy crash of Rine-os. The high-spirited, fun environment of the Rine lab gave me the strength to come to lab even when nothing was working. Each of the research chapters in this dissertation would not have been possible without the initial, keen observations of three previous Rine lab graduate students: Oliver Zill, Lenny Teytelman and Erin Osborne Nishimura. From these three individuals, I learned how to conceive a project and follow it through to the end—something I had never accomplished before. In addition to all the scientific support of the Rine lab, I also have made life-long friends. Weekends playing volleyball, afternoon diet coke, cookie and coffee breaks, March Madness, rehashing the Seahawks, hiding Sweetness, ridiculous quals parties, playing salad bowl, easter egg hunts in lab, letting me bother you when I am bored during a five minute incubation, large, loud lunches, Myers-Briggs personality types, meme generating, the awkward rhino and awesome frog and so much more: these are the every day things that made the Rine lab such an exceptional place to work. I will miss the sassy girls, three musketeers and crazy cat ladies that let me feel truly at home in my home away from home.

I am lucky to also have such great family support over the past six years. Even though my parents do not necessarily understand what I have been doing in graduate school, they encouraged me every step of the way and listened to me on the phone and when I would come to visit, giving me the self-confidence I needed to succeed in graduate school. I also have the three most wonderful sisters who through marriages and new nieces have given me the joy of an ever-expanding family. I especially want to thank Danielle for her mix tapes and study care packages got me through some long days in lab. Also, I thank Leah, Catherine and Liz. Although not scientists, they would listen to me talk about my work and support me, making me feel smart. Also, not only is graduate school challenging intellectually, but also emotionally and they gave me strength when I was at my wits end.

When choosing Berkeley for graduate school, I never knew that I would also be choosing a program that would give me so many life-long friends. From skyping biochemistry study sessions to blazing the trail on the PCT, the friends I developed through the MCB program made graduate school bearable. I will never forget all the shows (especially Phish shows) that Phil Cleves and I have seen. Releasing pent up lab energy by snowboarding in the winter and backpacking in the summer reenergized me for the next week. Also, I thank Dorothy and Alec for not caring when I would just show up at their house because I wanted to unwind with people after a long day. And even just the standing weekly appointment of TV club that gave me a reason to leave lab at a reasonable hour and go hang out with friends. I am sure that the friendships that I have made in graduate school will last a lifetime and I am grateful to have gotten to know each of you.

I also thank my best, furry friend who I couldn't have done graduate school without. As a third year, I adopted Jean Luc Picat at 10 weeks old. Since then he has become an integral part of my life and puts up with my mild torturing and demanding to hold him all the time. Whether its playing fetch with q-tips or just cuddling on the couch, JLPK makes me very happy every day.

Studies have shown that petting an animal can lower stress levels and I can 100% say that Jean Luc has lowered my stress levels throughout graduate school.

And last but not least I could not have finished graduate school without the love and support of Bryan Schmidt. As a friend from one of the first days I entered graduate school to my life partner now, he has been there for me through the highs and lows. He would always encourage me when I thought I couldn't keep going and put life into perspective for me when I was overreacting. He makes every day easier and more fun and I truly know that together we can do anything. So thanks to him I am confident that I can tackle the next task ahead of me.

Chapter 1: An Introduction to Silent Chromatin in *Saccharomyces cerevisiae*

1.1 Yeast Mating Type as a Model for Chromatin Regulation of Cell Identity

Within an organism, almost all cells have exactly the same genomic information, yet can have very different cellular identities. How the appropriate genes are expressed and repressed for that cell type, and how this expression pattern is maintained through mitosis, are frontier problems in genetics and development. To achieve this appropriate cell-type specific expression, eukaryotic cells exhibit many different scales of genetic regulation. The most thoroughly understood examples include mechanisms of promoter-dependent activation and repression of individual genes. At the other extreme, entire chromosomes are subject to a common regulatory influence, such as mechanisms of dosage compensation of sex chromosomes (Meyer 2010; Conrad and Akhtar 2011; Jeon et al. 2012). At intermediate scales, heterochromatin facilitates regional, promoter-independent repression, either constitutively, as in the pericentric regions of chromosomes in many species, or in a facultative fashion, such as repression of Hox genes by Polycomb group proteins in *Drosophila* (Ringrose and Paro 2004).

Mating type regulation in yeast is a simple, yet elegant model for studying heterochromatin control of cell identity. *Saccharomyces cerevisiae* has three different cell types: haploid **a** or α cells or diploid **a**/α cells. The haploid cells express specific patterns of gene expression making the cell responsive to the opposite mating-type pheromone and capable of mating. A diploid however, no longer has the capacity to mate, but rather, under correct nutrient conditions, is able to induce sporulation (Herskowitz 1988).

Mating type in yeast is controlled by the alleles at the actively transcribed *MAT* locus. However, there are additional copies of both the α and **a** genes located at loci, termed *HML* and *HMR,* at the distal ends of chromosome III that facilitate mating type switching (Figure 1.1) (Rine et al. 1979). In strains that are capable of switching their mating type, the site-specific HO endonuclease is expressed in a haploid, which cleaves its recognition sequence at the *MAT* locus, resulting in a double-strand DNA break. Through a gene conversion event, *HML* or *HMR* then act as the donor information to repair the break through homologous recombination, resulting in switching the mating type of the cell (Haber 2012). Even though the **a** and α alleles of *HML* or *HMR* have exactly the same promoters as the copies of these genes at the actively transcribed *MAT* locus, the mating type genes are not expressed when present at *HML* and *HMR*. This locus-specific repression is achieved through heterochromatic repression, and provides a simple, yet tractable context to explore the mechanism of promoter-independent repression.

1.2 Silencers and the Establishment of Silencing

The nucleation of chromatin proteins to the site of repression is critical to establishing heterochromatic repression. In *S. cerevisiae*, regulatory sites, termed silencers, flanking *HML* and *HMR* nucleate the localization of Silence Information Regulator (Sir) proteins, which make up the complex key for silencing in budding yeast (Kueng et al. 2013). The silencers are DNA sequences

that contain binding sites for the transcription factors Abf1 and Rap1 as well as the six-subunit Origin Recognition Complex (ORC), a complex that is critical for initiation of DNA replication (Figure 1.1). Interestingly, the silencers at *HML* and *HMR* exhibit different abilities to establish silencing: The *E* and the *I* silencers at *HML* are each sufficient for silencing; however, only the *E* silencer at *HMR* is necessary and sufficient for silencing, reflecting some of the intrinsic differences of *HML* and *HMR* (Brand et al. 1985; Mahoney and Broach 1989).

ORC is the only factor bound to all four silencers. ORC is the six-subunit complex necessary for replication initiation of eukaryotic DNA. Due to the presence of the ORC complex at silenced loci, it was hypothesized that there may be an intimate connection between replication and silencing. Each of the silencers can act as an autonomously replicating sequence (ARS) on a plasmid, however only *HMR-E* and *HMR-I* act as origins of replication on the chromosome (Rivier and Rine 1992). Interestingly, at *HMR* there is an S-phase-specific cell-cycle requirement for silencing, that is independent of DNA replication and seems to be dependent on an additional cis-element: a tRNA gene adjacent to *HMR* (Fox et al. 1997; Lazarus and Holmes 2011). Additionally, mutations have been isolated in Orc5 that effect its ability to silence, but not its replication abilities, indicating that ORC's silencing and replication roles are separable (Dillin and Rine 1997).

ORC's primary role at the silencer is to nucleate recruitment of the Sir complex, consisting of Sir2, Sir3 and Sir4, through interactions bridged between Sir1. Sir1 contains two ORC Interaction Regions, facilitating this interaction (Triolo and Sternglanz 1996; Zhang et al. 2002; Hou et al. 2005). Tethering Sir1 to the silencer bypasses the need for ORC binding to the silencers to recuit the other Sir proteins (Fox et al. 1997). Unlike loss of the other Sir proteins, which are all required for silencing, deletion of Sir1 creates two stable and phenotypically heritable populations: one expressing the silent mating loci and the other, in which these loci are repressed (Pillus and Rine 1989; Xu et al. 2006). This two-state observation has led to the suggestion that like the factors binding to the silencer, Sir1 is important for the establishment, rather than the maintenance of silent chromatin.

1.3 The Sir complex

The critical protein complex for silencing in *S. cerevisiae* consists of one copy each of the Sir2, Sir3, Sir4 proteins (Moazed et al. 1997). Deletion of the gene encoding any one of these components results in complete derepression of the silent mating loci (Rine and Herskowitz 1987). The Sir2, Sir3, Sir4 complex is also found at telomeres, where it mediates telomeric silencing. The complex consists of two structural components, Sir3 and Sir4, and the catalytic member, Sir2 (Kueng et al. 2013). Sir2, the founding member of the sirtuin family of proteins, is a NAD^+-dependent deacetylase (Imai et al. 2000; Landry et al. 2000; Smith et al. 2000). Sirtuins couple the hydrolysis of NAD^+ to the deacetylation of a protein, producing nicotinamide and 2-O-acetyl ADP ribose as reaction products (Tanner et al. 2000). This catalytic activity of Sir2's is necessary for silencing, as a point mutation in Sir2 that is structurally in tact but catalytically inactive, cannot silence (Imai et al. 2000). Its primary catalytic role is thought to deacetylate the N-terminal tails of H3 and H4, especially H4K16, to create a high-affinity binding site for Sir3. Through a binding surface near the N-terminus of Sir2, Sir2 interacts tightly with Sir4 (Rusché et al. 2002; Hoppe et al. 2002). Sir4 binds to both histones and DNA, but with little specificity (Martino et al. 2009). Sir2

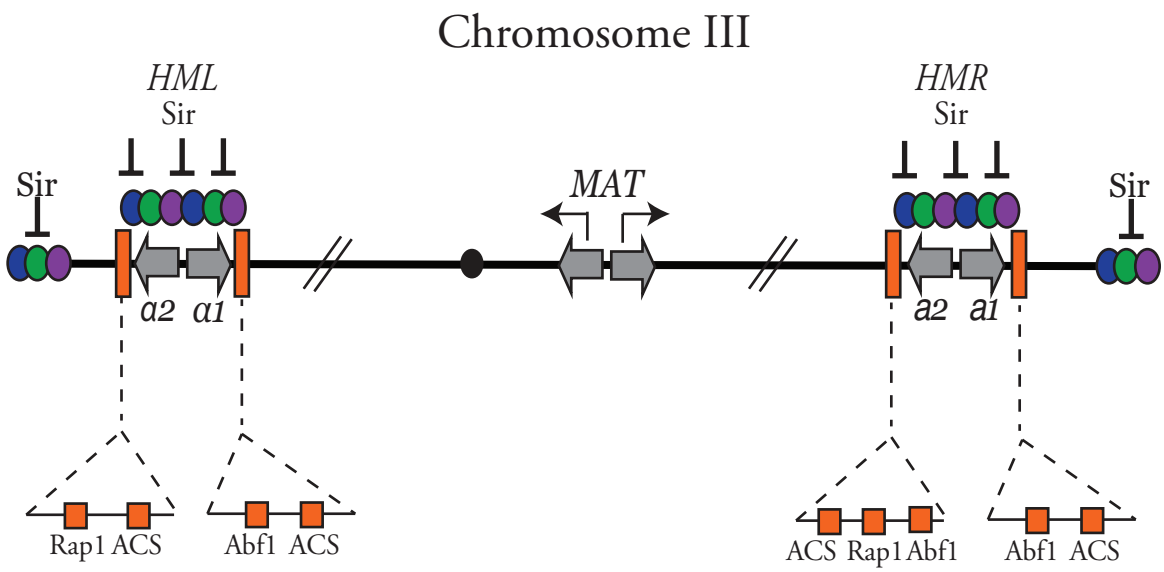

Figure 1.1 Chromosome III of *Saccharomyces cerevisiae*. Schematic of chromosome III highlighting the key features critical for yeast mating type. Near the centromere, the *MAT* locus harbors copies of the expressed mating type alleles. The distal ends of chromosome III bears the silenced copies of the α alleles at *HML* and the **a** alleles at *HMR*. Silencers flank *HML* and *HMR* with binding sites for transcription factors and ORC, which binds the Ars Consensus Sequence (ACS). These proteins recruit the Sir complex, which is critical for repression. Sir proteins are also found at the telomeres. Note the schematic is not drawn to scale.

is also important for suppression of rDNA recombination in a complex with Cdc14 and Net1 known as the RENT complex (Rusché et al. 2003).

The third member of the Sir complex, Sir3, is a structural member of the Sir complex that binds to hypoacetylated nucleosomes. Sir3 is a paralog of Orc1 resulting from the yeast whole genome duplication. Sir3 consists of a bromo-adjacent homology domain (BAH) and a degenerate AAA ATPase domain that is no longer catalytically active, but is suggested to bind other ATP-like analogs, which may be important for silencing (Norris and Boeke 2010; Ehrentraut et al. 2011). Genetic suppression experiments found that a single point mutation in the BAH domain of Sir3, *sir3D205N*, was able to suppress silencing defects of histone mutants mimicking the acetylated state (Johnson et al. 1990). This result suggested a key interaction between Sir3 and the nucleosome was important for silencing. Recent co-crystallization studies of Sir3's BAH with the nucleosome have confirmed this interaction and Sir3s affinity for hypoacetylated H3 and H4 (Simon and Kingston 2009; Wang et al. 2013). Additionally, overexpression of Sir3 leads to aberrant spreading of Sir complexes—likely due to its affinity for hypoacetylated histone tails (Hecht et al. 1996; Radman-Livaja et al. 2011). Together these three proteins comprise the Sir complex, which is indispensable for silencing at both the silent mating loci and telomeres in budding yeast.

1.4 The Nucleosome and Silencing: Modification and Positioning

In addition to the Sir complex associating with nucleosomes, histone hypoacetylation is key to the chromatin structure at the silenced loci. Initial genetic experiments identified H4K16 hypoacetylation as critical for silencing. Changing this residue to either an alanine (non-acetylatable) or glutamine (mimicking the acetylated state) almost completely abolishes silencing at *HML* (Park and Szostak 1990; Johnson et al. 1990). Mutations in additional H4 N-terminal tail lysines also effect silencing at *HML*, but to a much smaller degree than the single H4K16 acetylation. Thus, since Sir2 is a histone deacetylase, it was suggested that its main role in silencing was to hypoacetylate H4K16 (Braunstein et al. 1993). More recent biochemical studies of the association of Sir3 with the nucleosome has identified that acetylation of H4K16 disrupts a key interaction between the Sir3 BAH domain and the nucleosome (Armache et al. 2011; Wang et al. 2013). When Sir2 is not present, H4K16 is acetylated at silenced loci by the MYST-acetyltransferase Sas2, which typically counteracts deacetylation by Sir2 at the boundaries of silenced loci (Suka et al. 2002; Kimura et al. 2002). Interestingly however, mutations in *SAS2* have opposing effects at *HML* and *HMR*. In combination with *sir1Δ*, at *HML* silencing is completely lost (Reifnyder et al. 1997). However in combination with a weakened silencer at *HMR*, deletion of *SAS2* improves silencing (Ehrenhofer-Murray et al. 1997). These observations indicate fundamental differences between silencing at *HML* and *HMR*.

Additionally beyond just the H4 N-terminal tail, other modifications of nucleosomes are implicated in silencing. H3 is also hypoacetylated on its N-terminal tail and deletion of the H3 N-terminus disrupts the structure of silenced chromatin as measured by sedimentation analysis of the chromatin (Sperling and Grunstein 2009). Modification in the core of H3 also contributes to silencing. H3 is acetylated at K56 by the histone acetyltransferase Rtt109, which is critical for deposition of H3 into chromatin during replication and transcription (Recht et al. 2006; Fillingham et al. 2008). At telomeres, the other main region of Sir repression in yeast, point mutations in H3K56 disrupt Sir based silencing. Strains expressing a Sir2 catalytically dead point mutant show

an increase in H3K56 acetylation at telomeres and *HMR* and *HML* (Xu et al. 2007). However, this point mutation leads to loss of silencing and thus an increase in transcription at silenced loci. Since acetylation at H3K56 is a transcription-coupled mark, it is unclear whether this increase in acetylation at H3K56 is a cause or consequence of the loss of silencing. Additionally, there is contradictory evidence as to whether Sir2 is able to deacetylate H3K56 in vivo (Xu et al. 2007; Yang et al. 2008; Oppikofer et al. 2011). This has led to the hypothesis that other deacetylases may be important at silenced loci. In addition to Sir2, the yeast genome encodes four other sirtuin-class histone deacetylases: Hst1-4. Hst3 and Hst4 deacetylate H3K56 and may have roles at silenced loci, however this role seems more relevant at the telomeres than *HML* and *HMR* (Yang et al. 2008).

The positioning of the nucleosomes is also highly characterized at *HML* and *HMR*. Precise nucleosome mapping at *HML* and *HMR* reveals 12 well-positioned nucleosomes at *HMR,* positioned in pairs with very short linkers, and 20 nucleosomes at *HML* (Ravindra et al. 1999; Weiss and Simpson 1998). This nucleosome positioning is dependent on Sir3 as well as the N-terminal tail of H4. The 20 nucleosomes at *HML* are precisely positioned only directly adjacent to the silencers, and are less well positioned throughout the middle of the cassette with the exception of a pair of very precisely positioned nucleosomes directly over the HO recognition site at *HML* (Weiss and Simpson 1998). Thus the silencing complex and nucleosome modification important for silencing in yeast, and the positioning of the nucleosomes is critical to the organization of the silent chromatin at *HML* and *HMR*.

1.5 The Nucleation and Spreading Model

Chromatin Immunoprecipitation (ChIP) studies analyzed by PCR revealed that the Sir2, Sir3, Sir4 complex is enriched across the entire silent mating loci (Rusché et al. 2002; Hoppe et al. 2002). This association of Sir proteins throughout the loci is thought to be critical for repression of the silent mating loci, leading to the nucleation and spreading model for silenced chromatin as follows: The Rap1 and Abf1 sequence specific transcription factors and ORC bind to the silencers. Through interactions between Rap1 and Sir3 and Sir4, and between Sir4 and Sir1, the Sir complex is nucleated to the silencers (Figure 1.2A). Sir2, the NAD^+-dependent histone deacetylase, deacetylates the neighboring nucleosome, creating a high-affinity binding site for Sir3 and Sir4, resulting in the spreading of the Sir complex to the adjacent nucleosome (Figure 1.2B). Then, through iterative rounds of the deacetylation, the Sir proteins spread across the silenced loci, creating the repressive chromatin domain (Figure 1.2C-D). This repressive chromatin domain silences the loci at least in part through steric occlusion of the transcriptional machinery from their recognition sequences in silenced chromatin though others have suggested additional contributions to the mechanism of silencing (Singh and Klar 1992; Loo and Rine 1994; Chen and Widom 2005; Gao and Gross 2008).

The spreading of the Sir complex into neighboring euchromatin is prevented by boundary elements. Adjacent to *HMR*, an expressed $tRNA^{THR}$ is necessary and sufficient for preventing the spreading of Sir proteins (Donze and Kamakaka 2001). At *HML* there is not a distinct boundary element identified, but the orientation of the *HML-I* silencer may influence the direction of chromatin organization (Bi et al. 1999). Chromatin factors also help prevent the aberrant spreading of Sir proteins. Modification of histones by histone acetyltransferases and methyltransferases, such as Sas2 and Dot1, respectively, disrupt Sir-nucleosome interactions, preventing the spreading of the

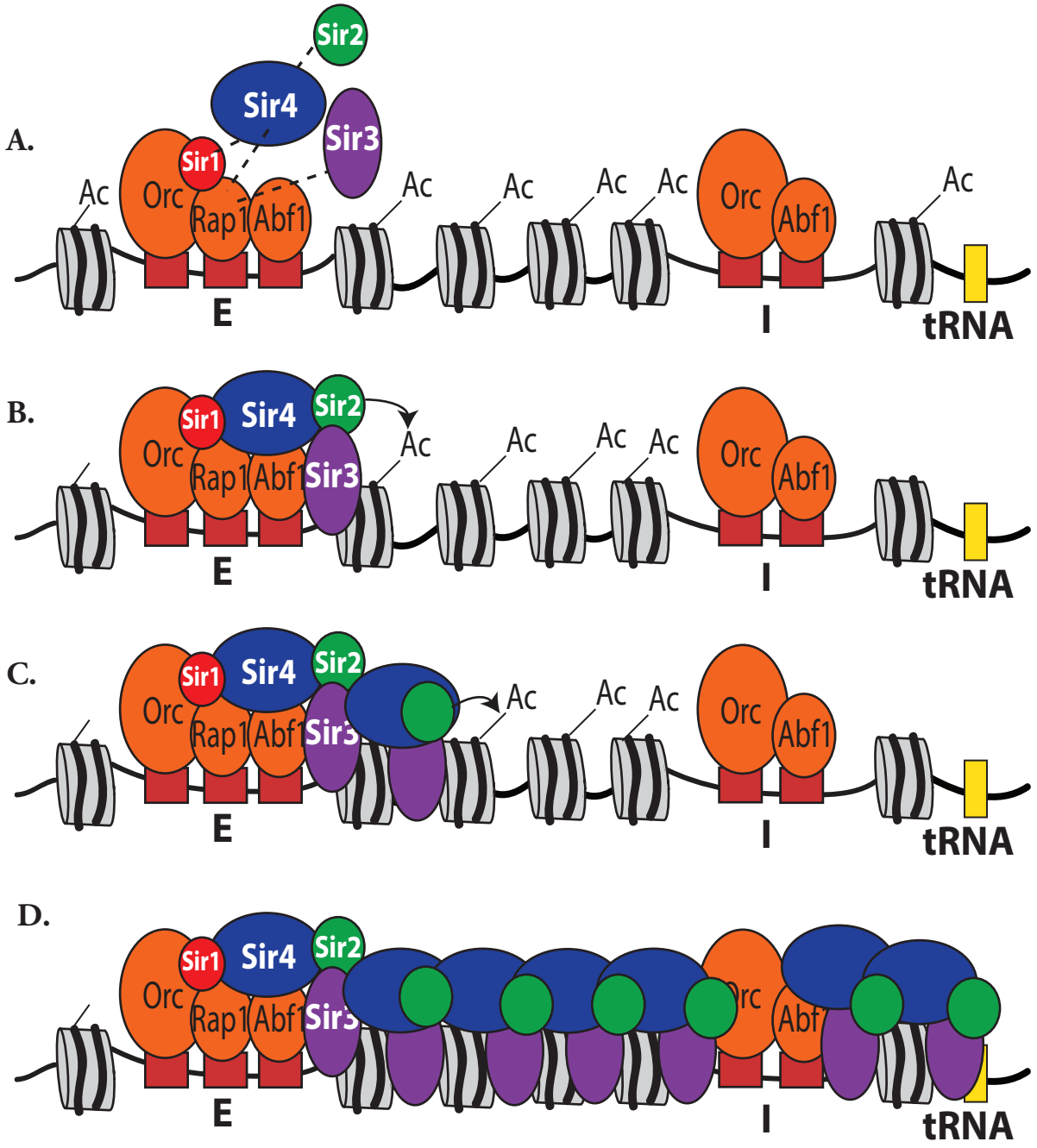

Figure 1.2 The nucleation and spreading model. (A) Through interactions with proteins that bind the silencers, the Sir2, Sir3, Sir4 protein complex is nucleated to the silent mating loci. (B) Sir2 deacetylates the neighboring nucleosome tail to create a high-affinity binding site for Sir3. (C) This deacetylation allows the complex to spread to the neighboring nucleosome, resulting in iterative rounds of deacetylation. (D) The Sir2, Sir3, Sir4 protein complex spreads across the silent mating loci, stopped by the adjacent tRNA, to create the repressive chromatin domain critical for silencing.

complex (Kueng et al. 2013). Additionally, a non-sirtuin histone deacetylase, Rpd3, may prevent Sir complex spreading by competing for Sir2's H4K16-acetyl substrate (Ehrentraut et al. 2011). When deacetylating H4K16 Sir2 not only creates a Sir3 binding site on the nucleosome, but also creates the small molecule OAAR, which may be critical for silencing (Liou et al. 2005; Johnson et al. 2009; Martino et al. 2009). Since Rpd3 is not a sirtuin, Rpd3 prevents the spreading of Sir proteins by not making this reaction byproduct. This suggestion of the sirtuin reaction mechanism and its byproduct as critical for silencing is explored in chapter 4. Additionally, Sir-nucleosome interactions may be disrupted due to insertion of the H2A.Z histone variant into the nucleosome core particle, blocking the aberrant spreading of Sir proteins to neighboring chromatin (Babiarz et al. 2006). The paradigm for the creation of heterochromatin domains in multiple species is modeled after nucleation of a key heterochromatic complex at a regulatory site followed by spreading of that complex to the target(s) of repression that is restricted by boundary elements to its appropriate domain described here in *S. cerevisiae*.

1.6 Telomeric Silencing

In addition to the silent mating loci, Sir2, Sir3 and Sir4 also mediate gene silencing at telomeres. Like at *HML* and *HMR*, Sir proteins are nucleated to the telomeres through interactions with ORC, Abf1 and Rap1 that are bound to different telomeric elements organized in two structural classes: those containing just an X-element (X) (Figure 1.3A), and those with both an X-element and Y'-element (X-Y') (Figure 1.3B). The X-element contains the Core X, where ORC and Abf1 bind, as well as the subtelomeric repeat sequence. Y' elements contain ORFs that encode proteins with sequence homology to helicases. At telomeres that contain only an X-element, the X-element is adjacent to the telomerase-generated telomeric repeats, where Rap1 binds (Figure 1.3A). At telomeres that contain both a Y'-element and X-element, the X-element is immediately centromere-proximal to the Y'-element, which is adjacent to the telomeric repeats (Figure 1.3B) (Louis 1995). Nucleation of the Sir proteins at telomeres is primarily mediated through interactions with Sir4, where Sir4 interacting with Rap1 at the $TG_{1\text{-}3}$ repeats nucleates the complex (Kueng et al. 2013). Additionally, the yeast Ku complex also binds telomeric ends and interacts with Sir4 to also facilitate Sir protein nucleation (Roy et al. 2004). Because the complex is primarily nucleated through interactions mediated by Sir4, Sir1 is not involved in telomeric silencing as determined for synthetic telomeres. Although there are data suggesting a role for Sir1 at a native telomere, recent data all but eliminate any role of Sir1 at *Saccharomyces cerevisiae* telomeres (A. Ellahi, personal communication).

Due to these different combinations of telomeric elements and their ability to recruit Sir proteins, initial studies of telomeric silencing, termed Telomere Position-Effect Variegation, in yeast utilized a reporter gene inserted directly adjacent to the telomeric repeats, deleting all the X and Y' sequences. Utilizing this reporter, it was found that expression of the reporter gene at *S. cerevisiae* telomere ends is stably silenced through mitotic divisions and this is dependent on Sir proteins (Gottschling et al. 1990; Aparicio et al. 1991). Interestingly, later studies examined the repression of a reporter gene at different telomeres with the natural telomeric features preserved. This study found that silencing at different yeast telomeres was extremely variable with some telomeres not exhibiting any silencing and the largest effect found when the reporter was inserted directly adjacent to the X-core region (Pryde and Louis 1999; Fourel et al. 1999). Advances in whole-genome microarray

A. X-Only Telomere

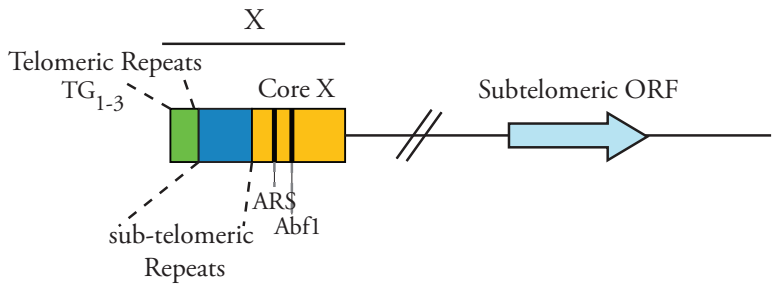

B. X-Y' Telomere

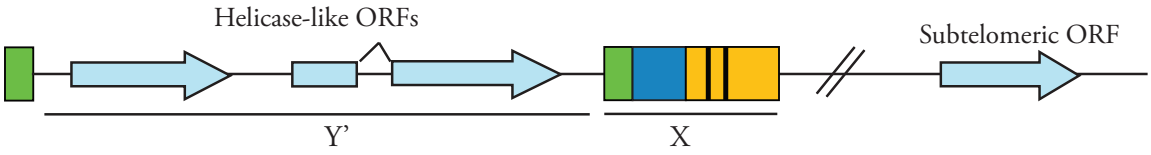

Figure 1.3 Telomeres of *Saccharomyces cerevisiae*. (A) X-only telomeres consist of the telomeric repeats generated by telomerase (green), the sub-telomeric repeats (blue) and the Core X sequence which contains binding sites for Abf1 and an ARS where ORC binds (orange). (B) X-Y' telomeres have the telomeric repeats generated by telomerase at the very end of the chromosome as well as a Y' region containing open reading frames (ORFs) with homology to helicases. Additionally on the centromere side of the Y' element, X-Y' telomeres also contain an X-element harboring the same features as when the X-element is found at X-only telomeres. Note the schematics are not drawn to scale.

technology made it possible to examine natural telomeres and the change in expression of native genes at the telomeres in a Sir-protein-dependent pattern. Surprisingly, very few of the natural genes at yeast chromosome ends change in response to silencing mutations, calling into question the generality of telomere position effect variegation in yeast (Takahashi et al. 2011).

1.7 Predictions and Untested Assumptions of Silencing in Yeast

The nucleation and spreading model for silencing at *HML*, *HMR* and telomeres makes many testable predictions about silencing in *S. cerevisiae*. First, the proposed histone deacetylation by Sir2 through iterative rounds of hypoacetylation of the adjacent nucleosome suggests that the Sir complex spreads linearly across the chromatin fiber. However, recent kinetic studies of the establishment of silencing have found that Sir protein association at *HML* and *HMR* happens evenly throughout the locus until steady-state levels are achieved, challenging the notion of linear spreading (Radman-Livaja et al. 2011; Lynch and Rusché 2009). Additionally, the notion of linear Sir protein spreading predicts each nucleosome to be occupied by the Sir complex to create a condensed chromatin fiber where Sir proteins associate evenly throughout the silenced domain. However, more recent studies of Sir protein association have indicated that there are regions of discontinuous Sir protein enrichment, raising the possibility that not all nucleosomes may be occupied by Sir proteins (Zill et al. 2010; Radman-Livaja et al. 2011).

The nucleation and spreading model only attributes Sir protein function to the silenced regions of *HML*, *HMR* and the telomeres, as well as the repression of recombination at the rDNA by Sir2. With the rise of whole genome sequencing techniques, others have suggested the presence of Sir proteins at euchromatic loci as well (Radman-Livaja et al. 2011; Li et al. 2013). This suggestion highlights an outstanding question for the Sir complex in yeast not addressed by the nucleation and spreading model: Does the Sir complex have roles in yeast outside the canonical silencing domains?

Lastly, according to the nucleation and spreading model as outlined above, the only role for Sir2's catalytic activity is the hypoacetylation of histones, especially H4K16. This model suggests that the requirement for Sir2's catalytic activity should be bypassed if the acetylation on H4K16 is preemptively removed. However, this is not the case. Studies where the H3 and H4 tails are genetically modified to mimic the hypoacetylated state, or the acetyltransferase, Sas2, is deleted so as the lysines are never acetylated at the silenced regions are unable to overcome the Sir2 catalytically dead silencing defect (Yang and Kirchmaier 2006). These results indicate that a key role of Sir2's catalytic activity is not accounted for in the model.

Throughout my thesis work, I have sought to test these predictions and assumptions of yeast silent chromatin. I definitively characterized Sir protein association at *HML* and *HMR* with high-resolution sequencing techniques, revealing unappreciated nucleation sites for Sir proteins at *HML* and *HMR* and a possible higher-order structure critical to silencing. Additionally in collaboration with Lenny Teytelman in Alexander Van Oudenaarden's lab, we discovered that there are regions of the genome vulnerable to non-specific ChIP enrichment. These analyses were made possible by exploiting the highly characterized nature of Sir protein function and biology, ensuring that the Sir proteins do not function elsewhere in the genome besides the already characterized silent chromatin. Additionally, I performed a forward genetics screen to understand what role of Sir2's catalytic activity has not been accounted for in the nucleation and spreading model. This screen identified other factors that restore silencing in the absence of Sir2 catalytic activity, highlighting key players

previously underappreciated for yeast silencing. Through this dissertation work I have refined the classic nucleation and spreading model, discovered a pervasive bias in ChIP studies and uncovered additional roles for a conserved enzyme, contributing to our understanding of regional repression across organisms.

Chapter 2: The Molecular Topography of Silenced Chromatin in *Saccharomyces cerevisiae*

(Portions of this chapter are adapted from: **Thurtle, D.M.** and Rine, J.R. (2014). *Genes & Development* 28, 245-258.)

2.1 Abstract

Heterochromatin imparts regional, promoter-independent repression of genes, and is epigenetically heritable. Understanding how silencing achieves this regional repression is a fundamental problem in genetics and development. Current models of yeast silencing posit that Sir proteins, recruited by transcription factors bound to the silencers, spread throughout the silenced region. To directly test this model at high-resolution, we probed the silenced chromatin architecture by ChIP-seq of Sir proteins, histones, and a key histone modification, H4K16-acetyl. These analyses revealed that Sir proteins are strikingly concentrated at, and immediately adjacent to the silencers, with lower levels of enrichment over the promoters at *HML* and *HMR*, the critical targets for transcriptional repression. The telomeres also showed discrete peaks of Sir enrichment, yet a continuous domain of hypoacetylated histone H4K16. Surprisingly, ChIP-seq of cross-linked chromatin revealed a distribution of nucleosomes at silenced loci that was similar to Sir proteins, whereas native nucleosome maps showed a regular distribution throughout silenced loci, indicating that cross-linking captured a specialized chromatin organization likely imposed by Sir proteins. This specialized chromatin architecture observed in yeast informs the importance of a steric contribution to regional repression in other organisms.

2.2 Introduction

There are four key features of heterochromatic repression essential to its role in genetic regulation: 1) its nucleation; 2) the mechanism of apparent spreading; 3) the mechanism of transcriptional repression; and 4) the mechanism of its epigenetic inheritance. Understanding the first two features of heterochromatin, its ability to nucleate from a specific site and its ability to then spread to create larger areas of regional repression, is critical to understanding the other two features. Formally, the apparent spreading of repression could occur through two classes of mechanisms: 1) physical spreading of chromatin associating proteins or histone marks from the nucleation site to the distal sites of repression; or 2) "action at a distance" where the nucleation site interacts with the distal site(s) of repression though long-range and potentially stochastic transient interactions. The function of heterochromatin in many organisms depends upon an interplay between noncoding RNA, enzymes that modify nucleosomes, and proteins that recognize and bind those modifications (Beisel and Paro 2011). In *Saccharomyces*, the silenced chromatin at *HML*, *HMR* (the silenced mating-type loci) and telomeres bear all the hallmarks of classically defined heterochromatin, yet achieve the four features of heterochromatin with no contribution from noncoding RNA (Grunstein and Gasser 2013). Hence, this example offers the opportunity to address fundamental mechanisms with one less layer of complexity.

The silent mating-loci in *Saccharomyces cerevisiae* harbor unexpressed copies of the mating-type alleles, that contain the same promoters as the actively transcribed alleles of the *MAT* locus (Hicks et al. 1979; Rine et al. 1979). Repression at the silent-mating loci is due to the nucleation and spreading of the Sir complex. The nucleation of silenced chromatin formation at *HML* and *HMR* is achieved by the *E* and *I* silencers, which are specific DNA sequences that flank both loci and contain binding sites for the widely-acting transcriptional activators, Abf1 and/or Rap1, as well as ORC, the initiation factor for DNA replication common to all eukaryotes (Brand et al. 1985; Rusché et al. 2003). These nucleation sites recruit the Sir proteins, which, through modification and subsequent binding to histone tails of nucleosomes, constitute silenced chromatin. The mechanism of silencing is, at least in part, due to steric occlusion of the transcriptional machinery from their recognition sequences in silenced chromatin (Singh and Klar 1992; Loo and Rine 1994; Chen and Widom 2005; Gao and Gross 2008).

Sir1 is recruited to the silencers through direct binding to ORC (Triolo and Sternglanz 1996; Zhang et al. 2002; Hou et al. 2005), facilitating the subsequent recruitment of Sir4-Sir2 dimers and Sir3, which also bind to Rap1 and Abf1 (Ghidelli et al. 2001; Hoppe et al. 2002; Chen et al. 2011). Sir2, the founding member of the Sirtuin family conserved throughout eukaryotes, is an NAD-dependent histone deacetylase that deacetylates the amino-terminal tail of histone H4 on lysine 16 (Imai et al. 2000; Landry et al. 2000; Smith et al. 2000). The deacetylase activity of Sir2 is necessary for silencing (Imai et al. 2000; Tanny et al. 1999). ChIP studies have shown Sir2, Sir3 and Sir4 to be enriched throughout the silenced domain at *HML* and *HMR* (Rusché et al. 2002; Hoppe et al. 2002). Sir3 has a higher affinity for deacetylated tails of histone H4 than for acetylated tails (Johnson et al. 2009; Martino et al. 2009). These observations and others have led to a widely-adopted model for how Sir proteins appear to spread throughout a silenced domain: following nucleation of a Sir-protein complex at the silencers, Sir2 deacetylates histone tails of adjacent nucleosomes, creating new high-affinity binding sites for additional Sir-protein complexes. Iterative rounds of deacetylation, followed by recruitment of additional Sir-protein complexes, leads to spreading of repression across the silenced locus. Boundary elements, best defined at *HMR*, restrict silencing to one side of the boundary, preventing aberrant Sir spreading into euchromatin (Donze and Kamakaka 2001; Oki and Kamakaka 2005).

Sir2, Sir3 and Sir4 also mediate telomere-position effects in *Saccharomyces*, causing genes positioned near telomeres to be stochastically expressed or repressed (Gottschling et al. 1990). Telomeres in *S. cerevisiae* consist of tandem repeats of sequences produced by telomerase, and other telomere-associated sequences, referred to as X-elements or Y'-elements (Louis 1995). Studies have reported considerable variation in the silencing capacity among telomeres. At natural telomeres, silencing is more pronounced directly next to the X-elements, and diminishing substantially within a few kilobase-pairs or less (Fourel et al. 1999; Pryde and Louis 1999; Takahashi et al. 2011). In contrast, studies of silencing at synthetic telomeres, especially with overexpression of Sir3, have indicated a more extensive domain of silencing (Gottschling et al. 1990; Hecht et al. 1996; Radman-Livaja et al. 2011).

Classic chromatin mapping studies at *HML* and *HMR* have identified well-positioned nucleosomes at the silent mating-type loci with the silencers being nucleosome free, reflecting their occupancy by ORC, Abf1 and/or Rap1 (Weiss and Simpson 1998; Ravindra et al. 1999; Henikoff et al. 2011). In contrast to the regular distribution of nucleosomes in silenced chromatin, limited higher resolution Chromatin Immunoprecipitation followed by Next-Generation Sequencing

(referred to throughout this work at ChIP-seq) studies revealed less homogeneous distributions of individual Sir proteins than suggested by prior methods, and by the model for Sir-protein spreading (Zill et al. 2010; Radman-Livaja et al. 2011; Li et al. 2013). To provide a definitive assessment of the silenced chromatin architecture as revealed by Sir-protein distributions at *HML*, *HMR*, telomeres and across the genome, we performed high-resolution ChIP-seq analysis of Sir2, Sir3 and Sir4, a catalytically inactive Sir2, as well as an evaluation of the distribution of nucleosomes and of acetylated H4K16. At this high-resolution, we found that the Sir proteins had a strikingly heterogeneous and highly reproducible pattern of enrichment at the *HML* and *HMR* loci, with the lowest apparent level of enrichment, paradoxically, over the promoter regions that are the targets of the silencing mechanism. In contrast, H4K16 hypoacetylation was homogeneous across the silenced loci. An integrated suite of chromatin analyses revealed a molecular topography of Sir proteins that suggested the existence of a chromatin superstructure at both *HML* and *HMR*, which provided insight into the steric dimension of the mechanism of silencing.

2.3 Materials and Methods

Yeast strains Used All yeast strains were derived from the W303 background and genotypes are indicated in Table 2.1. Deletions and epitope-tags were constructed through one-step integration of knockout cassettes (Longtine et al. 1998). C-terminal tagging of Sir gene ORFs was also conducted using one-step gene replacement with the 13xMyc tag. H4K16-acetyl and H3 ChIP-seq experiments were performed on JRY9316.

Chromatin Isolation by Sonication 70 OD units (A600) of logarithmically growing cells were cross-linked with 1% formaldehyde for either 15 minutes or for 1 hour at room temperature. Chromatin was prepared as previously described (Aparicio et al. 2005). Cells were lysed with 0.5-mm zirconia beads in 1 ml FA lysis buffer. Cell lysates were collected by centrifugation at 74,000 x g for 40 min then washed for 1 hour at 4°C in FA lysis buffer. Samples were then centrifuged at 74,000 x g for 22 min and sonication proceeded as described to an average size of 300-400 bp.

MNase Preparation of Chromatin 350 OD units (A600) of logarithmically growing cells were cross-linked with 1% formaldehyde for 15min at room temperature. For native chromatin preparation, the crosslinking step was omitted. Nuclei were prepared as in (Furuyama and Biggins 2007) with the following modifications. Cells were resuspended in 4 ml/g cell weight Buffer 1 and digested with 450 ug Zymolyase-100T. Spheroplasts were washed twice in 5 mls SPC + Protease Inhibitors and resuspended in 1 ml SPC + PI. This resuspension was added to 1 ml Ficoll buffer while gently stirring. Nuclei were collected by spinning at 9800 rcf for 20 min at 4°C. Nuclei were washed twice with 1 ml SPC + protease inhibitors. Nuclei were resuspended in a final volume of 1 ml SPC + protease inhibitors and flash frozen at -80°C overnight. 420 units of MNase (Worthington) was added to thawed nuclei and nuclei were digested for 20 min at 37°C. Cells were pelleted at 3700 rpm for 10 min at 4°C. Supernatant was passed four times through a 20 gauge needle and then four times through 25 gauge needle and spun twice at 1300 rcf at 4°C. This clarified MNase digested chromatin was used for immunoprecipitations.

Table 2.1: Yeast Strains Used in Chapter 2

Name	Genotype
JRY9316	*matΔ::HygMX lys2 his3-11 leu2-3,112 trp1-1 ura3-52 can1-100*
JRY9317	*matΔ::HygMX lys2 his3-11 leu2-3,112 trp1-1 ura3-52 can1-100 SIR4-13xMyc::KanMX*
JRY9318	*matΔ::HygMX lys2 his3-11 leu2-3,112 trp1-1 ura3-52 can1-100 SIR3-13xMyc::KanMX*
JRY9319	*matΔ::HygMX lys2 his3-11 leu2-3,112 trp1-1 ura3-52 can1-100 SIR2-13xMyc::KanMX*
JRY9498	*matΔ::HygMX lys2 his3-11 LEU2::sir2N345A trp1-1 ura3-52 can1-100 SIR3-13xMyc::KanMX sir2Δ::HISMX*
JRY9499	*matΔ::HygMX lys2 his3-11 LEU2::sir2N345A trp1-1 ura3-52 can1-100 SIR4-13xMyc::KanMX sir2Δ::HISMX*

Immunoprecipitations Chromatin was immunoprecipitated with the following antibodies as described in the supplementary materials and methods. For Sir ChIP-Seq samples, chromatin was immunoprecipitated with 120 µl of Anti-c-Myc Agarose (Sigma, Cat. 7470) overnight at 4°C. For both H4K16-acetyl IPs and H3 IPs, prior to immunoprecipitation, chromatin was precleared for 1 hr at 4°C with 40µl Protein A Sepharose bead slurry (17-5280-01, GE Healthcare). Pre-cleared chromatin was immunoprecipitated with the appropriate antibody, either 5 µl anti H3 (abcam, ab1791) or 15 µl anti H4K16-acetyl (Millipore, Cat. 07-595) overnight at 4°C. 120 ul of Protein A Sepharose bead slurry was then added, and samples incubated for at least 4 hours at 4°C. Washes, elutions, and isolation of DNA were performed as previously described (Aparicio et al. 2005). For MNase samples, after the reversal of crosslink with Proteinase K, 0.1 ug of RNase A was added to both inputs and IPs and samples were incubated at 37°C for 1-2 hours then DNA was isolated with Qiagen PCR clean up kit.

Library Preparation The first biological replicate of Sir sonication libraries, the second biological replicate of Sir3 and Sir4 libraries and the first replicate of the no-tag libraries were prepared with modifications to the Illumina paired-end library protocol as in (Zill et al. 2010). Libraries were loaded into one lane each and sequenced using the Illumina Genome Analyzer II as 45bp or 36bp paired-end reads. All MNase libraries, Sir3 and Sir4 libraries from the *sir2N345A* mutant, the Sir2 biological replicate and H4K16-acetyl library were constructed using the Illumina Tru-Seq library preparation kit with the following modifications: Upon end repair, samples were cleaned up using a Qiagen minelute column. Adapters were used at a 10-fold diluted concentration as to that provided. Samples were indexed and sequenced in four lanes on the Illumina HiSeq 2000 as 100 bp paired-end reads. All sequences have been deposited in the NCBI Short Read Archive under accession [**to be determined**].

Data Analysis Reads were mapped using BWA (Li and Durbin 2009) to a modified Sac Cer 2 genome in which the *MAT* locus was replaced with the Hyg-MX cassette. Duplicate reads were removed using Picard (http://picard.sourceforge.net) and per-base-read counts determined using Samtools (Li et al. 2009). The number of reads used per sample, after mapping and duplicate processing are documented in Table 2.2.

For the MNase samples, mapped reads were then trimmed to 40 bp and only reads with an insert length less than 250 bp were used to ensure mononucleosome resolution. The reads were further processed, including coverage calculations, signal smoothing and peak detection using nucleR (Flores and Orozco 2011). A threshold value of 50% was used for peak detection and peaks were filtered for those with a score greater than .4. All graphs were created using R (R Core team 2012). Median coverage was calculated for 100 bp windows, sliding along each chromosome in 50 bp steps. The genome-wide median was calculated by determining the median of the sliding windows for each data set (Table 2). The genome-wide correlations were determined by pairwise comparison of the same 100 bp sliding windows between the appropriate datasets and then determining the Pearson correlation in R (R Core Team 2012).

Table 2.2: Number of Reads Mapped for Each Experiment in Chapter 2

Experiment	Non-Duplicate Aligned Reads	Genome-Wide Median
Sir2-13xMyc Sonication IP Biological Replicate 1	15896635	39
Sir2-13xMyc Sonication input Biological Replicate 1	27831502	75
Sir3-13xMyc Sonication IP Biological Replicate 1	13638677	31
Sir3-13xMyc Sonication input Biological Replicate 1	16599252	42
Sir4-13xMyc Sonication IP Biological Replicate 1	8002066	25
Sir4-13xMyc Sonication input Biological Replicate 1	20552580	57
No-tag Sonication IP	24771036	60
No-tag Sonication input	51552632	153
Sir2-13xMyc Sonication IP Biological Replicate 2	5633361	28
Sir3-13xMyc Sonication IP Biological Replicate 2	20388061	33
Sir4-13xMyc Sonication IP Biological Replicate 2	14392654	21
Sir2-13xMyc MNase IP	15465564	94
Sir2-13xMyc MNase input	32617038	230
Sir3-13xMyc MNase IP	9793451	65
Sir3-13xMyc MNase input	14099839	84
Sir4-13xMyc MNase IP	17719118	112
Sir4-13xMyc MNase input	22055185	152
No-tag MNase IP	17582264	120
No-tag MNase input	35748898	258
H4K16-acetyl Sonication IP	28071876	222
H4K16-acetyl Sonication input	14677332	98
Sir3-13xMyc Sonication in *sir2N345A* IP	11896642	73
Sir3-13xMyc Sonication in *sir2N345A* input	22866844	163
Sir4-13xMyc Sonication in *sir2N345A* IP	23318195	155
Sir4-13xMyc Sonication in *sir2N345A* input	18734513	131
H3 Native MNase IP	8930151	58
H3 Native MNase input	32645311	234
H3 Cross-linked MNase IP	25238204	188
H3 Cross-linked MNase input	19095249	117
H3 Cross-linked Sonication IP	19881390	157
H3 Cross-linked Sonication input	20919986	152
H3 Cross-linked 1 hour MNase IP	26830653	198
H3 Cross-linked 1 hour MNase Input	9915194	60
H3 Cross-linked 1 hour Sonication IP	34197316	280
H3 Cross-linked 1 hour Sonication input	22451529	158
H3 Cross-linked in *sir2N345A* (JRY9498) IP	14684023	100
H3 Cross-linked in *sir2N345A* (JRY9498) input	17521211	124

2.4 Results

2.4.1 Sir Proteins Showed Heterogeneous Distribution at *HML* and *HMR*

To characterize the chromatin positions occupied by the Sir proteins more precisely than previously possible, we performed ChIP-seq of myc-tagged Sir2, Sir3 and Sir4. Chromatin that was not immunoprecipitated, the input chromatin, was also sequenced, providing a baseline reference for the immunoprecipitated (IP) sample. Based on previous ChIP-qPCR and ChIP-chip results, we expected a homogenous distribution of Sir proteins across *HML* and *HMR* (Hoppe et al. 2002; Rusché et al. 2002). However the picture at both loci was more complex than expected. As anticipated, Sir proteins were enriched at the *E* and the *I* silencers well above the genome-wide median (Figure 2.1). Enrichment at these positions presumably reflects Sir2, Sir3 and Sir4 association with Rap1, Abf1, ORC and Sir1. The most striking enrichment for all three Sir proteins was immediately internal to each of the silencers, corresponding to the well-positioned nucleosomes adjacent to the silencers at *HMR* and *HML* (Weiss and Simpson 1998; Ravindra et al. 1999). However, the pattern of Sir-protein enrichment appeared to be more heterogeneous than expected throughout the rest of the loci (Figure 2.1). The extent of Sir-protein enrichment at the promoter regions of *HML* and *HMR* and at the *a1* open reading frame was somewhat higher than the signal from the input chromatin, yet was much lower than the enrichment at the silencers and at positions immediately adjacent to the silencers. This striking quantitative difference was surprising given that the promoters of *HML* and *HMR* are the critical targets of silencing.

In addition to the peaks associated with the silencers and the adjacent nucleosomes, we observed a third large peak of Sir-protein enrichment at both *HML* and *HMR*. At *HML*, this third peak was in the middle of the locus, centered approximately over the Yα and Z1 border, corresponding to the HO endonuclease recognition sequence cleaved by HO to facilitate mating-type switching (Strathern et al. 1982). This peak of Sir-protein enrichment was consistent with genetic evidence of a protosilencer element that stabilizes Sir-protein association within *HML* independently of the *E* and *I* silencers, possibly involving interactions between Rap1 bound to the promoter and Sir proteins (Cheng and Gartenberg 2000). At *HMR*, the third peak of enrichment of Sir proteins was immediately to the right of the locus, and corresponded to the tRNA-Thr gene that serves as a boundary element for the silenced domain at *HMR* (Donze and Kamakaka 2001; Li et al. 2013). A slight increase in non-specific binding of the tRNA gene to the anti-myc beads was evident in the immunoprecipitated sample from cells lacking any myc-tagged proteins (top, right panel Figure 2.1). However, this enrichment was minor compared to the Sir protein enrichment, and is thoroughly documented and discussed in a report on non-specific ChIP-seq enrichment (Teytelman et al. 2013). The left side of *HMR* also exhibited a discrete boundary for enrichment of all three Sir proteins directly to the left of the ORC, Abf1 and Rap1 binding sites in the *E* silencer (Figure 2.1, right panels). This discrete decrease in Sir-protein enrichment was in contrast to reporter assays showing the silenced domain to extend about 500 bp to the left of *HMR-E* (Donze et al. 1999).

Consistent with genetic studies of *HML*, and unlike the discrete boundary for Sir protein enrichment at *HMR*, enrichment at *HML* was continuous for over 15 kb from the left telomere of chromosome III to *HML* (Figure 2.2). Curiously, the extent of enrichment oscillated with a period of approximately 1 kb. This extended domain of Sir-protein enrichment corresponded to the

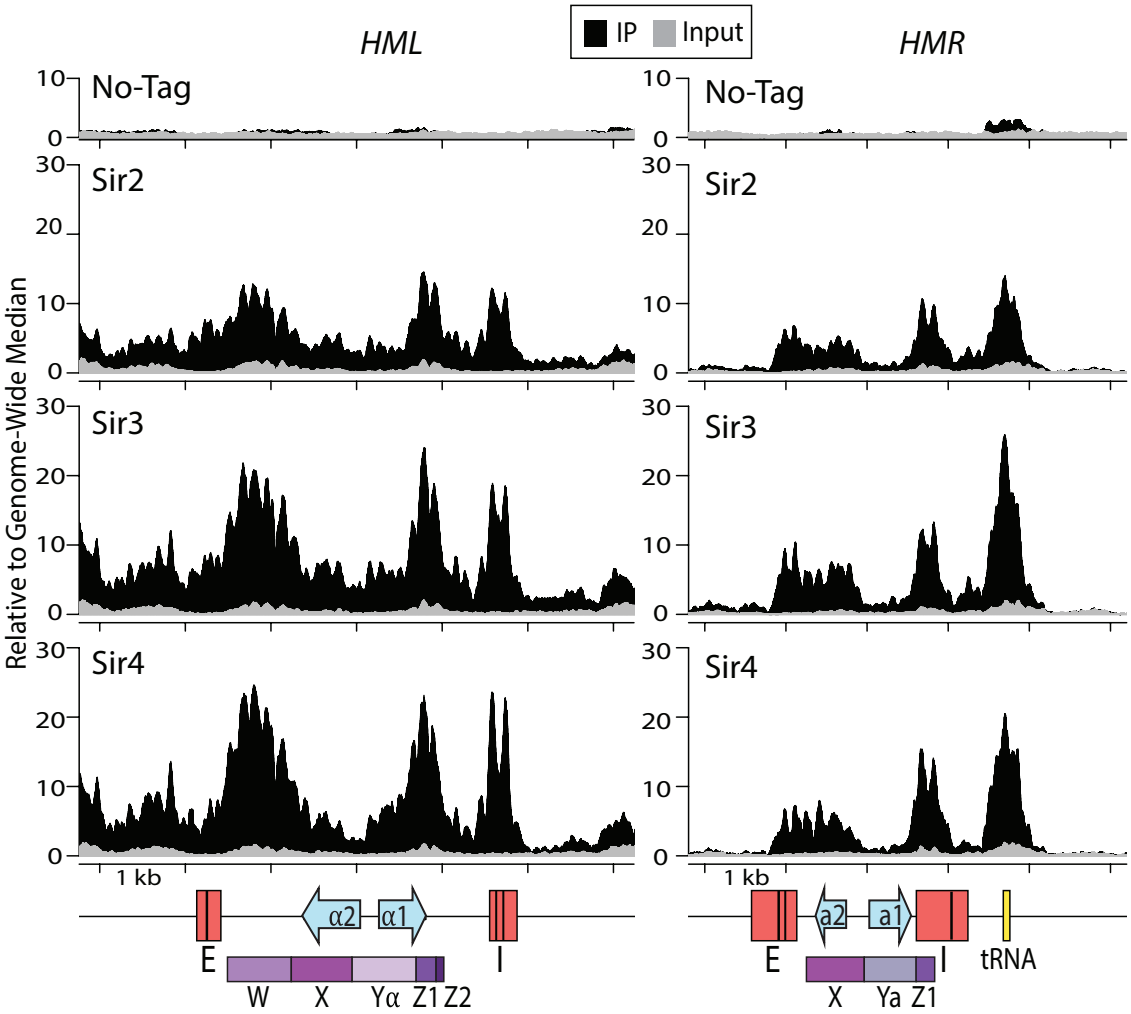

Figure 2.1 Sir protein ChIP-seq of sonicated chromatin showed heterogeneous distribution at *HML* and *HMR*. ChIP-seq of formaldehyde cross-linked chromatin sheared by sonication was performed on a no-tag control sample, and on strains with Sir2, Sir3 or Sir4 tagged with the 13x-myc epitope. The left panel shows 6 kb centered on *HML* (Chr III coordinates 10000-16000), the right panel shows 5 kb around *HMR* (Chr III coordinates 291793-296793). Tick marks denote 1 kb increments. Salient features are shown for each locus below: the red rectangles denote the silencers as defined in the *Saccharomyces* Genome Database, black bars within the red rectangles indicate the binding sites for ORC, Rap1 or Abf1; blue arrows denote the open reading frames, and the yellow box deotes the position of the tRNA-Thr. The purple boxes show the W, X, Y and Z regions (as defined in Nasmyth and Tatchell 1980). The distribution of sequence reads for the immunoprecipitate (IP) for each sample is shown in black and the sequence reads from the input chromatin for that sample in grey. The Y-axis units are sequencing reads normalized to the genome-wide median for that sample. To facilitate accurate and unambiguous mapping of the sequence reads to both *HML* and *HMR,* the *MAT* locus was deleted. Still, some reads could not be uniquely mapped because of the X region is identical between *HML* and *HMR*. However, there were reads within the X region whose paired-end read mapped uniquely to either *HML* or *HMR*, indicating that Sir proteins were at both X regions.

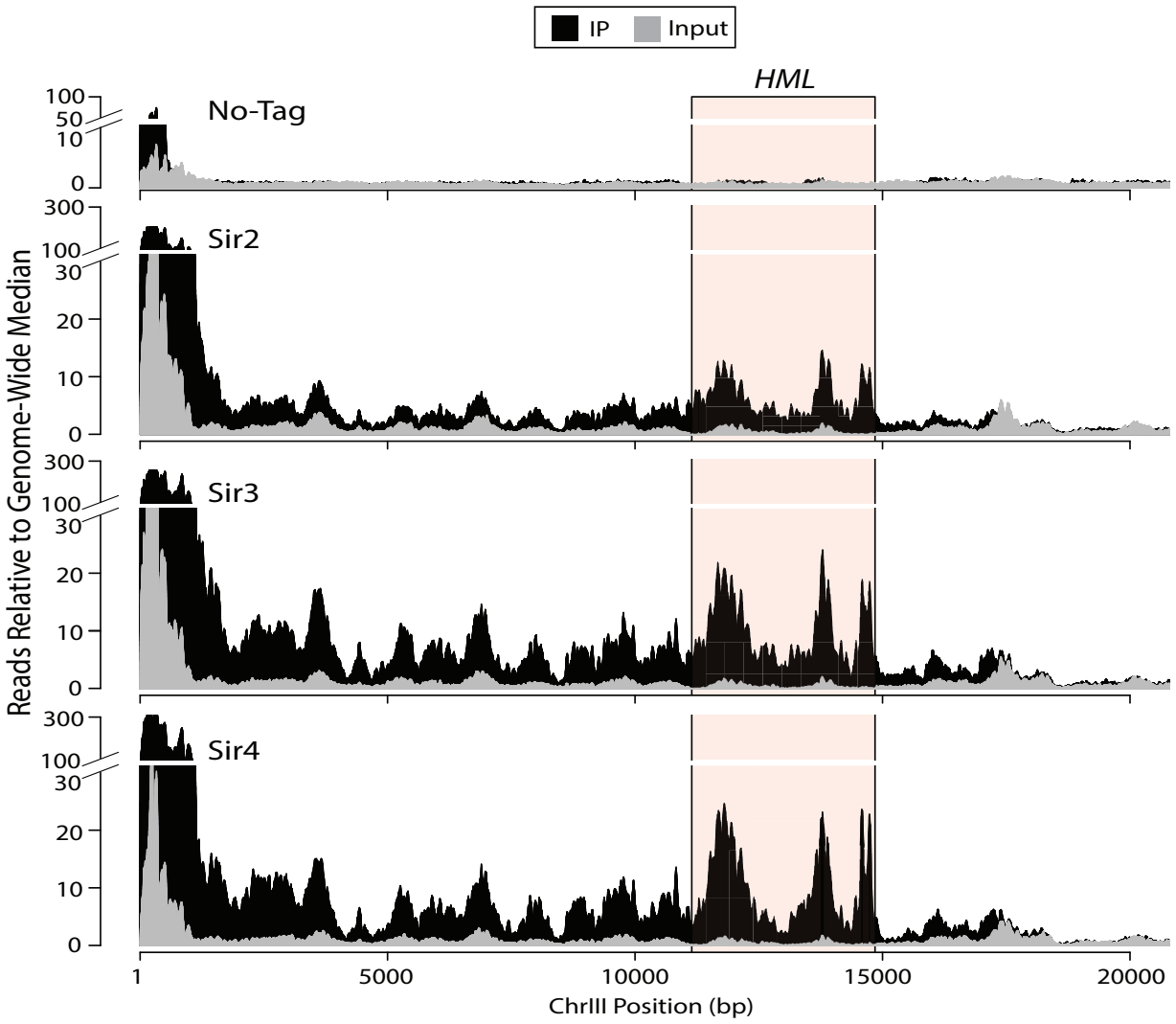

Figure 2.2 Sir-proteins showed continuous, though quantitatively variable enrichment from *HML* to the left telomere of Chromosome III. ChIP-seq was performed on a no-tag control sample, and on strains with Sir2, Sir3 or Sir4 tagged with the13x-myc epitope. *HML* from the *E* to the *I* silencer (chromosomal coordinates 11146-14849) is shown as a shaded pink box. The X-axis represents chromosomal position in 5 kb increments from the left telomere to 20 kb toward the centromere. The distribution of sequence reads for the immunoprecipitate (IP) for each sample is shown in black and the sequence reads from the input chromatin for that sample in grey.

extended domain of telomeric silencing between the telomere and *HML,* and was also consistent with lower-resolution ChIP-chip studies of Sir proteins (Hecht et al. 1996; Lieb et al. 2001). Additionally, to the right of *HML-I*, Sir-protein enrichment was evident for about 1 kb, though the level of enrichment was lower than within or to the left of *HML* (Figure 2.1). Further to the right, there was no detectable enrichment. Together, these data supported earlier suggestions of a lack of a clear boundary for silencing on the telomere proximal side of *HML* (Bi et al. 1999) and the lack of a distinct boundary element on the centromere proximal side of *HML* (Figure 2.1 and Figure 2.2) and established distinct structural differences between the silenced chromatin in and near *HML* from the more discrete domain at *HMR.*

The genome-wide reproducibility between the IP samples from a biological replicate of each of the Sir proteins showed high correlation between each biological replicates: .920, .989 and .964 for Sir2, Sir3 and Sir4, respectively. Additionally, the pattern from one Sir protein was nearly indistinguishable from that of the others, emphasizing the robustness of this surprisingly complex topography (Figure 2.1). Thus the features of chromatin responsible for this pattern were robust and highly reproducible.

Chromatin structures can impact the efficiency of fragmentation by sonication, especially of silenced chromatin as we discovered previously and as can been seen in the input chromatin distribution (Teytelman et al. 2009). To provide an independent assessment of this unexpected distribution of Sir proteins, and as a further control for fragmentation bias, we employed a different method of chromatin fragmentation to characterize the distribution of Sir proteins. Specifically, Sir-protein chromatin association was evaluated through ChIP-seq of Sir proteins with cross-linked chromatin that was digested to mononucleosomes with Micrococcal Nuclease (MNase), rather than sonicated, as above. Additionally, to ensure the extended crosslinking time often used to capture chromatin-associating proteins that do not directly bind DNA did not influence the topology observed, we used a more limited, 15-minute cross-linking time for the following MNase preparations.

At the level of mononucleosomes, Sir proteins appeared to be primarily associated with the nucleosomes adjacent to the silencers (Figure 2.3). The extent of enrichment of Sir proteins at the silencers in the MNase treated chromatin was somewhat lower than their enrichment as assayed with sonicated chromatin. At this higher-resolution, Sir3 and Sir4 at *HMR-E* showed more association with the silencer than did Sir2, likely reflecting the directness of the interaction between Sir3 and Rap1 (Chen et al. 2011), and between Sir4 and Sir1 and Rap1 (Triolo and Sternglanz 1996). At mononucleosome resolution, the peak of enrichment at *HML* internal to the silencers and adjacent nucleosomes was resolved into distinct features: a single peak and a double peak (Figure 2.3, left panels). The double peak over the Yα-Z1 border is consistent with the previously described tightly-packed nucleosome pair over the HO recognition site (Weiss and Simpson 1998). The single peak possibly reflected protein association with the internal protosilencer element that stabilizes Sir-protein associations within *HML* (Cheng and Gartenberg 2000).

The third peak at *HMR* at the tRNA gene resolved into three peaks of Sir protein association. Two peaks corresponded to nucleosomes on either side of the tRNA gene flanking a third distinct peak of enrichment directly over the tRNA gene, which is nucleosome free (Oki and Kamakaka 2005). There the Sir-proteins formed stable associations with non-nucleosomal factors that bound the tRNA gene, as discussed below. The paradoxical paucity of Sir enrichment over the promoters at both *HML* and *HMR* was even more evident than in the sonicated-chromatin data

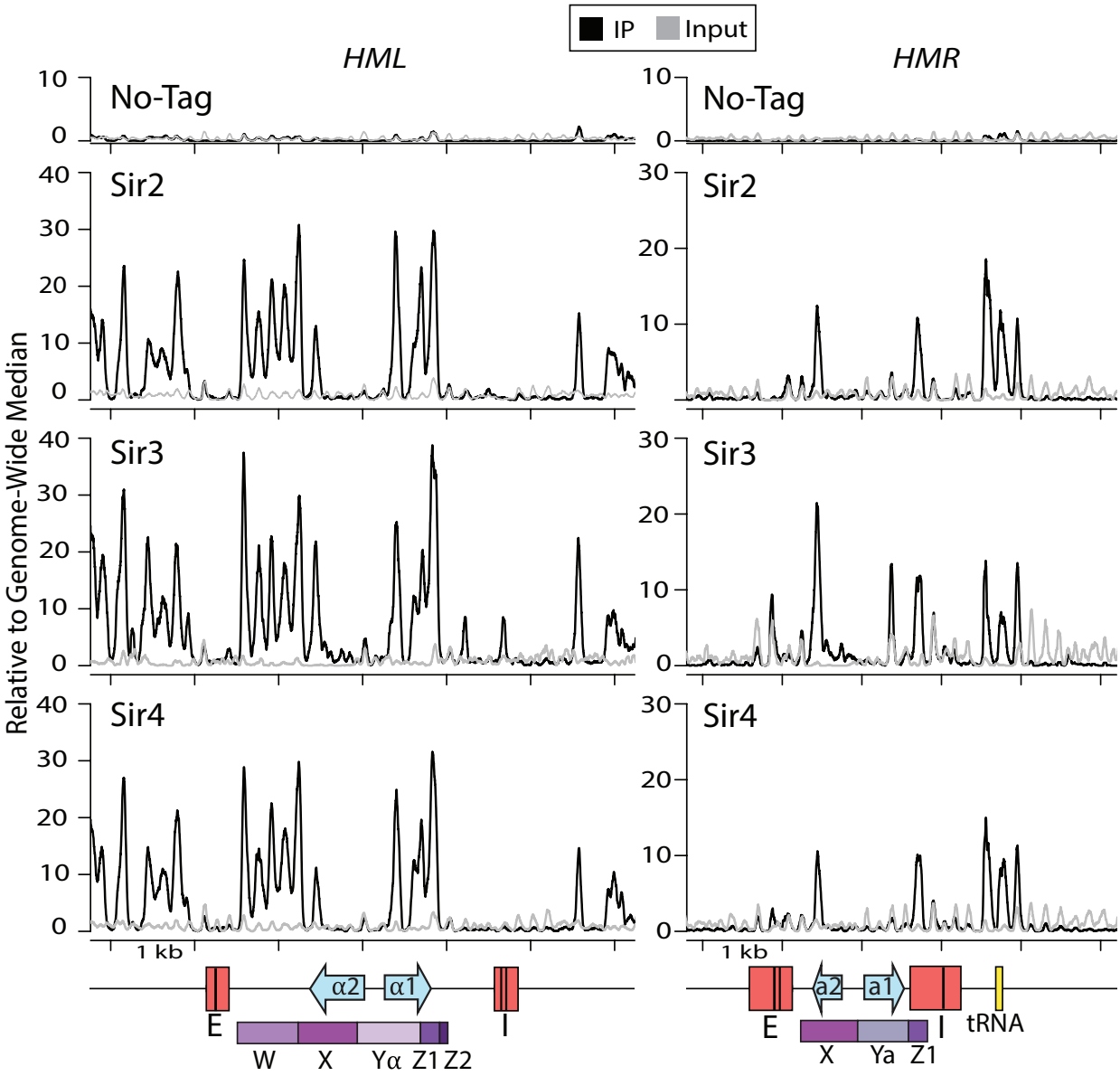

Figure 2.3 Sir protein ChIP-seq at *HML* and *HMR* on cross-linked chromatin digested with MNase. The left panel shows 6 kb centered on *HML* (Chr III coordinates 10000-16000), and the right panel shows 5 kb around *HMR* (Chr III coordinates 291793-296793). Tick marks denote 1 kb increments. Salient features are as in Figure 1. The distribution of sequence reads for the immunoprecipitate (IP) for each sample is shown as a black line and the sequence reads from the input chromatin for that sample as a grey line. To better define the peaks to nucleosome resolution, trimming of the reads was performed with nucleR (Flores and Orozco 2011).

(Figure 2.3). (The MNase ChIP no-tag sample also showed low non-specific binding to the myc beads, as did the sonication no-tag sample.) Thus two independent chromatin preparation methods clearly demonstrated that the unusual pattern of enrichment of Sir proteins in silenced chromatin was a fundamental property of silenced chromatin rather than an artifact of either method of analysis. Importantly, the greater resolution of the mononucleosome analysis highlighted what appeared to be positions at which the nucleosomes lacked Sir proteins. As discussed below, this appearance resulted from a property of a chromatin superstructure in the domain of silenced chromatin.

2.4.2 H4K16 was Hypoacetylated Across Silent Mating-Type Loci

Sir2, an NAD-dependent histone deacetylase, acts on lysines on the N-terminal tails of histones H3 and H4, creating high-affinity binding sites for Sir3 and Sir4 (Grunstein and Gasser 2013). This hypoacetylation, especially of H4K16-Acetyl, is a key feature of silenced chromatin in yeast (Johnson et al. 1990; Park and Szostak 1990). Thus we tested whether the distribution of hypoacetylated H4K16 was homogeneous across silenced loci, or exhibited the uneven distribution of the Sir2 deacetylase. ChIP-Seq analysis of the distribution of H4K16 acetylation revealed that H4K16 was uniformly hypoacetylated across *HML* and *HMR* (Figure 2.4). Additionally, H4K16 hypoacetylation was apparent for the entire left end of Chromosome III, from the telomere to *HML* (Figure 2.4a). Thus although Sir2 exhibited a complex pattern of enrichment at positions across *HML* and *HMR*, the consequence of its catalytic activity, H4K16 hypoacetylation, was more uniformly distributed across these loci than were the apparent distributions of the Sir proteins themselves (Figure 2.4b).

2.4.3 Sir Proteins Showed Discrete Enrichment at Natural Telomeres

Given the surprising discrepancy between the heterogeneous Sir protein distribution and the larger, more homogeneous H4K16 hypoacetylation, we determined if this difference applied to the other major class of Sir-silenced loci, the chromatin of telomeres. *S. cerevisiae* has telomeres of two structural classes: those containing just an X-element (X), and those with both an X-element and Y'-element (X-Y'). The X-element contains the Core X, where ORC and Abf1 bind, as well as the subtelomeric repeat sequence. Y' elements contain an ORF that encodes a protein with sequence homology to helicases. At telomeres that contain only an X-element, the X-element is adjacent to the telomerase-generated telomeric repeats, where Rap1 binds. At telomeres that contain both a Y'-element and X-element, the X-element is immediately centromere-proximal to the Y'-element, which is adjacent to the telomeric repeats (Louis 1995) (Figure 2.5). We examined enrichment of all three Sir proteins at an X-element telomere (*TELXVL*) and a X-Y' telomere (*TELVIIIR*). Sir protein enrichment was in discrete peaks, similar to the large peaks at the silencers at *HML* and *HMR*, rather than a continuous gradient of Sir-protein association expected from the studies of telomere position effects with the synthetic telomeres (Gottschling et al. 1990). At the X-element telomere, enrichment of all three Sir proteins overlapped and was coincident with both the Rap1 binding-site array in the telomeric repeats and the ORC and Abf1 binding sites within the Core X (Figure 2.5a). These binding patterns were consistent with the reported silencing capacity of natural telomeres, which is primarily evident immediately adjacent to the X-element (Pryde and Louis 1999). Similar

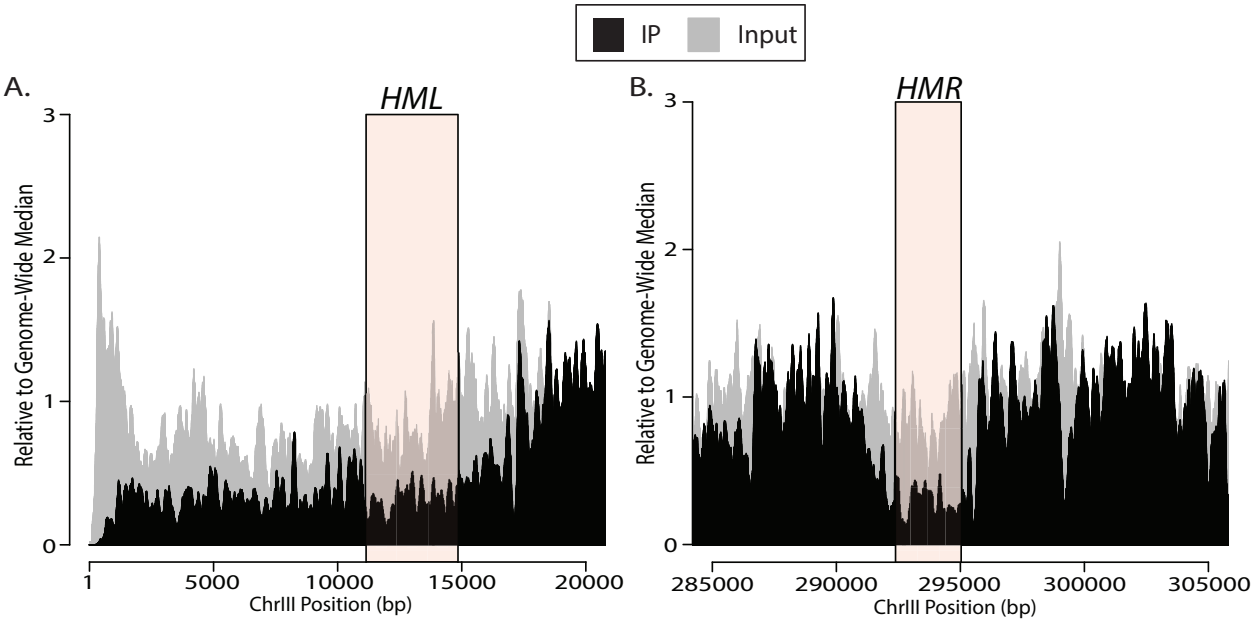

Figure 2.4 H4K16 was hypoacetylated throughout *HML* and at *HMR*. ChIP-seq of sonicated sheared chromatin against H4K16-acetyl from the left telomere of Chromosome III through *HML* (a) and 20 kb centered around *HMR* (b). In (a) *HML* from the *E* to the *I* silencer (chromosomal coordinates 11146-14849) is shown as a shaded pink box and (b) shows *HMR* from the *E* to the *I* silencers (chromosomal coordinates 292388 to 295034) is shown as a shaded pink box. The X-axis represents chromosomal position in 5 kb increments. The distribution of sequence reads for the immunoprecipitate (IP) for each sample is shown in black and the sequence reads from the input chromatin for that sample in grey.

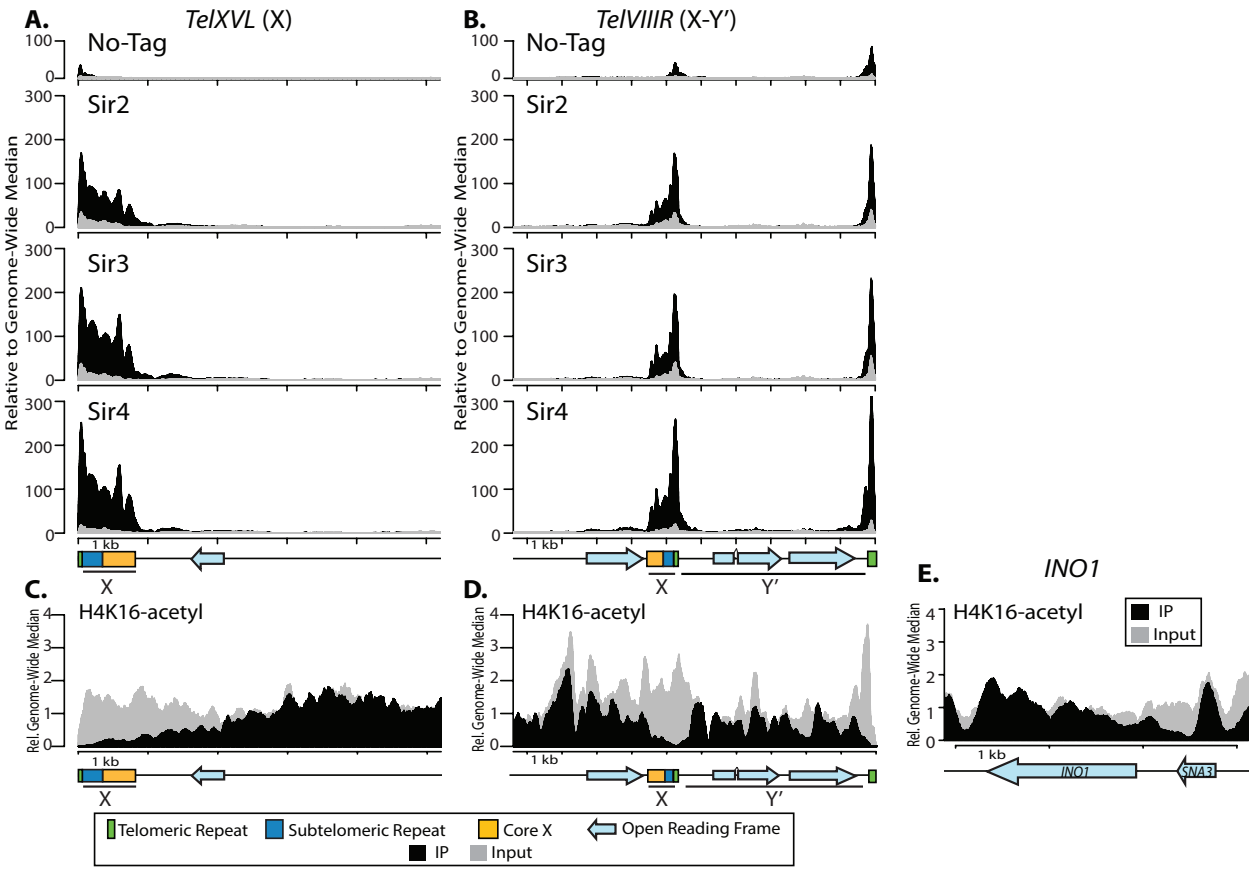

Figure 2.5 Sir protein enrichment at telomeres was discrete. (a) Enrichment for each of the Sir proteins in sonicated ChIP-seq samples at an X-Element telomere (5 kb *TELXVL*) and (b) a X- Y' telomere (10 kb of *TELVIIIR*). (c) and (d) show ChIP-seq of cross-linked and sonicated chromatin of H4K16-acetyl for *TELXVL* and *TELVIIIR,* respectively. Salient features are shown below the X-axis with telomeric repeats in green, subtelomeric repeats in dark blue and the Core X in orange, open reading frames are blue arrows and the X and Y' elements underlined. (e) H4K16-acetyl ChIP-seq data for *INO1*, where the 3' end of the ORF has previously been shown to be acetylated (Suka et al. 2002) X-axis tick marks represent 1 kb on all graphs. Black is the IP samples and gray is the input samples. Y-axis is reported at reads relative to the genome-wide median.

Sir-protein distributions were also seen at the Y' telomere where enrichment was concentrated at two discrete regions: at the sites of the telomeric repeats and at the X-element. No Sir protein enrichment was observed within the Y' region (Figure 2.5a). These enrichment patterns were consistent with the *URA3* reporter gene not being silenced when inserted within the Y'-element (Pryde and Louis 1999) and with previous studies that found little Sir-protein enrichment within the Y'-element (Zhu and Gustafsson 2009; Zill et al. 2010).

Next, we compared the distribution of H4K16-acetyl, a mark imparted by the histone acetyltransferase Sas2, to the restricted Sir-protein enrichment at the natural telomeres (Kimura et al. 2002; Suka et al. 2002). Interestingly, similar to the theme at the silenced mating-type loci, the region of H4K16 hypoacetylation was much larger than the region of Sir-protein enrichment (Figure 2.5c-d). At the X-element telomere H4K16 was hypoacetylated for about 3 kb inward from the end of the chromosome, but Sir-protein enrichment was limited to 1 kb from the end (Figure 2.5b). This extended domain of H4K16 hypoacetylation was even more apparent at X-Y' telomeres with hypoacetylation extending thoughout the Y'-element, although without Sir-protein enrichment in this region (Figure 2.5d). The nucleosome distribution at telomeres is needed to interpret the H4K16-acetyl signal. For example, telomeric repeats and the Core X showed extremely low coverage in the H4K16-acetyl IP not because the nucleosomes there were hypoacetylated, but rather because these areas are nucleosome free (Loney et al. 2009; Zhu and Gustafsson 2009). However, the amount of H4K16-acetyl IP signal across the Y'-element was still below the genome-wide average for this sample, and less than the input signal for this region, indicating that it was hypoacetylated. Additionally, a well-studied region previously reported to be acetylated at H4K16, the 3' end of the *INO1* gene (Suka et al. 2002), showed clear H4K16-acetyl enrichment in the immunoprecipitated chromatin (Figure 2.5e), as expected. The region of H4K16 hypoacetylation was much larger than the region of Sir-protein enrichment. Therefore, models invoking an antagonism of Sir2 function, such as a positioned H4K16 acetylase near telomeres could not account for the discrete enrichment of Sir proteins at telomeres.

2.4.4 Restricted Sir3 and Sir4 Enrichment in Cells Lacking Sir2 Catalytic Activity

In all previous models of Sir-based silencing, sequential deacetylation of histone tails was envisioned to create new binding sites for additional Sir-protein complexes (Grunstein and Gasser 2013). Such models predict that in the absence of Sir2's catalytic activity, the distribution of Sir proteins should be restricted to the sites of initial recruitment. Previous lower resolution studies established that in the *sir2N345A* mutant Sir proteins nucleate at the silencers, but do not spread within the locus (Rusché et al. 2002). To distinguish recruitment sites from sites of secondary occupation, we performed ChIP-Seq on myc-tagged Sir3 and Sir4 in a *sir2N345A* mutant, which has an amino-acid substitution in the active site of Sir2 rendering it catalytically inactive, but structurally intact (Imai et al. 2000).

Enrichment of both Sir3 and Sir4 at *HML* and *HMR* in cells lacking Sir2 catalytic activity was overall reduced. However enrichment was evident at three of the four silencers confirming that these three silencers could be considered nucleation sites for the silenced domain (Figure 2.6). Sir3 and Sir4 enrichment were almost completely absent from *HMR-I* in the absence of Sir2 function. The absence of a signal at *HMR-I* was consistent with genetic observations that *HMR-I* is neither necessary nor sufficient for silencing (Rivier et al. 1999) presumably, as shown here, because *HMR-I*

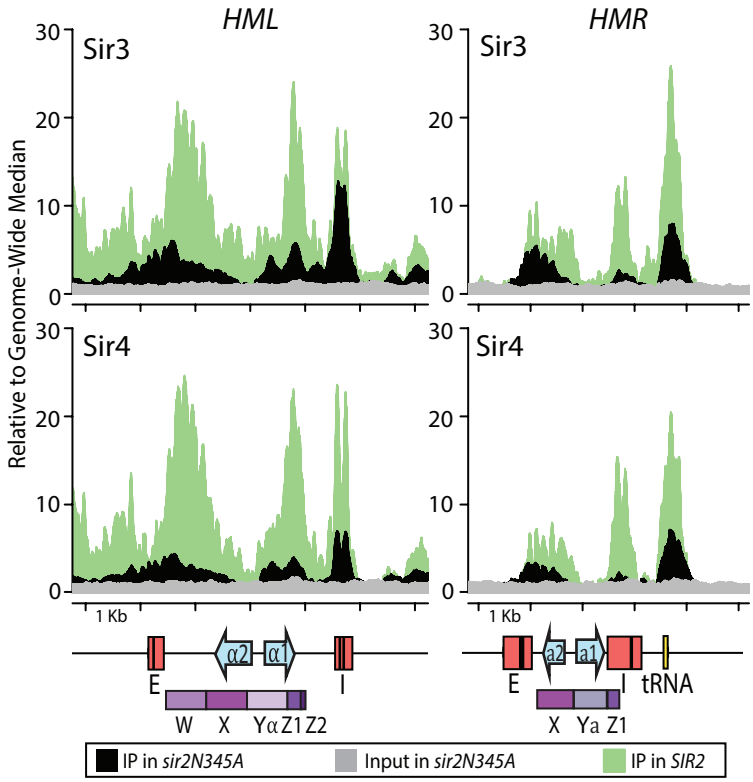

Figure 2.6 Sir3 and Sir4 enrichment in a strain lacking Sir2 catalytic activity revealed nucleation sites. 13x myc-tagged Sir3 (top) and Sir4 (bottom) enrichment in a *sir2N345A* mutant shown at *HML* (left) and *HMR* (right). Salient features in the genome are shown below the X-axis, as above. Values are reported as sequence reads relative to the genome-wide median for the IP (black) and the input (grey). For a reference, the green track shows the distribution of the Sir3 or Sir4 immunoprecipitate (IP) in chromatin from cells with wild-type Sir2, as in Figure 2.1.

is unable to nucleate Sir proteins. The widespread reduction in Sir3 and Sir4 enrichment at internal positions, and apparent absence from others, implied that Sir2's catalytic activity was necessary either for interactions between Sir3 and Sir4 with nucleosomes at some positions within these loci, or for stabilizing these interactions. Interestingly, Sir2's catalytic activity was not necessary for establishing the Sir3 and Sir4 association at the internal region near the HO recognition sequence and protosilencer at *HML,* or at the tRNA gene flanking *HMR* (Figure 2.6). There was also clear evidence, albeit at slightly lower levels in the *sir2N345A* mutant, for some Sir3 and Sir4 occupancy of nucleosomes internal to the silencers at *HML* and *HMR*. These data suggested that deacetylated H4K16 was not an absolute requirement for Sir-protein enrichment on nucleosomes at these positions.

2.4.5 Formaldehyde Crosslinking Captured a Unique Feature of Silenced Chromatin Architecture

Because Sir proteins associate with nucleosomes, it was possible that their binding to nucleosomes disturbed the underlying nucleosome architecture, explaining the heterogeneous distribution of Sir proteins. However, nucleosome position has been interrogated extensively in yeast both globally and specifically at the silent mating-type loci, with no indication of unusual distributions (Weiss and Simpson 1998; Ravindra et al. 1999; Henikoff et al. 2011). To assess independently whether the previously reported distribution of nucleosomes applied to our strains, we used the standard anti-H3 antibody to map nucleosomes on native chromatin digested with MNase by ChIP-seq, as others have done. The critical difference between this analysis and the analysis of Sir-protein ChIP-seq above was that no formaldehyde was needed due to the tight associations of nucleosomes and DNA. We found a regular distribution of nucleosomes very similar to those previously published for both silenced loci (Figure 2.7a). Thus the heterogeneous distribution of the Sir proteins could not be explained by a peculiar distribution of nucleosomes in our strains.

One clear, possible explanation for the discrepancy between the nucleosome positioning data and Sir-protein enrichment data could be that the use of formaldehyde cross-linking allowed the Sir-protein ChIP-seq procedure to capture a unique chromatin architecture that was not preserved on non-cross-linked, native chromatin preparations. To investigate this possibility, we performed ChIP-seq against H3 of cross-linked chromatin fragmented by sonication or by MNase digestion. This approach allowed us to interrogate the potential contribution of formaldehyde crosslinking to nucleosome position independently of the fragmentation method. There were two possible distributions of H3 from such an experiment that would be illuminating: 1) if the cross-linked H3 distribution indicated regularly spaced nucleosomes as in their native distribution, then the Sir-proteins must occupy only some of the nucleosomes in the silenced domain; or 2) if the cross-linked H3 distribution were heterogeneous, similar to the heterogeneous Sir-protein distribution, then crosslinking would cause the specific under-recovery of certain nucleosome and the proteins bound to them. Unlike the distribution of H3 in native chromatin, the distribution of H3 in cross-linked chromatin, either sheared by sonication or cleaved by MNase, was heterogeneous, qualitatively similar to each other, and similar to the Sir-protein distribution (Figure 2.7b-c). Most notably, at both *HML* and *HMR* there were fewer nucleosomes captured in the H3 IP at the promoter region and across *α1* and *a1,* respectively, in cross-linked chromatin than in the native chromatin

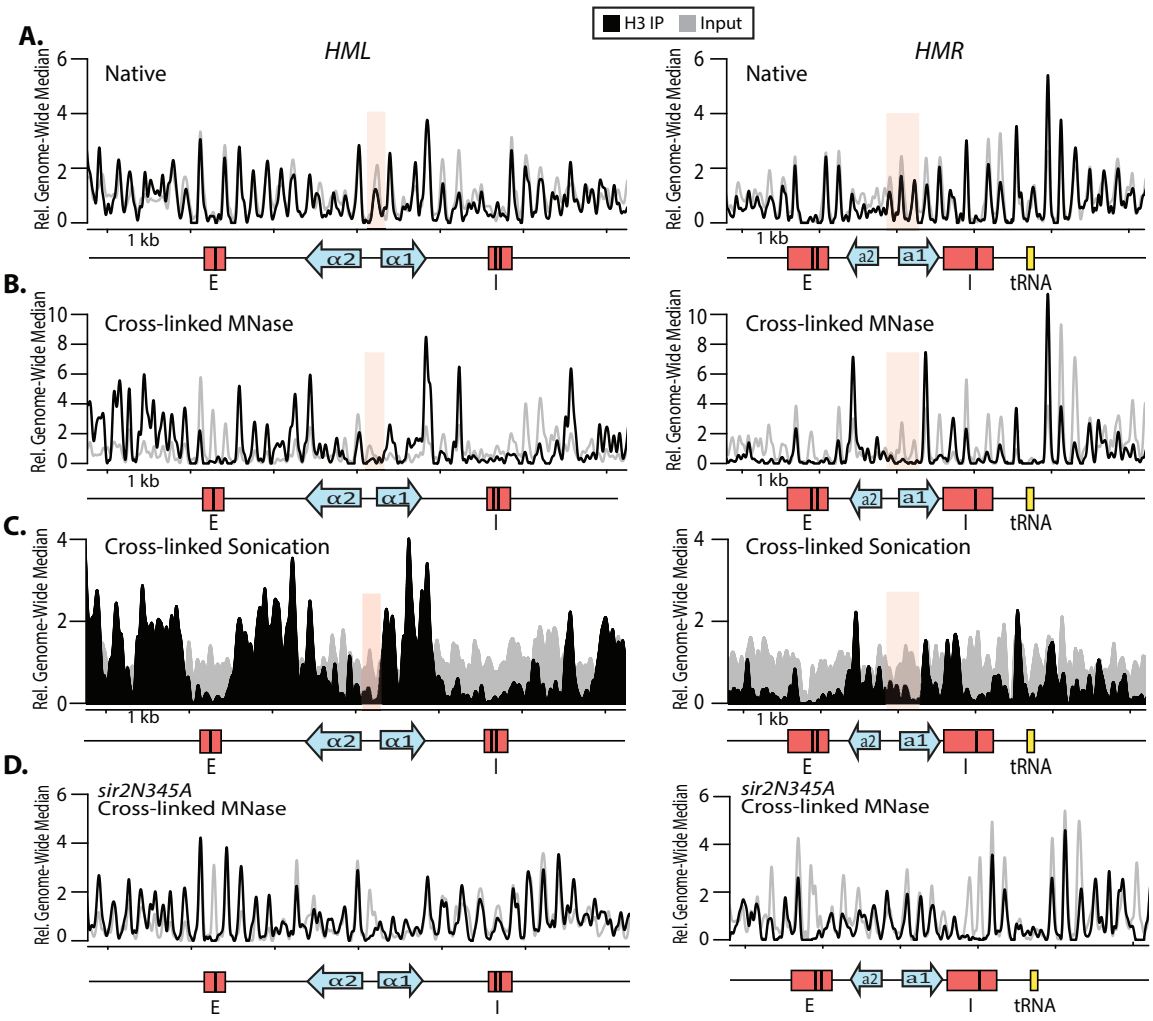

Figure 2.7 H3 was differentially recovered in immunoprecipitates from native versus cross-linked chromatin. (a) H3 ChIP-seq of native chromatin treated with MNase, (b) H3 ChIP-seq from chromatin cross-linked for 15 minutes at room temperature and treated with MNase, (c) H3 ChIP-Seq of sonicated chromatin and cross-linked for 15 minutes at room temperature. The pink shaded region in each graph highlights an area where nucleosomes are detected in the H3 IP in the native preparation (a), but not in either of the cross-linked chromatin preparations (b and c). (d) H3 ChIP-seq in cells expressing only the catalytically inactive version of Sir2 (*sir2N345A*) (JRY9498). Chromatin was cross-linked for 15 minutes and treated with MNase. The black track shows the reads for the H3 immunoprecipitate (IP) and input is shown in grey. Nucleosomes appeared less well positioned in the X region because reads could not be uniquely mapped between *HML* and *HMR*. Tick marks denote 1 kb intervals and salient features shown below the X-axis as above. All reads have been trimmed and mapped with NucleR to facilitate nucleosome mapping (Flores and Orozco 2011).

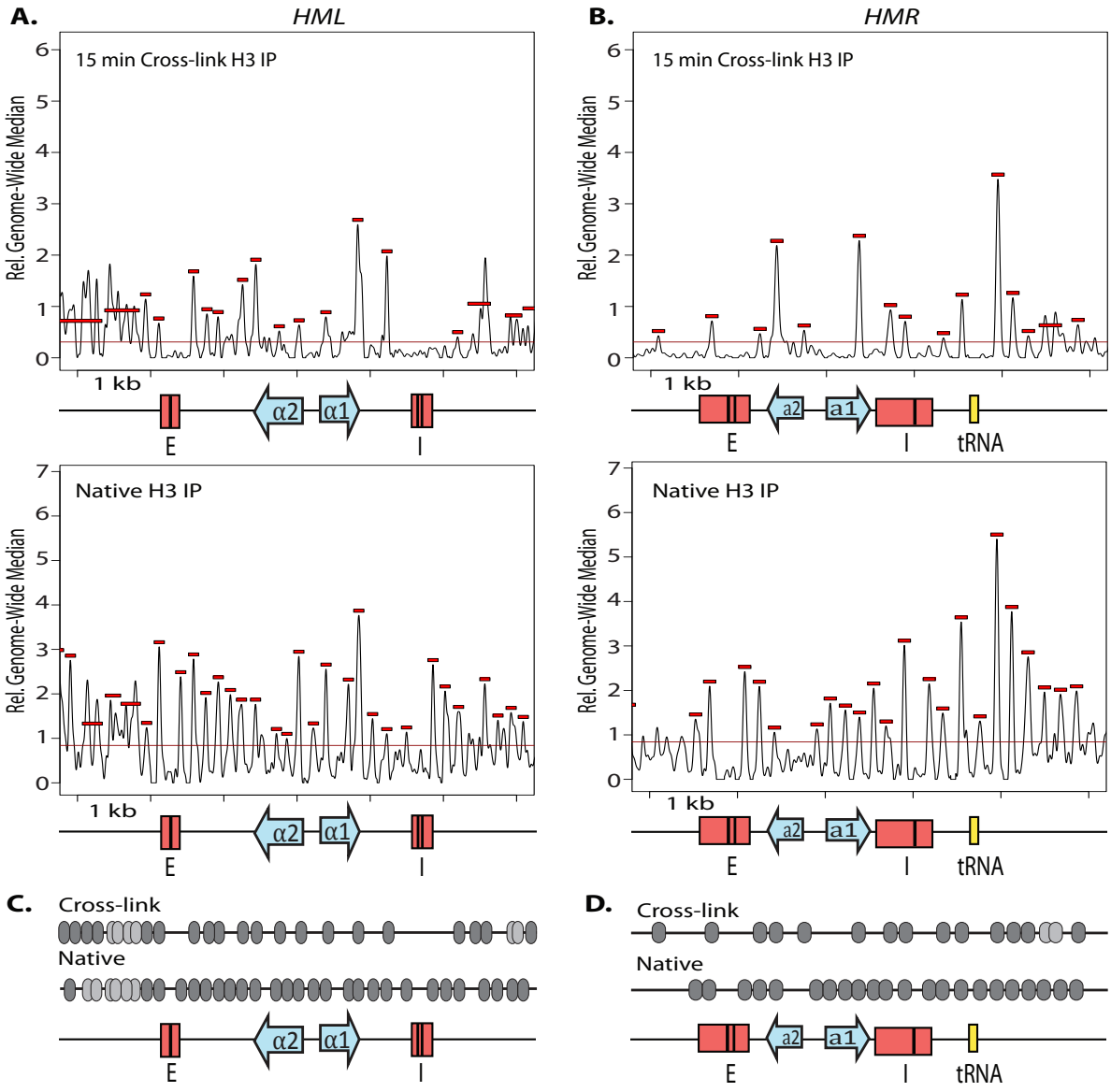

Figure 2.8 Nucleosome occupancy between crosslinked and native chromatin preparations varies dramatically at silenced regions. Nucleosome occupancy was determined using nucleR (Flores and Orozco 2011) with the threshold value shown as a horizontal red line and nucleosome calls as red rectangles above peaks at *HML* (a) and *HMR* (b) on cross-linked (above) and native (below) H3 IP samples of MNase digested chromatin. A schematic of nucleosome occupancy at each condition from those nucleosome calls is shown for *HML* (c) and *HMR* (d) Dark grey nucleosome represent well positioned nucleosomes and light grey represent overlapping, less well-positioned nucleosome calls.

(highlighted by pink shading in Figure 2.7), which was especially evident when nucleosome occupancy was determined by peak calling (Figure 2.8). This paucity in nucleosome enrichment in the cross-linked chromatin coincided precisely with the positions of the lowest Sir-protein enrichment. The lack of H3 at positions within *HML* and *HMR* in the cross-linked chromatin could not be explained by under-recovery of this chromatin per se, because these regions were well represented in the data from the input chromatin (Figure 2.7, gray lines). The input chromatin trace represented data from a MNase-seq experiment, which allowed the determination of nucleosome position by patterns of sequences protected from MNase, further emphasizing the presence of nucleosomes in this region. Rather, the "missing nucleosomes" resulted from under-recovery due to position-dependent epitope masking of certain positions specifically in the immunoprecipitated chromatin from cross-linked samples. H3 enrichment was also evaluated using the 1-hour cross-linking time originally used for Sir protein preparations (Figure 2.9). These samples showed a similar distribution to the 15 minutes. crosslinking preparations, indicating that varying crosslinking time did not change the H3 ChIP profile. As discussed below, it was the inability to detect both H3, which was present in the native H3 distribution, and Sir proteins at key positions in cross-linked chromatin that provided strong evidence that both were there, but in an inaccessible chromatin superstructure that resulted in epitope masking of both H3 and Sir proteins within the core, promoter region of the silenced loci, but not in flanking regions.

To test whether the inability of the antibody to recover H3 across the promoter region in cross-linked treated chromatin was specific to silenced cells, we performed MNase-Seq followed by an H3 IP of cross-linked chromatin in cells expressing only the catalytically inactive version of Sir2 (*sir2N345A*). As with the native chromatin, in this strain all nucleosomes were recovered in the IP, indicating that silencing was necessary for the inaccessible chromatin structure resulting in position-dependent epitope masking of H3 (Figure 2.7D).

2.4.6 The Chromatin Superstructure Appeared Specific to Silenced but not Repressed Genes

We tested whether the chromatin structure implied by the difference in the H3 distribution in cross-linked versus native H3 mapping was a general property of the chromatin at repressed genes, or was potentially particular to silenced chromatin. To answer this question we compared nucleosome positions in native and cross-linked chromatin digested with MNase at the repressed *GAL1-GAL10* gene pair (Figure 2.10a) and at the α-specific gene *STE3* (Figure 2.10b), which are repressed in these strains. Unlike at *HML* and *HMR*, the nucleosomes mapped on native chromatin occupied essentially identical positions to those mapped on cross-linked chromatin (Figure 2.10 and Figure 2.11). Thus, in contrast to the transcriptionally repressed locations tested, the silenced chromatin exhibited a unique architecture, captured by formaldehyde cross-linking, and recognized by its under-recovery in the immunoprecipitation of specific and highly reproducible positions - within the silenced domain.

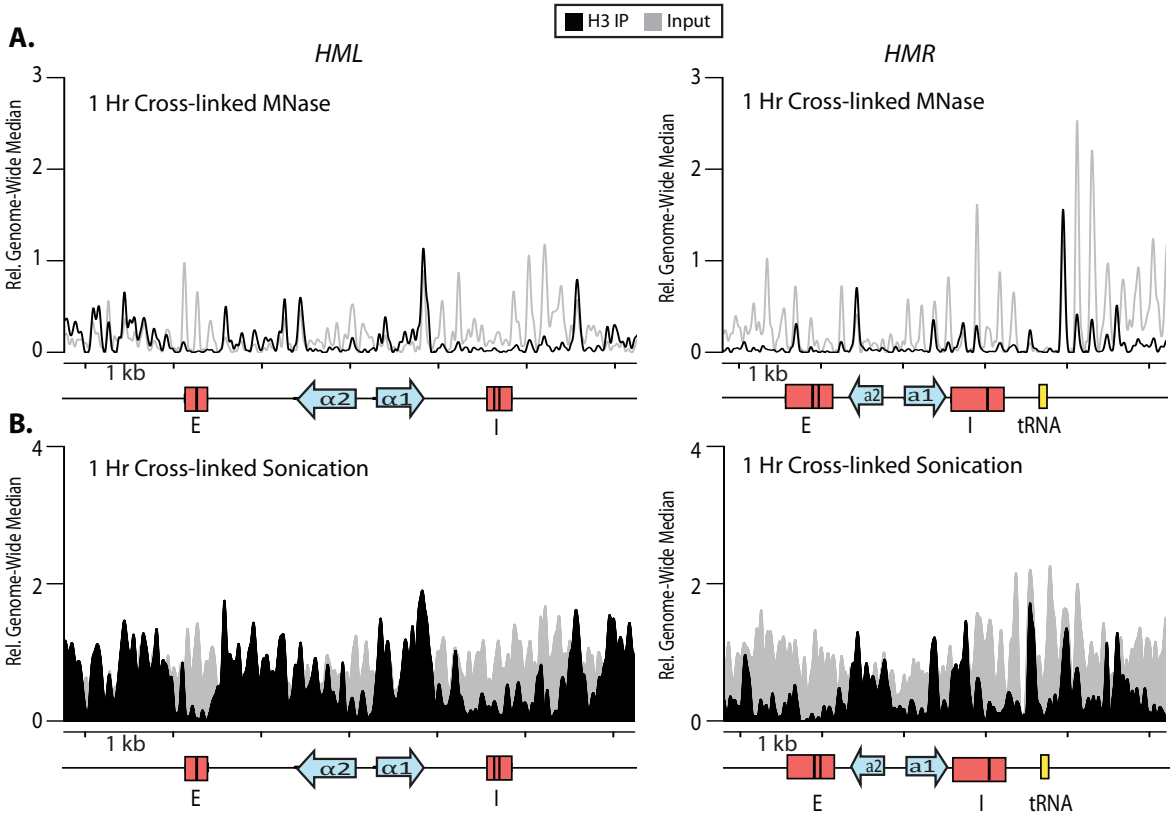

Figure 2.9 Increased cross-linking time shows similar H3 ChIP distribution. H3 ChIP-seq was performed on MNase treated chromatin (a) and sonicated chromatin (b) after 1 hour crosslinking. The black track shows the reads for the H3 immunoprecipitate (IP) and input is shown in grey. Tick marks denote 1 kb intervals and salient features shown below the X-axis as above. All reads have been trimmed and mapped with NucleR to facilitate nucleosome mapping (Flores and Orozco 2011).

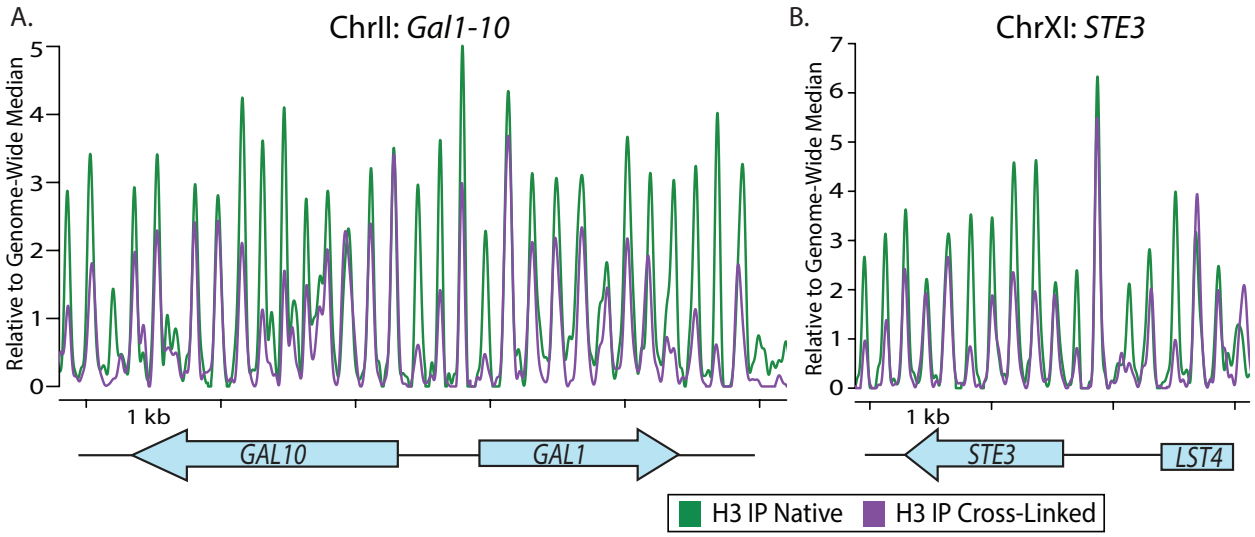

Figure 2.10 H3 can be recovered in cross-linked samples at loci of site-specific transcriptional repression. Comparison of ChIP-seq of MNase treated H3 immunoprecipitate (IP) from native chromatin (green) and chromatin cross-linked for 15 minutes (purple) at the *GAL1-10* gene pair (a) and *STE3* (b). Tick marks denote 1 kb intervals, and ORFs are shown below the X-axis. Reads were trimmed with NucleR to facilitate nucleosome mapping (Flores and Orozco 2011).

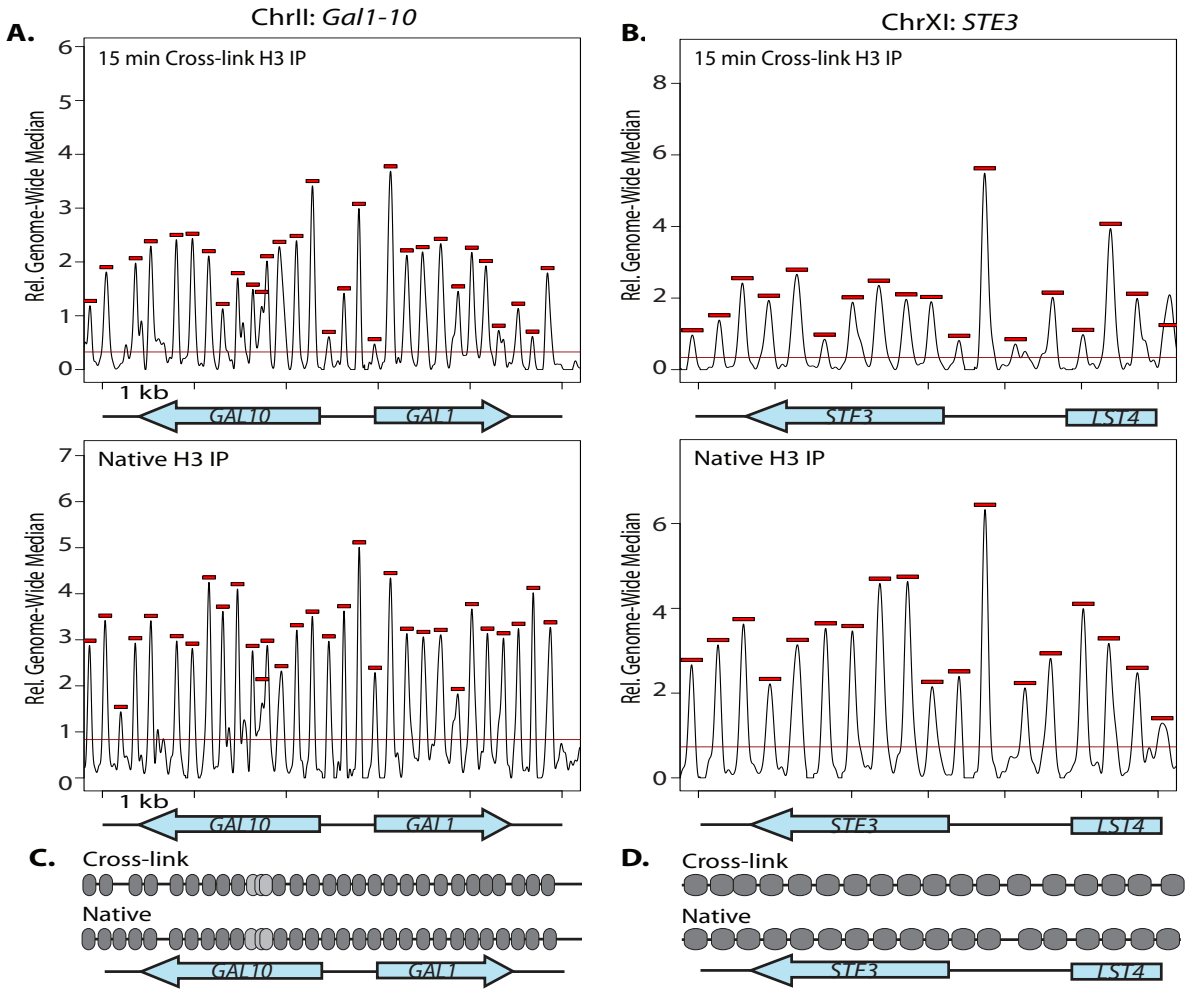

Figure 2.11 Nucleosome occupancy was very similar between native and cross-linked samples at loci of site-speci_c repression. Nucleosome occupancy was determined using nucleR (Flores and Orozco 2011) with the threshold value shown as a horizontal red line and nucleosome calls as red rectangles above peaks at GAL1-10 (a) and STE3 (b) on cross-linked (above) and native (below) H3 IP samples of MNase digested chromatin. A schematic of nucleosome occupancy at each condition from those nucleosome calls is shown for GAL1-10 (c) and STE3 (d) Dark grey nucleosome represent well positioned nucleosomes and light grey represent overlapping, less well-positioned nucleosome calls.

2.5 Discussion

We characterized at higher resolution than previously possible, the structure of the silenced chromatin of *Saccharomyces* formed by the association of Sir2, Sir3 and Sir4 at the two canonical silenced regions of the yeast genome: the silent mating-type loci, which harbor the unexpressed copies of mating-type regulatory genes, and representatives of the two classes of telomeres. This characterization revealed a much more complex topology of Sir-protein distribution at *HML* and *HMR* than anticipated, provided a high-resolution test of the nucleation and spreading model for the formation of silenced chromatin, and uncovered several unanticipated dimensions that informed the mechanism of Sir protein silencing.

2.5.1 Crosslinking Captured a Higher-order Chromatin Super Structure

The surprising patterns of Sir-protein enrichment described here, and for Sir2 in Li et al. (Li et al. 2013), along with evidence that sonication is influenced by specific chromatin structures, motivated a thorough investigation of the structure of the underlying chromatin of silenced regions (Teytelman et al. 2009). Through interrogation of the chromatin by two different fragmentation methods, MNase and sonication, and two different chromatin preparations, not cross-linked (native) or cross-linked by formaldehyde, we found that in the cross-linked samples the nucleosome distribution was similar to the pattern of Sir-protein enrichment, with some positions appearing devoid of nucleosomes as assayed by recognition by the H3 antibody even though these same positions were fully occupied by nucleosomes in the native chromatin.

We considered multiple explanations for how the distribution of nucleosomes, and presumably the distribution of Sir-proteins, could be so dramatically influenced by crosslinking. Under-recovery of certain regions of the genome in the chromatin preparation from cross-linked samples could not explain the paucity of Sir proteins or nucleosomes at particular positions because there was abundant signal at those positions in the input samples (Figure 2.7, gray lines). Similarly, the cross-linking procedure per se did not harm the H3 epitope recognized by the antibody as shown by the robust mapping of nucleosomes in cross-linked chromatin over the rest of the genome. Thus at *HML* and *HMR*, cross-linking appeared to capture a chromatin superstructure resulting in position-dependent masking of the H3 and anti-myc epitopes, leading to the appearance of an uneven distributions of nucleosomes, which the native samples and non-silenced chromatin showed were evenly distributed.

The H3 antibody used in these and most nucleosome mapping studies recognizes the last 20 residues of the C-terminus of H3 (ab1791). Thus the cross-linking may capture a local chromatin architecture in which the nucleosomes at the promoter region of *HMR* and *HML,* for example, are positioned such that crosslinking occludes the antibody recognition site for H3. Because the regions of under recovery of the H3 IP correlated with the regions of low Sir-protein occupancy shown above, the chromatin architecture captured by the cross-linking likely contributed to the heterogeneous distribution of Sir proteins observed at the same positions, indicating that a chromatin-superstructure resulted in masking of both the H3 and anti-myc epitopes at the promoter region of silenced chromatin. It was not possible to test this inference directly because the association of Sir proteins with nucleosomes was insufficiently tight to allow ChIP-Seq analysis in the absence of cross-linking (unpublished observations). However, we hypothesize that Sir proteins

are associated throughout the locus, but like the H3 distribution, are under-recovered in the IP when cross-linked.

Previous studies have also implicated a higher-order structure for silenced chromatin, though none have addressed the structure with this resolution (Sperling and Grunstein 2009; Yu et al. 2011). Chromatin-confirmation-capture studies, which exploit formaldehyde cross-linking to capture long-range interactions between sequences suggest that the *E* and the *I* silencers of *HMR* physically interact to form a looped structure in a Sir-dependent manner (Dekker et al. 2002; Valenzuela et al. 2008). Our data implied that the loop's structure was sufficiently complex to facilitate cross-links that cause differential recovery of relatively precise regions in immunoprecipitations, perhaps burying the promoter region and associated Sir proteins in the silenced superstructure. One possible model consistent with the data presented and also compatible with current views of the possible higher-order chromatin structures would be an additional, internal looping or coiling beyond the loop detected by 3C between the two silencers (Figure 2.12). This structure would allow nucleosomes and associated Sir proteins immediately adjacent to the silencers to be accessible to antibody recognition by being on the outer part of the loop, and the promoter region buried within the silenced structure would have less accessibility to antibodies upon crosslinking, resulting in epitope masking of the proteins buried within the structure.

2.5.2 The Contribution of the Chromatin Superstructure to Silencing

This architecture of silenced chromatin was distinct from two canonical examples of site-specific repression: *GAL1-10* repression in cells grown on glucose medium and repression of *STE3* in *MATa* cells; and hence the special architecture appeared specific to Sir-based gene silencing (Figure 2.9). Additionally, in non-silenced cells nucleosomes were accessible across *HML* and *HMR*, indicating that the differential accessibility, as probed by recovery with the H3 antibody, was dependent on silencing (Figure 2.7D). The paradox in the data from figures 2.1 and 2.3 was why the very promoters that must be silenced by Sir proteins exhibited the lowest enrichment of Sir proteins. Since it now appears that the structure that exists at those promoters has the capacity, upon crosslinking, to mask recognition by the anti-H3 and anti-myc antibodies, that same structure might occlude RNA polymerase form the resident promoters, thus suggesting a structural component to the steric occlusion mechanism of regional, promoter-independent repression.

Other striking features of the enrichment data of Sir proteins at *HMR* were the clear boundaries, one on the left side of *HMR-E* and immediately to the right of the tRNA-Thr gene. That tRNA gene creates a boundary, limiting Sir-based silencing on one side from affecting the expression of a reporter gene on the other (Donze and Kamakaka 2001; Oki and Kamakaka 2005). The tRNA gene and associated cohesin might function as a boundary by providing a structural scaffold for constraining the silenced domain at *HMR* through interaction with *HMR-E*. This may be akin to cohesin's chromatin organizational role in other organisms, such as the CTCF/cohesin interactions in mammals (Phillips-Cremins et al. 2013). If so, perhaps the tRNA gene relieved the selective pressure for a functional I- silencer at *HMR* would be reduced. *HML*, however, showed a less discrete domain of enrichment than *HMR*, possibly reflecting its relative proximity to the Chromosome III left telomere.

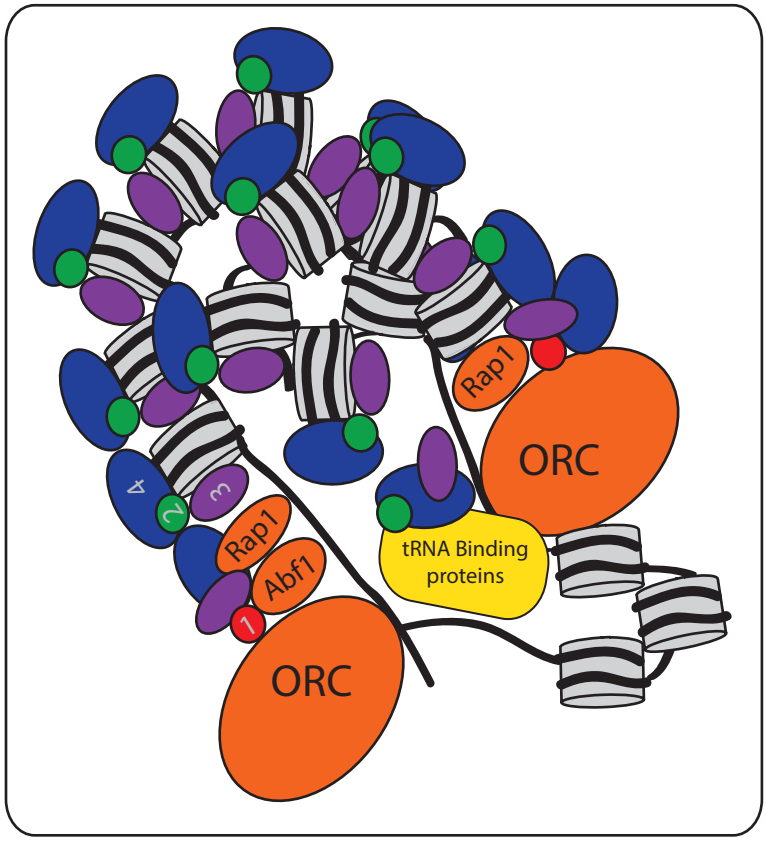

Figure 2.12 A model for a silenced superstructure at *HMR*. The *E* and the *I* silencers interact to form a loop, creating distinct boundaries for Sir-protein association. Nucleosomes are tightly packed throughout the loci with a secondary loop burying the promoter in the chromatin superstructure, excluding access by RNA polymerase in vivo and by antibodies in cross-linked chromatin in vitro. Sir proteins associate with the nucleosomes throughout the locus and are also buried within the confirmation at the promoter region. The tRNA gene associates with the silenced superstructure and interacts with the Sir complex mediated by Sir2 cohesin binding.

2.5.3 Nucleation and Sir-Protein Association at Silenced Chromatin

The working model for the assembly of silenced chromatin, drawn from low-resolution ChIP-qPCR studies, has been the nucleation of a Sir protein complex at the silencers though association of individual Sir proteins with ORC, Abf1 and Rap1. In the model, nucleation is followed by spreading of Sir complexes across the region by iterative cycles of deacetylation of histones by Sir2, leading to recruitment of additional Sir-protein complexes, ultimately occupying a region of chromatin and repressing transcription within it (Rusché et al. 2002). Our data have substantially refined this view. Sir3 and Sir4 enrichment in cells lacking Sir2 catalytic activity was substantially reduced or missing from internal regions of *HML* and *HMR*. However, we still observed some clear, though reduced, Sir3 and Sir4 occupancy at nucleosomes adjacent to the silencers. According to the spreading model, and with support from the structure of Sir3 bound to a nucleosome, deacetylation of H4K16 is required to produce the highest affinity interactions between Sir3 and nucleosomes (Armache et al. 2011; Wang et al. 2013). However, since Sir2 must bind to H4K16-acetyl before the deacetylation reaction, it stands to reason that the Sir2-3-4 complex would still bind H4K16-acetyl, though with less affinity and perhaps less stability than the deacetylated histone tail. Indeed, in vitro studies have demonstrated a slightly higher affinity of the Sir2-4 complex with acetylated H4K16 than with the deacetylated H4K16, supporting our in vivo studies of Sir-protein association independent of Sir2 catalytic activity (Oppikofer et al. 2011).

This distribution of Sir3 and Sir4 independent of Sir2 catalytic activity also revealed additional nucleation sites at both *HMR* and *HML*. At *HML*, there was apparent nucleation at a region overlapping the HO recognition sequence. This internal peak may correspond to a genetic entity, called the protosilencer, internal to *HML*. This peak supports the hypothesis that the Rap1 binding site in the promoter region of *HML* might actually be occupied by Rap1 in silenced chromatin, perhaps providing stabilizing interactions with Sir3 and Sir4, just as it does at the silencer (Cheng and Gartenberg 2000). Additionally, Sir3 and Sir4 associated with the tRNA gene adjacent to *HMR,* largely independently of Sir2's catalytic activity. That tRNA gene recruits Scc1 cohesin, which in turn interacts with a non-catalytic domain of Sir2, presumably mediating the peak of Sir3 and Sir4 enrichment precisely over the tRNA gene (Wu et al. 2011). As a note of caution, we have recently identified tRNA genes and other highly expressed loci to be susceptible to non-specific enrichment in ChIP protocols (Teytelman et al. 2013). However, the magnitude of that non-specific enrichment could not account for the majority of the Sir-protein enrichment at this tRNA gene.

Several observations have been difficult to reconcile with the notion that spreading occurs in iterative cycles of histone deacetylation and Sir-complex recruitment across a linear silenced region. For example, studies on the kinetics of silencing have yet to detect time-revolved distinctions of where in a silenced domain Sir proteins first bind (Radman-Livaja et al. 2011; Lynch and Rusché 2009). The initial nucleation of Sir proteins to the silencers, as evidenced by the Sir3 and Sir4 enrichment in the absence of Sir2 catalytic activity, and the resulting looped structure, may facilitate efficient, non-linear assembly of silent chromatin by allowing Sir2 to access all the nucleosomes from one or more positions at the locus. Therefore, there may be no obligate order of Sir proteins associating with nuclesomes across the silenced domain.

2.5.4 The Domains of Hypoacetylated H4K16

At *HML, HMR* and the telomeres, the regions of H4K16 hypoacetylation were larger than the regions of Sir-protein enrichment. There were at least three possible explanations for how the hypoacetylated domain could be larger than the domain occupied by Sir proteins: 1) Sir proteins bound to one nucleosome could potentially deacetylate H4K16-acetyl on nearby nucleosomes; 2) there could be differences in the stability of Sir-protein association with some hypoacetylated H4K16 nucleosomes relative to others; 3) the extended H4K16 hypoacetylation could be the result of a different histone deactylase, such as Rpd3 (Ehrentraut et al. 2011). At telomeres, these larger regions of H4K16 hypoacetylation were consistent with the apparent ability of Sir3, especially upon over-expression, to spread inward from telomeres (Hecht et al. 1996; Radman-Livaja et al. 2011), exerting a telomere-position effect, due to Sir3's affinity for nucleosomes hypoacetylated at H4K16 (Armache et al. 2011; Wang et al. 2013). Formally, because we were unable to efficiently IP H3 from the internal silencer regions, we cannot completely discount the possibility that the chromatin is acetylated at some positions within *HML* and *HMR*, yet was unable to be immunoprecipitated by the H4K16-acetyl antibody. This explanation seems less likely though, as many studies have shown that acetylated H4K16 is not conducive to a tightly packed heterochromatin structure (Johnson et al. 2009; Martino et al. 2009). Additionally, genetic evidence shows that an H4K16-acetyl mimic is detrimental to silencing (Park and Szostak 1990).

2.5.5 Chromatin Architecture Facilitating Regional Repression

Increasingly, a three-dimensional architecture of chromatin has become a critical missing dimension in our understanding of chromatin regulation. Looping of silencer elements has been shown to be important for heterochromatin regulation in other organisms, such as Polycomb-bound regions and promoters in *Drosophila* and mammals (Bantignies et al. 2011). The high-resolution picture of silenced chromatin described here will be an important benchmark in relating the structure of domains of gene silencing to mechanisms of repression.

Chapter 3: Highly expressed loci are vulnerable to misleading ChIP localization of multiple unrelated proteins

(Portions of this Chapter are adapted from: Teytelman, L.*, **Thurtle D. M.***, Rine, J., and van Oudenaarden A. (2013). *Proceedings of the National Academy of Science* 46, 18602-7. These authors contributed equally to this work)

3.1 Abstract

Chromatin Immunoprecipitation (ChIP) is the gold-standard technique for localizing nuclear proteins in the genome. We used ChIP, in combination with deep sequencing, to study the genome-wide distribution of the Sir silencing complex in *Saccharomyces cerevisiae*. We analyzed ChIP-Seq peaks of the Sir2, Sir3, and Sir4 silencing proteins and discovered 238 unexpected euchromatic loci that exhibited enrichment of all three. Surprisingly, published ChIP-Seq datasets for the Ste12 transcription factor and the centromeric Cse4 protein indicated that these proteins were also enriched in the same euchromatic regions with the high Sir protein levels. The 238 loci were in highly-expressed regions with strong Pol II and Pol III enrichment signals, and the correlation between transcription level and ChIP enrichment was not limited to these 238 loci but extended genome-wide. The apparent enrichment of various proteins at hyper-ChIPable loci was not a consequence of artifacts associated with deep sequencing methods, as confirmed by ChIP-qPCR. The localization of unrelated proteins, including the entire silencing complex, to the most highly transcribed genes was highly suggestive of a technical issue with the immunoprecipitations. ChIP-Seq on chromatin immunoprecipitated with a nuclear-localized GFP reproduced the above enrichment in an expression-dependent manner: induction of the *GAL* genes resulted in an increased ChIP signal of the GFP protein at these loci, with presumably no biological relevance. While ChIP is a broadly valuable technique, some published conclusions based upon ChIP procedures may merit re-evaluation in light of these findings.

3.2 Introduction

Chromatin immunoprecipitation, followed either by microarrays (ChIP-chip) or deep sequencing (ChIP-Seq) is the standard method for *in vivo* genome-wide protein localization analysis (reviewed in (Hanlon and Lieb 2004; Park 2009; Furey 2012)). Since the first applications of deep sequencing to ChIP in 2007, the ChIP-Seq technique has quickly become accepted as superior to ChIP-chip hybridization and is now the dominant and most preferred approach for studying DNA- and chromatin-interacting proteins (Park 2009; Ho et al. 2011; Chen et al. 2012). Because of known biases in chromatin preparation and sequencing, nearly all ChIP-Seq studies compare the mapped reads of the immunoprecipiated sample to an input control with chromatin that is cross-linked but not immunoprecipitated(Park 2009; Chen et al. 2012; Kidder et al. 2011). We applied ChIP-Seq to study the distribution of the silencing protein complex, consisting of Sir2, Sir3, and Sir4, in *Saccharomyces cerevisiae.* Unexpectedly, the well-characterized biology of silencing enabled the resulting data to illuminate a technical artifact introduced by the ChIP technique.

Silencing in *S. cerevisiae* is established by the Sir2, Sir3, and Sir4 protein complex that binds and deacetylates key positions on nucleosomes, forming a heterochromatic structure that inhibits transcription (reviewed in (Rusché et al. 2003)). Prior work raised the possibility that the Sir proteins could occasionally be recruited in error to euchromatic regions (Teytelman et al. 2012). Hence, we asked whether there were any signals of euchromatic silencing in Sir2, 3, and 4 ChIP-Seq data.

In line with a recent report of euchromatic Sir3 localization (Radman-Livaja et al. 2011), we identified numerous loci with peaks of Sir2, 3, and 4 proteins, suggesting the presence of the entire silencing complex. However, the nature of the euchromatic signals and their overlap with highly transcribed genes were suspicious and inconsistent with the expectations from decades of study of silencing proteins and previously published literature (Teytelman et al. 2012; Lieb et al. 2001; Marchfelder et al. 2003). Careful investigation of the euchromatic binding sites of the Sir complex led us to discover that strongly expressed loci were reliably hyper-ChIPable; multiple unrelated proteins exhibit increased ChIP levels at these sites. There was no meaningful biology in these ChIP signals. Because of the widespread use of ChIP-based methods and the range of conclusions drawn, this discovery has wide applicability.

3.3 Materials and Methods

Yeast Strains and Plasmids Strains are listed in Table 3.1. All yeast strains were generated in the W303 background. Deletions and tags were constructed through one-step integration of knockout cassettes (Longtine et al. 1998). C-terminal tagging of Sir genes was also conducted using one-step gene replacement with the 13xMyc tag. The NLS-GFP plasmid was acquired from Addgene (24038).

Sir-Myc Chromatin Immunoprecipitation 70 OD (600nm) units of logarithmically growing cells were crosslinked with 1% formaldehyde for 1 hour at room temperature. Chromatin was prepared as previously described (Aparicio et al. 2005) with minor modifications. Cells were lysed with 0.5-mm zirconia beads in 1 ml FA lysis buffer. Cell lysates were collected by centrifugation at 74,000 x g for 40 min then washed for 1 hour at 4°C in FA lysis buffer. Samples were then centrifuged at 74,000 x g for 22 min, and then sonicated as described to an average size of 300-400 bp. Chromatin was immunoprecipitated with 120 µl of Anti-c-Myc Agarose (Sigma, Cat. 7470) overnight at 4°C. Washes, elution, and isolation of DNA were performed as previously described (23).

GFP Chromatin Immunoprecipitation Cells were grown overnight at 30°C in CSM-Leucine with raffinose (2%) as the sole sugar source. These cultures were then seeded at an OD of 0.2 into 100 ml of YP Dextrose (2%) or YP Galactose (2%) and grown at 30°C for two doublings (about 4 hours). Cells were fixed for 1 hour at room temperature in 1% formaldehyde and chromatin isolated as described above. Prior to immunoprecipitation, chromatin was precleared for 1 hr at 4°C with 40µl Protein A Sepharose bead slurry (17-5280-01, GE Healthcare). Pre-cleared chromatin was immunoprecipitated with 5 µl anti-GFP antibody (Abcam, ab290) overnight at 4°C. Then a 120ul aliquot of Protein A Sepharose bead slurry was added and samples incubated for 4 hours at 4°C.

Table 3.1 Yeast strains used in chapter 3

Name	Genotype
JRY9316	*matΔ::HygMX lys2 his3-11 leu2-3,112 trp1-1 ura3-52 can1-100*
JRY9317	*matΔ::HygMX lys2 his3-11 leu2-3,112 trp1-1 ura3-52 can1-100 SIR4-13xMyc::KanMX*
JRY9318	*matΔ::HygMX lys2 his3-11 leu2-3,112 trp1-1 ura3-52 can1-100 SIR3-13xMyc::KanMX*
JRY9319	*matΔ::HygMX lys2 his3-11 leu2-3,112 trp1-1 ura3-52 can1-100 SIR2-13xMyc::KanMX*
JRY9443	*mat**a** lys2 his3-11 leu2-3,112 trp1-1 ura3-52 can1-100 [Addgene 24041 NLS-GFP]*
JRY4012	*mat**a** lys2 his3-11 leu2-3,112 trp1-1 ura3-52 can1-100*

Sequencing and Mapping Sir-Myc libraries were prepared with modifications to the Illumina paired-end library protocol as in (Zill et al. 2010). Libraries were loaded into one lane each and sequenced using the Illumina Genome Analyzer II as 45bp paired-end reads.

GFP libraries were constructed using the Illumina Tru-Seq library preparation kit with the following modifications. Upon end repair, samples were cleaned up using a Qiagen MinElute column. Adapters were used at a 10-fold diluted concentration as to that provided. Samples were indexed and sequenced in a single lane on the Illumina HiSeq 2000 as 100 bp paired-end reads. Sir-myc reads were mapped to the S288C genome using MAQ (Li et al. 2008). GFP libraries were mapped with BWA and Samtools (Li and Durbin 2009; Li et al. 2009). The number of reads mapped for each sample is outlined in Table 3.2. All sequences have been deposited in the NCBI Short Read Archive under accession SRP030670.

Quantitative PCR Quantitative PCR on isolated chromatin from ChIP preparations was conducted with Dynamo HS SYBR green kit (Thermo Scientific) on a MX3000P qPCR machine (Agilent). The following primers were used for amplification: *SEN1* (Forward: ACCAAAGGTGGTAATGTTGATGTC, Reverse: GGGAGGCGATGGTTTAGCCTGTAG), *MET3* (Forward: TTCTTGCAATTCGGTGGTGG, Reverse: GACTCTAGCTGAATATCGGC), GCN4 (Forward: CATCAAGACTGAAGAGGATCCAAT, Reverse: AGTGGTAACTGGAATGTCATTGTC) and *LSR1* (Forward: GCTTTCTGTTTCTCCCTTAGTTTG, Reverse: GCGAAGAAATCAACAATAAGAGCG).

Data Analysis

IP/Input Ratios Every base of the genome was assigned the total number of sequence reads overlapping it, separately for the input and IP sequence reads. Subsequent normalization and analysis was performed on median read coverage across 100 bp windows, sliding along each chromosome in 50 bp steps. The median IP coverage of each 100 bp interval was divided by the median input coverage for the same window. The IP/input ratios of each interval were normalized, dividing by the median genome-wide IP/input. Positions with fewer than 20 input reads were excluded from all subsequent analysis because of unreliable enrichment associated with division by low numbers.
Sir-enriched euchromatic loci We searched for all 100bp euchromatic intervals, 50KB or more from chromosome ends, with the normalized IP/input ratio of the Sir2, Sir3, and Sir4 greater than 2. All adjacent locations within 2,000 bp were merged into single contiguous interval, giving the 238 Sir-enriched euchromatic loci. We also used the MACS peak-calling software on the Sir ChIP-Seq datasets using the following parameters: a gsize of 1.2×10^7, mfold value of 2 and tsize (tag size) of 45 (Zhang et al. 2008). All other parameters were used with the default settings.
Ste12, Cse4, Pol II datasets We used the published ChIP-Seq datasets for the Ste12, Cse4, and Pol II proteins (Lefrançois et al. 2009). Mapped reads were downloaded from the NCBI Gene Expression Omnibus, accession GSE13322. For each IP, we summed the read counts across the 3 replicate experiments at each base pair of the *S. cerevisiae* genome; the same for the input samples of each protein.
ChIP levels as a function of expression All genomic positions were split into those within 1,000 bp of an annotated tRNA gene start or stop (tRNA-proximal dataset) or more than 1,000 bp of tRNA gene start or stop (tRNA-distal dataset). The tRNA-proximal dataset was used to make the scatterplot of ChIP level versus increasing distance from the tRNA genes, and the tRNA-distal set

Table 3.2 Number of reads mapped for each experiment in chapter 3

Sample	Number of Mapped Reads
Sir2-myc IP	21044014
Sir2-myc input	30157356
Sir3-myc IP	19387854
Sir3-myc input	18570868
Sir4-myc IP	15095288
Sir4-myc input	22515576
Anti-myc No-tag IP Replicate #1	12117692
Anti-myc No-tag input Replicate #1	12130227
Anti-myc No-tag IP Replicate #2	26035511
Anti-myc No-tag input Replicate #2	52290472
Anti-myc No-tag IP Replicate #3	25776880
Anti-myc No-tag input Replicate #3	23380531
GFP Dextrose IP	9151398
GFP Dextrose input	15784778
GFP Galactose IP	11037364
GFP Galactose input	21171368
Anti-GFP Galactose IP (No GFP)	17150787
Anti-GFP Galactose input (No GFP)	14606780
Anti-GFP Dextrose IP (No GFP)	7299173
Anti-GFP Dextrose input (No GFP)	21382880

was used to plot the ChIP levels as a function of Pol II ChIP signal.
Glucose versus Galactose GFP ChIP-Seq Average IP/input ratios from the GFP-glucose and GFP-galactose ChIP-Seq experiments were calculated for each annotated *S. cerevisiae* gene. Boxplots were plotted for all genes, compared to the galactose-induced *GAL1, GAL2, GAL7,* and *GAL10.* The scatter plot comparing GFP ChIP-Seq of chromatin from cells grown in glucose and galactose media was also plotted on gene-level averages.
Heat maps The y-axis is a list of Sir3-enriched regions. The regions were selected as follows. 1) All 100 mers with Sir3 IP/input>2 were merged into a contiguous block if separated by less than 2KB. 2) The regions were ordered by descending level of average Sir3 IP/input ratio. 3) The heat maps were constructed for 2,000 bp to the left and right of the center of each Sir3-enriched region. 4) The heat maps were plotted separately for euchromatic regions, greater than 50KB from chromosome ends, and subtelomeric regions that were within 10KB of chromosome ends.
Using GFP to enrich for Sir and Cse4 true binding events Sir-enriched regions were defined as above, where there were contiguous blocks of >2x IP/input ratios of Sir2, 3, and 4. For each such subtelomeric or euchromatic region, we calculated the average GFP IP/input ratio across the entire region. We used the GFP in galactose ChIP-Seq dataset because it had higher sequence coverage. Regions with average GFP IP/input ratio>1.5 were deemed "high-GFP" and those with an IP/input ratio of <=1.5 were deemed "low-GFP". Cse4 targets were from the supplementary information of the published ChIP-Seq study (Lefrançois et al. 2009). Cse4 targets were partitioned into "centromeric" and "euchromatic/non-centromeric" according to the designation in the published supplementary table. High-GFP and low-GFP thresholding was the same as for the Sir-protein analysis above.
Statistical Analyses All statistical tests and fits were performed using Matlab.

3.4 Results

3.4.1 Unrelated Proteins show Overlapping Enrichment in ChIP-Seq Datasets

The well-described Sir protein silencing complex in yeast is important for silencing the cryptic mating-type loci and some subtelomeric regions. However, we were interested in the potential for euchromatic Sir-protein enrichment because the silencer-binding proteins that recruit the Sir proteins to silencers also bind at many positions in euchromatin. To investigate this possibility, we performed ChIP-Seq experiments on myc-tagged Sir2, Sir3, and Sir4 and analyzed the genome-wide IP/input ratios in euchromatin, operationally defined as sequences 50 kilobases or farther from chromosome ends. To identify euchromatic loci with Sir complex occupancy, we imposed a stringent standard for enrichment requiring Sir2, Sir3 and Sir4 to each be enriched two-fold or greater, with many of these loci exhibiting substantially higher enrichment of individual Sir proteins. Using this strict standard we found a total of 238 distinct loci (Figure 3.1, Table 3.3). Given that no euchromatic function has been ascribed to the Sir complex, this was a surprisingly high number of distinct euchromatic loci to be enriched for all Sir proteins.

These peaks reflected high read coverage in the immunoprecipitated DNA, rather than low representation in the input sample (Figure 3.2). We also used the popular peak-calling software MACS on the three Sir datasets, and 76 of the 238 peaks were confirmed by the program as statistically significant at the default p-value of 10^{-5} (Table 3.3). Additionally, this euchromatic

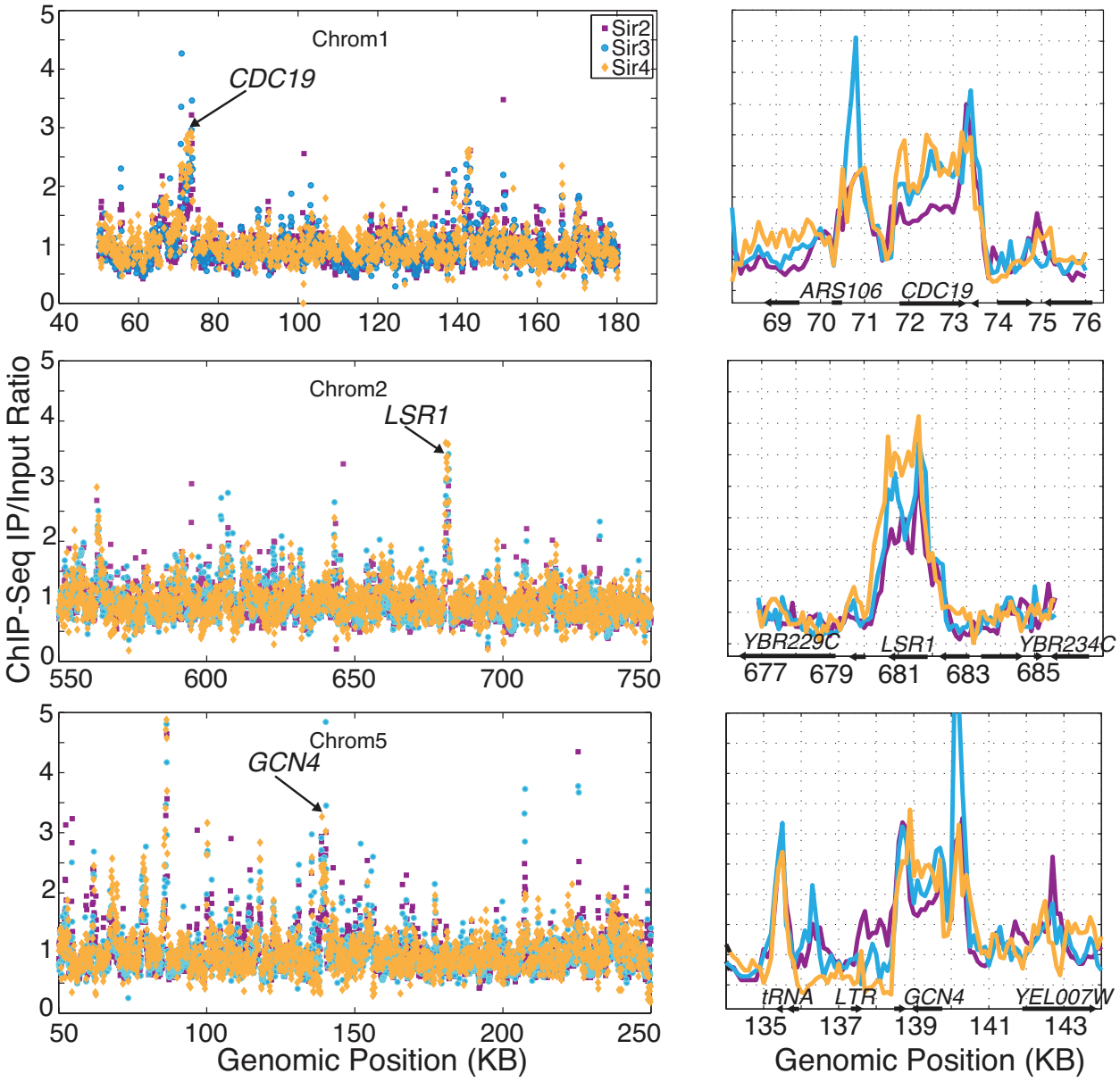

Figure 3.1. Euchromatic enrichment of the Sir complex in ChIP-Seq datasets. Examples of the 238 euchromatic loci with two-fold or higher ChIP-Seq enrichment of the Sir2, Sir3, and Sir4 proteins. The left panels are chromosome-level views and the right panels are zoomed in tracks for the *CDC19, LSR1,* and *GCN4* loci. For each protein, the IP/input ratios are normalized to the genome-wide median.

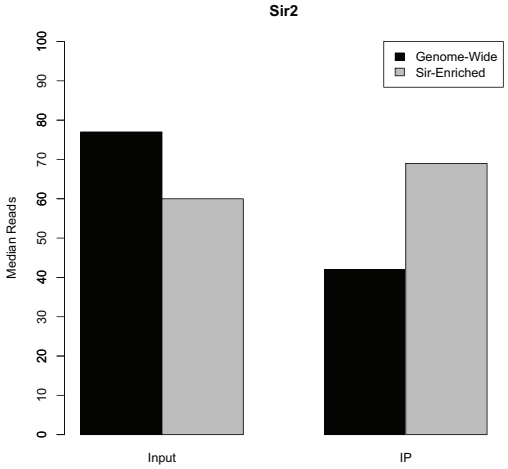

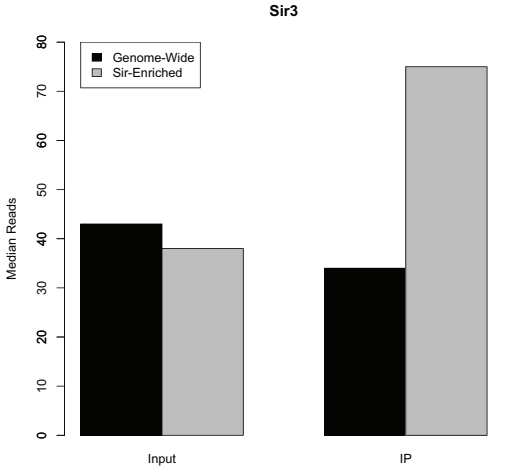

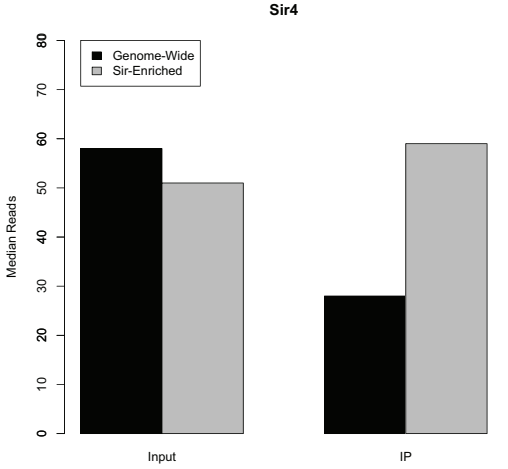

Figure 3.2 Enrichment Due to High Read Coverage in the Immunoprecipitate. Bar graphs show median number of reads for the input and immunoprecipitate (IP) samples genome-wide (black) and at Sir-enriched loci (grey) for Sir2, Sir3 and Sir4.

enrichment was not due to an artifact resulting from next-gen sequencing methods as ChIP-qPCR of myc-tagged Sir4 reproduced the ChIP-Seq enrichment at the highly-expressed *LSR1, CDC19,* and *GCN4* genes, which were prominent among the enriched genes in the ChIP-Seq datasets; Sir4-myc was not enriched at *MET3*, a gene not identified as enriched in the ChIP-Seq samples (Figure 3.3). To check for statistical significance, we asked how many loci had the inverse – input/ip ratio greater than 2 for all three proteins. In contrast to the 238 loci with high ip/input, only a single locus passed the inverse threshold. The discovery of a significant fraction of euchromatin being occupied by all three members of the silencing complex suggested either unanticipated roles of Sir proteins, or the existence of a systematic bias in the data.

The sites of the Sir complex enrichment across the yeast genome were inconsistent with prior knowledge of Sir-mediated silencing. The Sir proteins play roles in silencing telomeric and subtelomeric loci (Lieb et al. 2001; Barton and Kaback 2006; Gottschling et al. 1990; Vega-Palas et al. 2000; Wyrick et al. 1999), and in control of rDNA recombination, but no reproducible derepression of euchromatic genes is observed in *sir* mutants (Marchfelder et al. 2003). Moreover, predictions for possible euchromatic Sir targets in a prior study (Teytelman et al. 2012) did not overlap with the 238 Sir-enriched loci reported here. Hence, we considered the possibility of a ChIPability issue that could result in strong but misleading peaks, despite normalization to the "input-Seq" sample, a commonly used method of normalization(Park 2009; Chen et al. 2012; Kidder et al. 2011).

We reasoned that if certain genomic regions were more susceptible to immunoprecipitation per se, they would show increased ChIP signals for unrelated DNA-binding and chromatin-binding proteins. To test this hypothesis we analyzed published ChIP-Seq datasets for the Ste12 transcription factor and the Cse4 centromere protein specifically at the 238 euchromatic loci already identified as being enriched for Sir 2, 3, and 4 (Lefrançois et al. 2009). These 238 euchromatic loci also exhibited increased Ste12 and Cse4 signals (Figure 3.4, Figure 3.5, Table 3.3). Therefore, these regions were not specifically bound by Sir proteins and did not reveal new Sir-protein biology. Rather they revealed loci that were commonly enriched in ChIP datasets. We called these regions of overlapping peaks of unrelated proteins "hyper-ChIPable."

3.4.2 The Hyper-ChIPable Regions Coincided with Highly Expressed Genes

Investigations of common characteristics about these "hyper-ChIPable" loci where many unrelated factors were enriched revealed that these loci were frequently coincident with highly-expressed Pol II-transcribed genes and tRNA genes, also known to be heavily transcribed by Pol III (Dieci and Sentenac 1996; Roberts et al. 2003; Moqtaderi and Struhl 2004). Of the 238 regions, 145 (61%) overlapped tRNA genes, and another 47 (20%) had more than 10-fold enrichment of Pol II (Table 3.3). Additionally, this relationship was also evident with qPCR analyses, in which three genes with high expression showed Sir4 signal, but *MET3*, which is not expressed under these conditions, did not show enrichment of Sir4 (Figure 3.3). This concordance of the 238 Sir-enriched euchromatic loci being coincident with highly-expressed genes led us to investigate the genome-wide ChIP-to-expression-level correlation by comparing the ChIP levels of the Sir2, 3, and 4 and Cse4 proteins to RNA Pol II occupancy or tRNA gene proximity genome wide. There was a striking positive relationship between ChIP enrichment and the level of RNA Pol II (Figure 3.6A-B, Figure 3.7), extending the correlation between increased ChIP capacity with increased transcription beyond

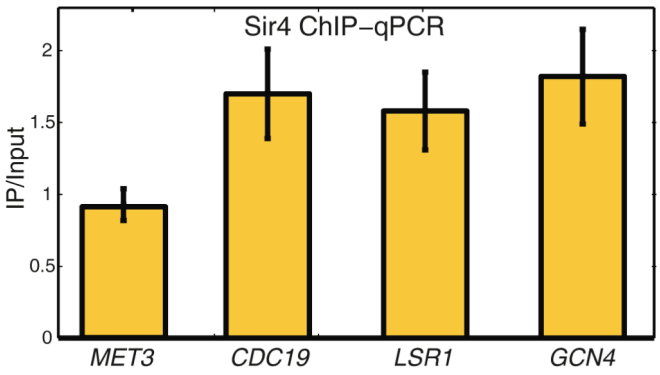

Figure 3.3 Confirmation of ChIP enrichment at highly expressed genes by ChIP-qPCR. Sir4 ChIP-qPCR reproduces the ChIP-Seq enrichment at highly expressed *CDC19, LSR1,* and *GCN4*. No enrichment is seen at the uninduced *MET3* negative control. The error bars show the SEM values from 3 biological replicates.

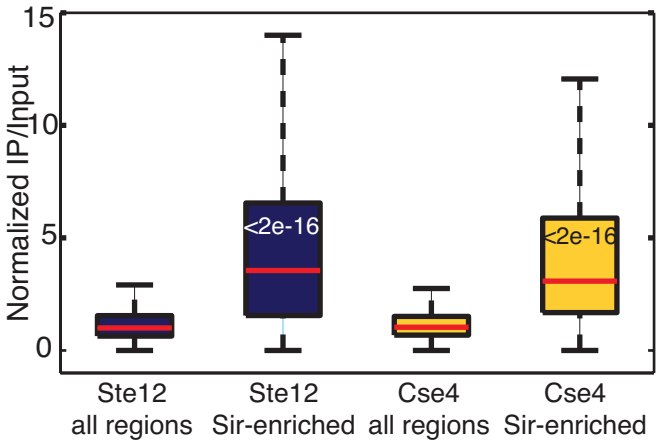

Figure 3.4 Sir-enriched euchromatic loci are hyper-ChIPable. Boxplots of ChIP-Seq levels for the transcription factor Ste12 and the centromeric Cse4 protein, comparing the genome-wide distribution versus the 238 Sir-enriched loci. The top of each box indicates the 75th percentile, the bottom the 25th percentile, and the thick bar inside the box is the median. The whiskers extend out to the most extreme data point that is at most 1.5 times the interquartile range from the box. Wilcoxon-Mann-Whitney p-values comparing the genome-wide and Sir-enriched distributions are shown in the Sir-enriched boxes.

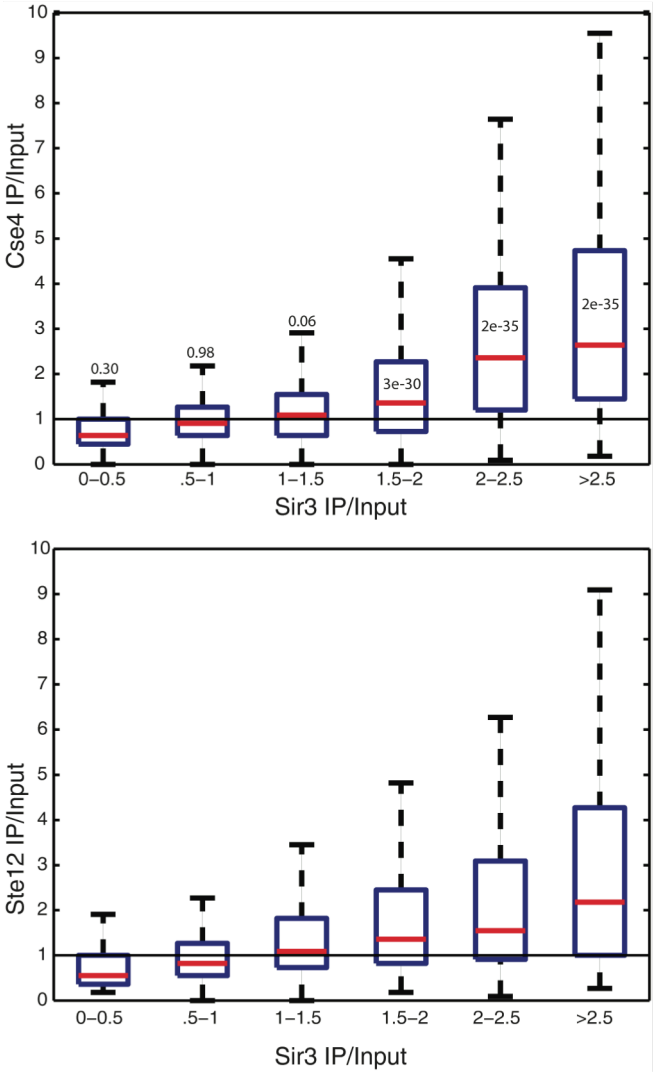

Figure 3.5 Sir3 levels correlate with ChIP-Seq signals for Ste12 and Cse4. Boxplots of Cse4 and Ste12 ChIP-Seq levels, as a function of Sir3 enrichment.

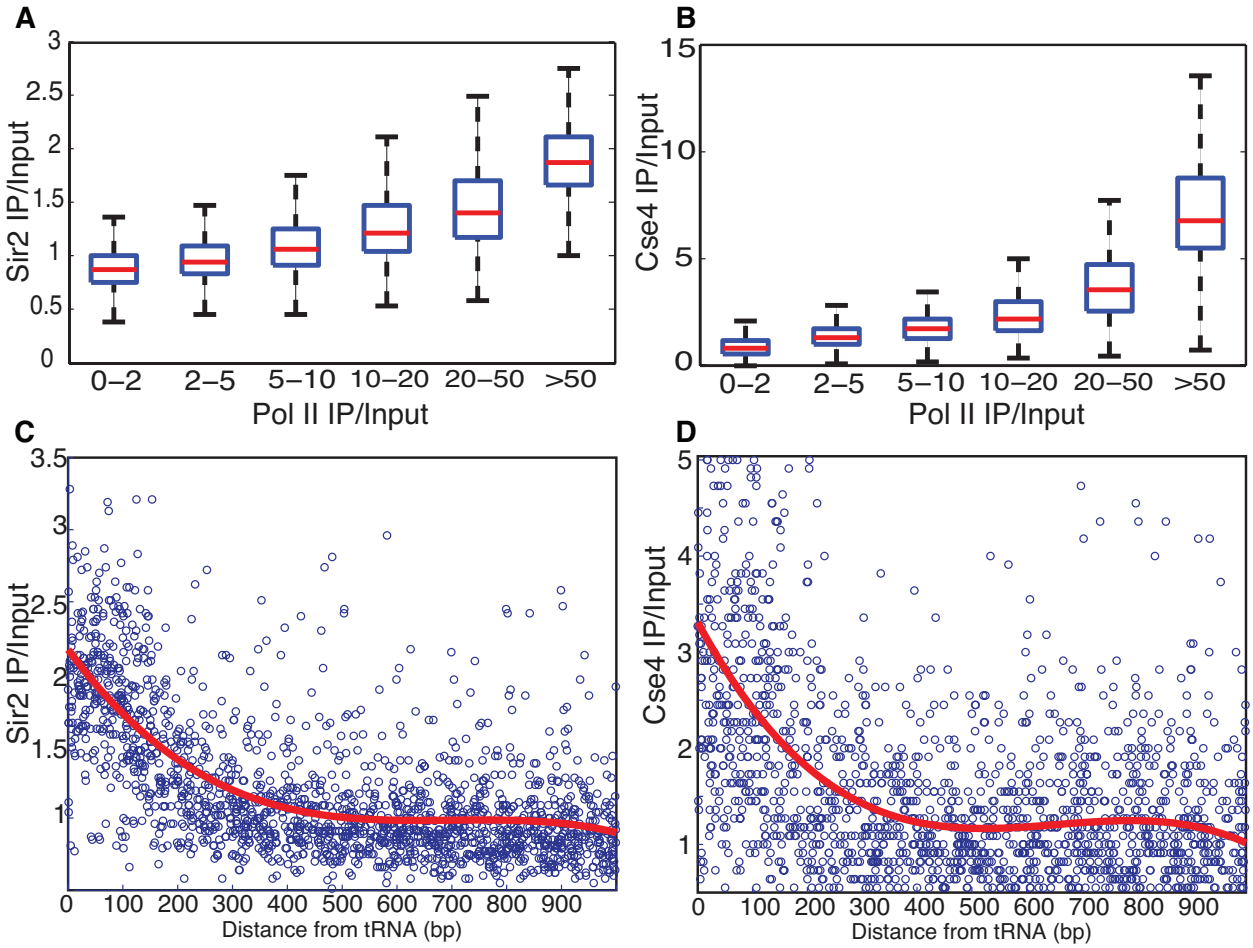

Figure 3.6 Highly expressed loci are hyper-ChIPable. Boxplots of the Sir2 (**A**) and Cse4 (**B**) genome-wide ChIP-Seq levels, as a function of Pol II enrichment. Sir2 (**C**) and Cse4 (**D**) genome-wide ChIP-Seq levels, as a function of the distance from all *S. cerevisiae* annotated tRNAs. The red curve is a polynomial fit to the scatterplot.

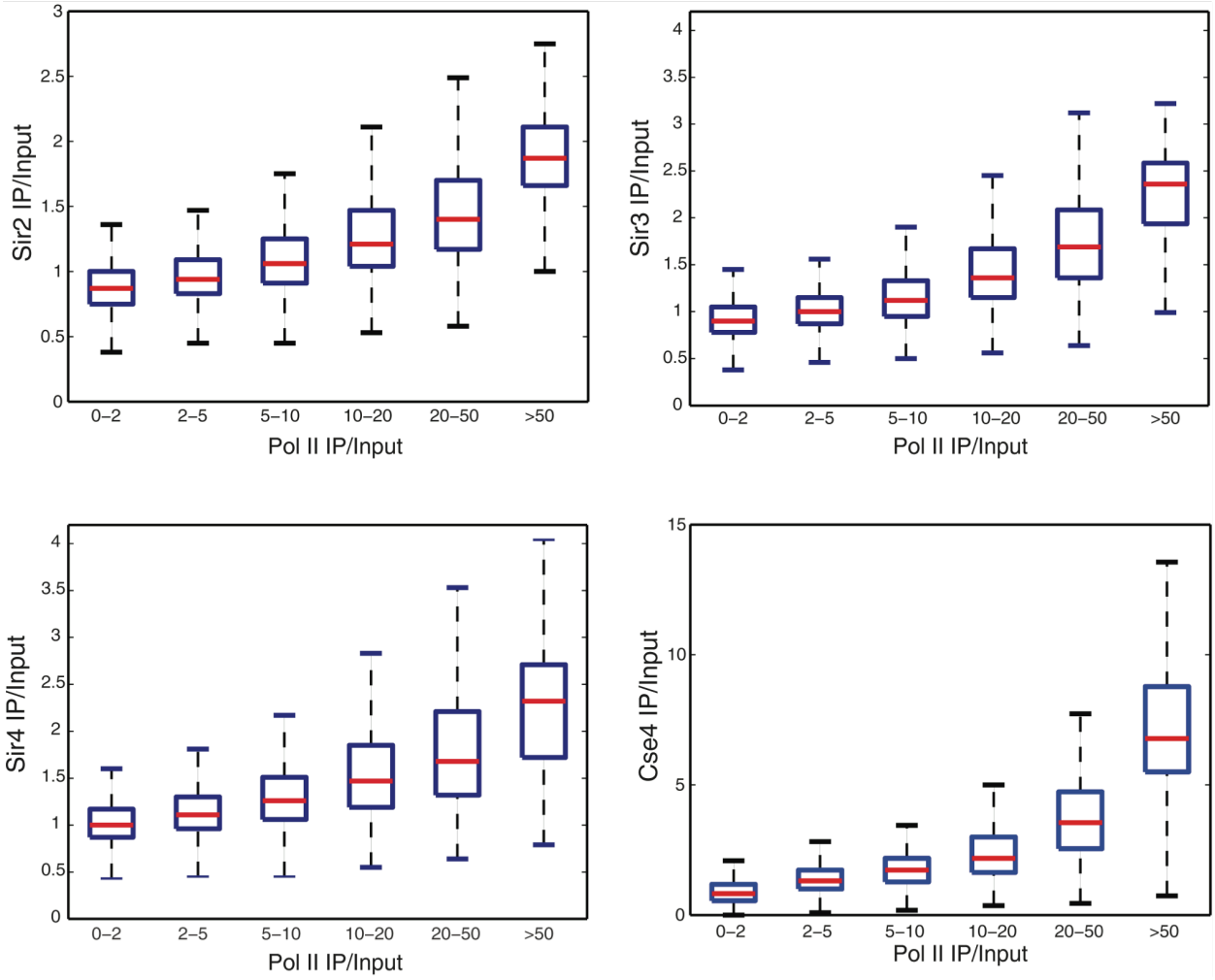

Figure 3.7 Pol II levels correlate with ChIP-Seq signals for Sir2, Sir3, Sir4, and Cse4. Boxplots of Sir2, Sir3, Sir4, and Cse4 ChIP-Seq levels, as a function of Pol II enrichment.

the originally identified 238 loci. Similarly, the ChIP levels of Cse4, Ste12, Sir2, Sir3, and Sir4 correlated with proximity to tRNAs (Figure 3.6C-D, Figure 3.8).

This positive genome-wide relationship between ChIP enrichment and RNA Pol II occupancy suggested that the hyper-ChIPability of loci was due to increased transcription. If so, the ChIP-specific enrichment signal would be expected to extend across the entire gene body. Representative loci showed consistent enrichment of Sir proteins over a continuous stretch of 1,000-2,000 base pairs (Figure 3.1, right panel). To test the generality of this trend, we analyzed the ChIP levels of the Sir2, 3, and 4 proteins as a function of distance from the 5' end of the 200 most highly transcribed genes in the *S. cerevisiae* genome. As predicted, a metagene analysis of these loci showed unambiguous enrichment of all three silencing proteins deep inside the open reading frames (Figure 3.9). Therefore the 238 initially identified hyper-ChIPable loci illuminated the genome-wide phenomenon that more highly expressed genes showed increased enrichment independent of the transcription factor or chromatin protein assayed. This presence of the Sir protein silencing complex over the most heavily transcribed genes was exactly the opposite of the expected distribution for Sir-based gene silencing. Thus, combined with the ChIP signals for the distribution of the unrelated Ste12 and Cse4 proteins over the most expressed genes, the data were strongly suggestive of a technical issue, rather than interesting new biology.

3.4.3 Green Fluorescent Protein was Enriched at Highly-Expressed Loci by ChIP-Seq Analyses in an Expression-Dependent Manner

The analyses described above linked high expression level with increased IP/input ChIP signals for unrelated chromatin- and DNA-interacting proteins. To challenge the possibility that this correlation might reflect an unappreciated dimension of chromatin protein biology, we tested whether immunoprecipitation of the heterologous green fluorescent protein (GFP) with a nuclear localization signal (NLS) and lacking any histone or DNA-binding domain, would reproduce ChIP peaks over the highly-expressed genes. The GFP ChIP-Seq data recapitulated the Cse4, Ste12, and Sir-protein results: GFP enrichment signals were higher in the 238 Sir-enriched loci than the rest of the genome (Figure 3.10A). Additionally, the GFP enrichment correlated with Pol II levels, and increased with proximity to tRNA genes (Figure 3.11A, Figure 3.11B). Again, we confirmed these enrichments of GFP by ChIP-qPCR: GFP enrichments were higher at the *LSR1, CDC19,* and *GCN4* genes, compared to the non-expressed *MET3* locus (Figure 3.10B). The GFP antibody was the third antibody displaying hyper-ChIPability, illustrating the pervasiveness of this enrichment at highly expressed loci (anti-Myc for Sir2, 3, 4, Cse4; anti-GFP, and anti-HA for Ste12). Therefore, by performing ChIP-Seq of a protein that we did not expect to be associating with DNA, we demonstrated that hyper-ChIPable loci were not regions of unexpected binding of chromatin proteins, but rather an artifact of the ChIP method.

The correlation between ChIP levels and highly expressed loci suggested that high-level expression per se could contribute to hyper-ChIPability. Moreover, Fan and Struhl reported artifactual ChIP signal under inducing conditions of TBP and Hsf1 over the *GAL1* coding region and of TBP and Gal4 over a heat shock gene (Fan and Struhl 2009). However, it was possible that some other feature of genes with the capacity for high-level expression led to their enrichment during chromatin immunoprecipitations. To directly test the effect of expression on the enrichment of these loci in the ChIP immunoprecipitates, we performed ChIP-Seq of chromatin from cells expressing

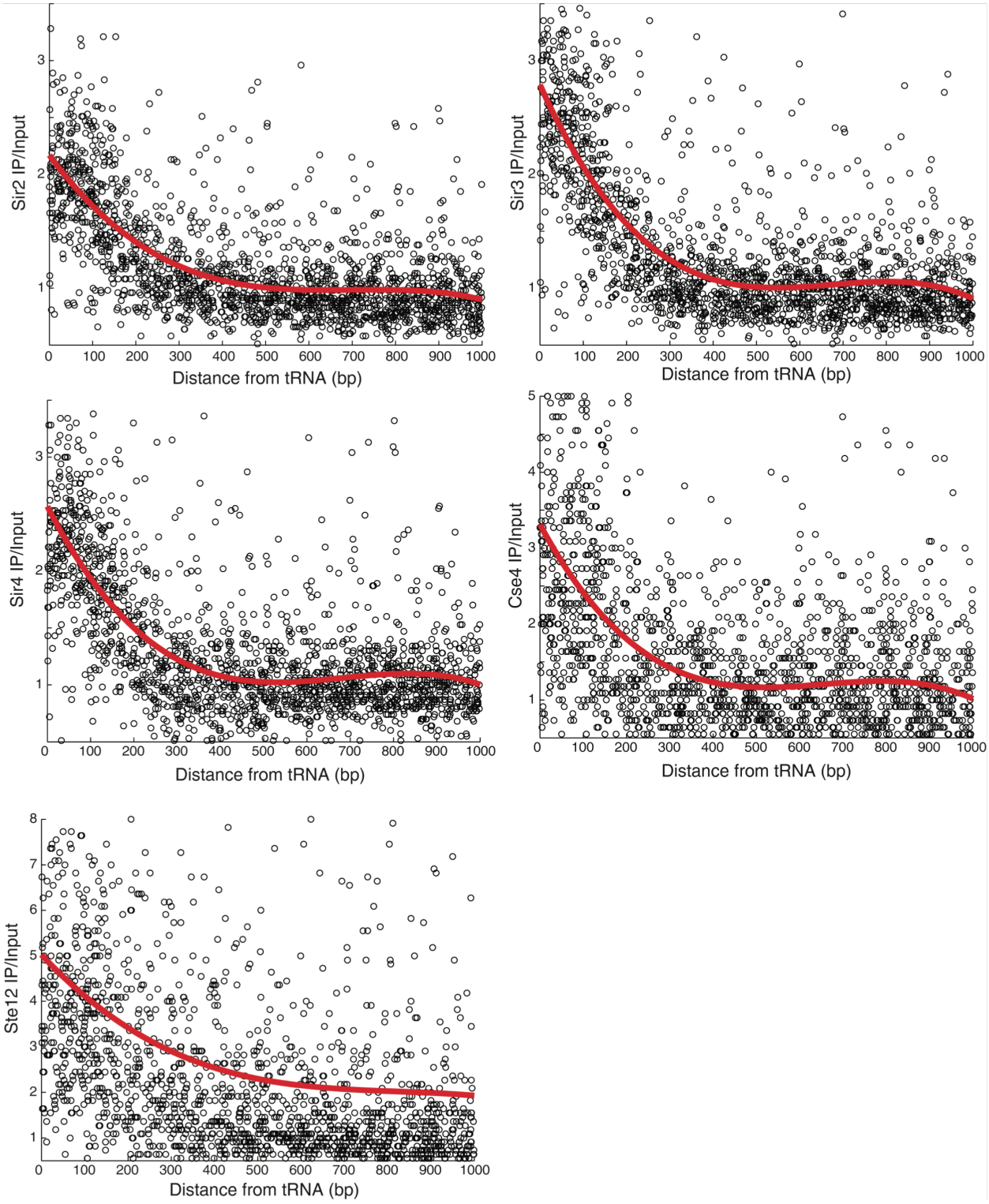

Figure 3.8 tRNA proximity correlates with ChIP-Seq signals for Sir2, Sir3, Sir4, Cse4, and Ste12. Sir2, Sir3, Sir4, Cse4, and Ste12 ChIP-Seq levels, as a function of the distance from *S. cerevisiae* annotated tRNAs. The red curve is a polynomial fit to the scatterplot.

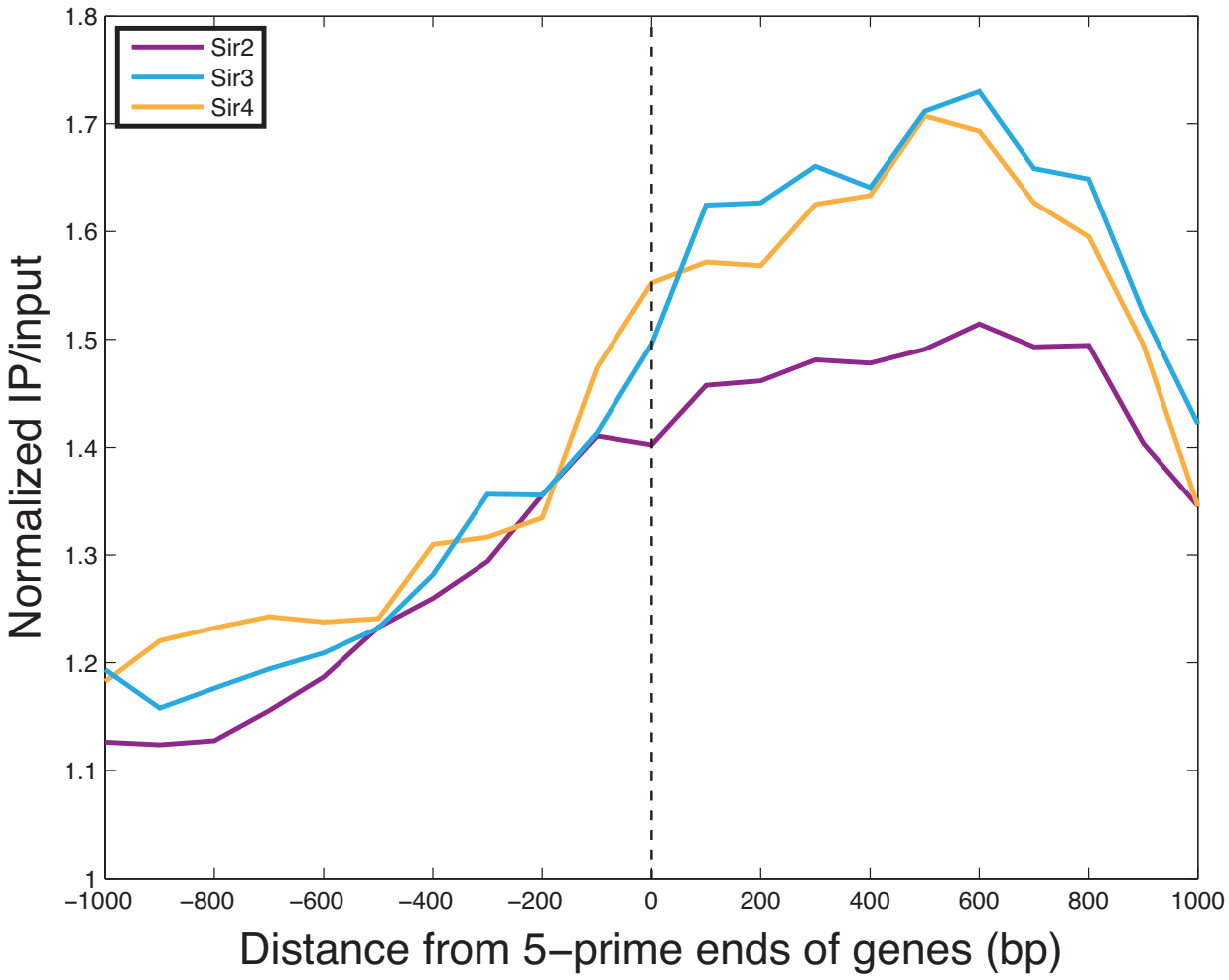

Figure 3.9 Sir proteins are enriched across the entire Open Reading Frame. Sir2, Sir3, and Sir4 ChIP-Seq levels, as a function of the distance from the 5' starts of the 200 most highly-expressed genes in the *S. cerevisiae* genome.

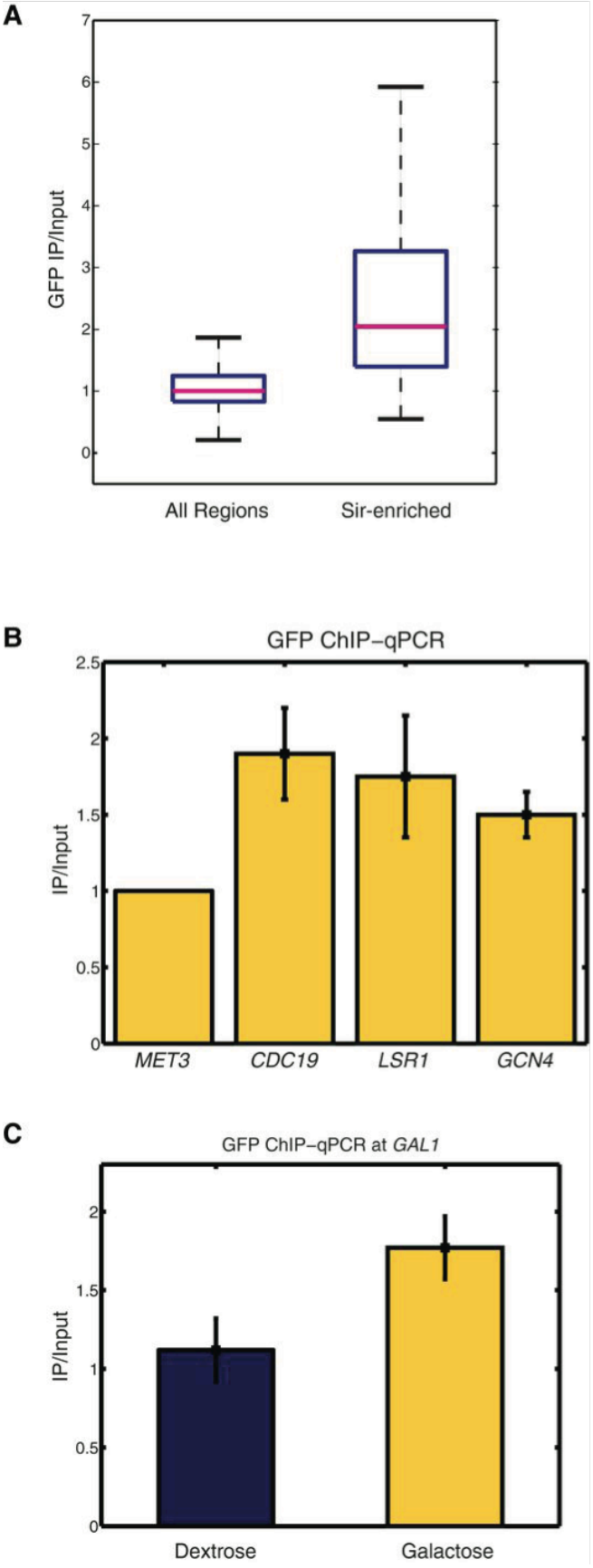

Figure 3.10 Confirmation of GFP hyper-ChIPability. **(A)** Boxplots comparing the GFP ChIP-Seq levels genome-wide versus the 238 Sir-enriched euchromatic loci. Data are from the glucose condition. **(B)** GFP ChIP-qPCR in glucose reproduces the ChIP-Seq enrichment at highly expressed *CDC19, LSR1,* and *GCN4*. All values are shown as relative to the uninduced *MET3* negative control. The error bars show the SEM values from 3 biological replicates. **(C)** ChIP-qPCR values, normalized to *SEN1,* of an NLS-tagged GFP protein. Induction-dependent enrichment of the *GAL1* gene; enrichment is seen only in the induced galactose condition. The error bars show the SEM values from 3 biological replicates.

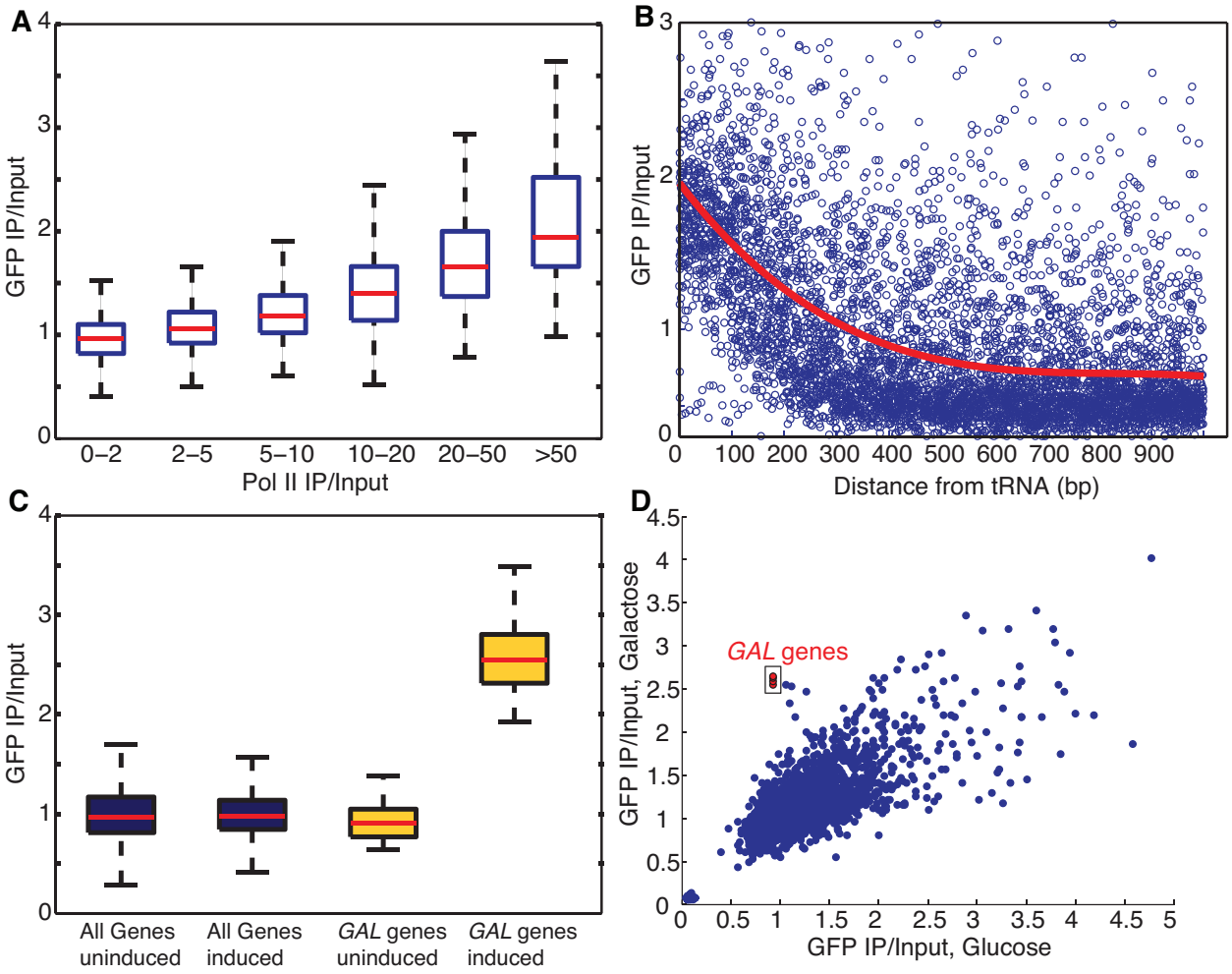

Figure 3.11 ChIP-Seq of nuclear-localized GFP shows hyper-ChIPability. **A.** GFP ChIP-Seq levels, from YPD (2% glucose) media, as a function of Pol II enrichment. **B.** GFP ChIP-Seq levels, from YPD (2% glucose) media, as a function of increasing distance from tRNAs. **C.** Boxplots of GFP ChIP-Seq levels, showing increase for the *GAL1, GAL2, GAL7,* and *GAL10* genes, specifically under the induced galactose condition. For the induction, cells were shifted from overnight growth in raffinose to galactose media for four hours. **D.** Average GFP ChIP-Seq levels for all genes, comparing dextrose versus galactose-shifted media. The *GAL1, GAL2, GAL7,* and *GAL10* genes are highlighted in the red rectangle; they show normal levels in dextrose but are enriched after the shift to galactose.

the NLS-GFP shifted from medium with glucose to medium with galactose as the sole carbon source. There was a clear spike in the GFP ChIP levels at the galactose-inducible *GAL* genes *(GAL1, GAL2, GAL7, GAL10)*, upon induction of these genes (Figure 3.11C). The GFP results were highly reproducible genome-wide, with the exception of the activated *GAL* loci, which were not enriched in glucose media (where the genes are tightly repressed), but enriched in chromatin from galactose-grown cells (Figure 3.11D). Similarly, as measured by ChIP-qPCR, the GFP signal also increased after induction of the *GAL1* gene by shifting from glucose to galactose-containing medium (Figure 3.10C). This result established that increased transcription was sufficient for hyper-ChIPability.

3.4.4 No-Tag Controls Did Not Eliminate Hyper-ChIPability

The discovery of expression-dependent GFP ChIP enrichment led us to ask whether the antibody target itself contributed to the signal, or whether this enrichment depended only on the immunoprecipitation with an antibody. We performed ChIP-Seq on chromatin immunoprecipitated with anti-Myc in a strain lacking a Myc tag on any protein. Likewise, we tested the GFP antibody in a strain without any GFP. The resulting hyper-ChIPability was variable in these no-tag or no-GFP experiments. In contrast to the strong enrichment over highly expressed loci observed in seven out of seven ChIP-Seq datasets above (Sir2, 3, 4, Cse4, Ste12, GFP-glucose, GFP-galactose), only two out of the five no-tag/no-GFP datasets showed an enrichment quantitatively similar to the tagged datasets; another two showed enrichments in the immunoprecipitated chromatin with a weak correlation with published Pol II levels, and one set showed no hyper-ChIPability whatsoever (Figure 3.12).

The variable extent of the enrichment at highly expressed loci in these "negative control samples" implied that no-tag controls could not be reliably utilized to remove spurious cases of hyper-ChIPability. Despite the variability, the presence of hyper-ChIPability in some of the extracts from cells lacking the target of the antibody was striking. It indicated that the enrichment was due, at least in part, to something that happened *in vitro* from the IP step itself interacting with this more "open" chromatin, rather than due to increased interaction between a nuclear protein and highly-transcribed regions *in vivo*.

3.4.5 Utilizing GFP ChIP-Seq to Remove False Positive Targets

Our detection of the hyper-ChIPable loci, despite normalization by input-Seq, and the variability in no-tag experiments above, implied that neither no-tag nor input samples are sufficient controls to remove false positive ChIP peaks. Hence, we considered whether the GFP ChIP-Seq data could be used to discriminate between real and artifactual localization signals.

In principle, known silenced chromatin should be specifically enriched for the Sir2, 3, and 4 proteins, without the corresponding GFP increase, in contrast to the hyper-ChIPable euchromatic loci where Sir proteins and GFP seemed to co-localize. As predicted, subtelomeric sequences, within 10KB of chromosome ends, had enrichment of all three Sir proteins, without a high GFP signal (Figure 3.13). Therefore, we applied a simple GFP-enrichment threshold for all putative Sir-enriched loci, requiring the average IP/input GFP enrichment to be below 1.5-fold before a signal was considered tentatively meaningful. Among subtelomeric Sir targets, only 1 out of 53 regions (2%) had a high GFP level; however, in the euchromatic Sir-enriched regions, 201 out of 238 (84%)

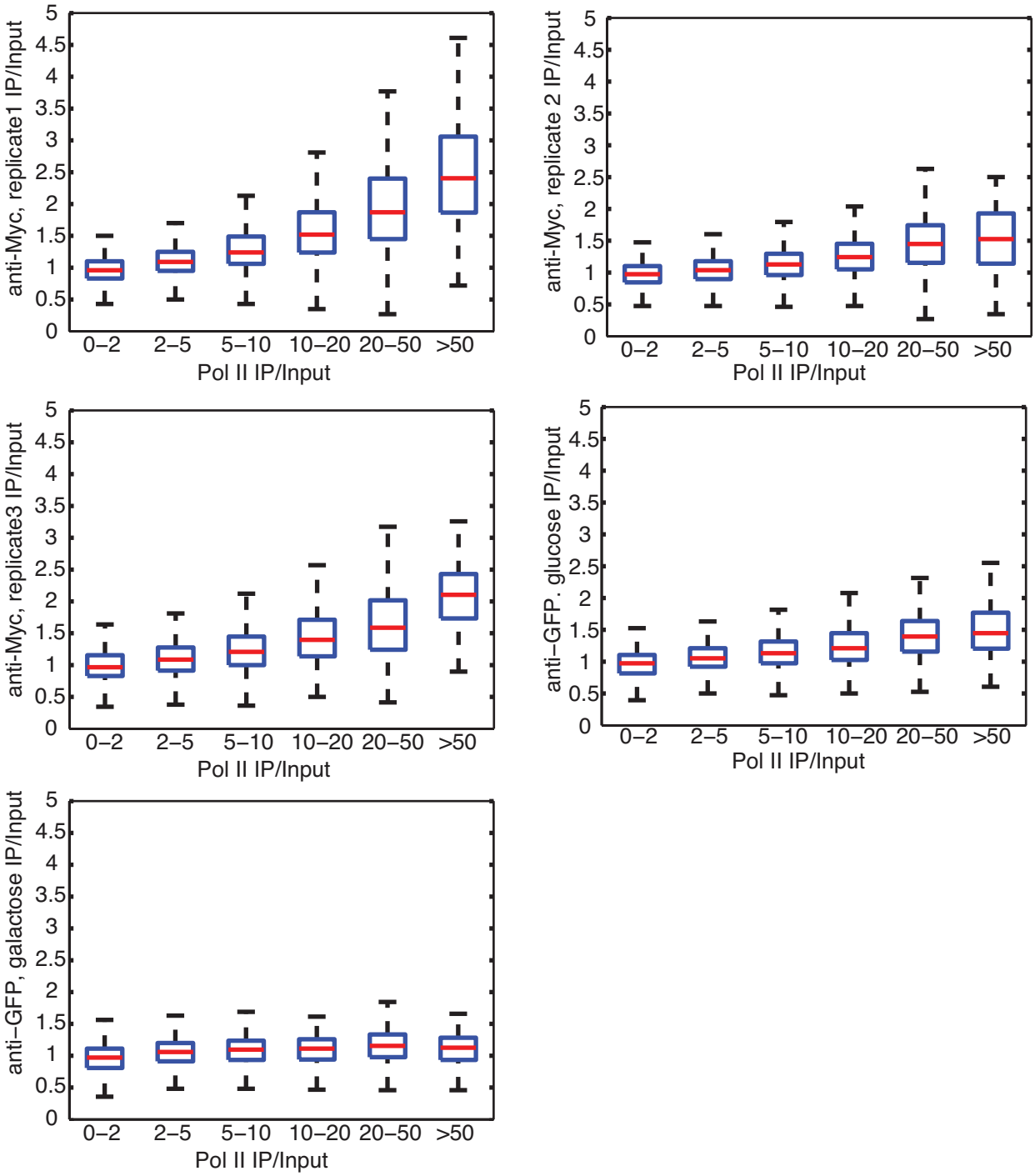

Figure 3.12 Hyper-ChIPability is present but variable in no-tag and no-GFP ChIP-Seq. Boxplots of ChIP-Seq levels for immunoprecipitations in a strain with no protein tags and no GFP, as a function of Pol II enrichment. Shown are 3 biological replicates using anti-Myc antibody, and an IP performed using the anti-GFP antibody for glucose- and galactose-grown cells.

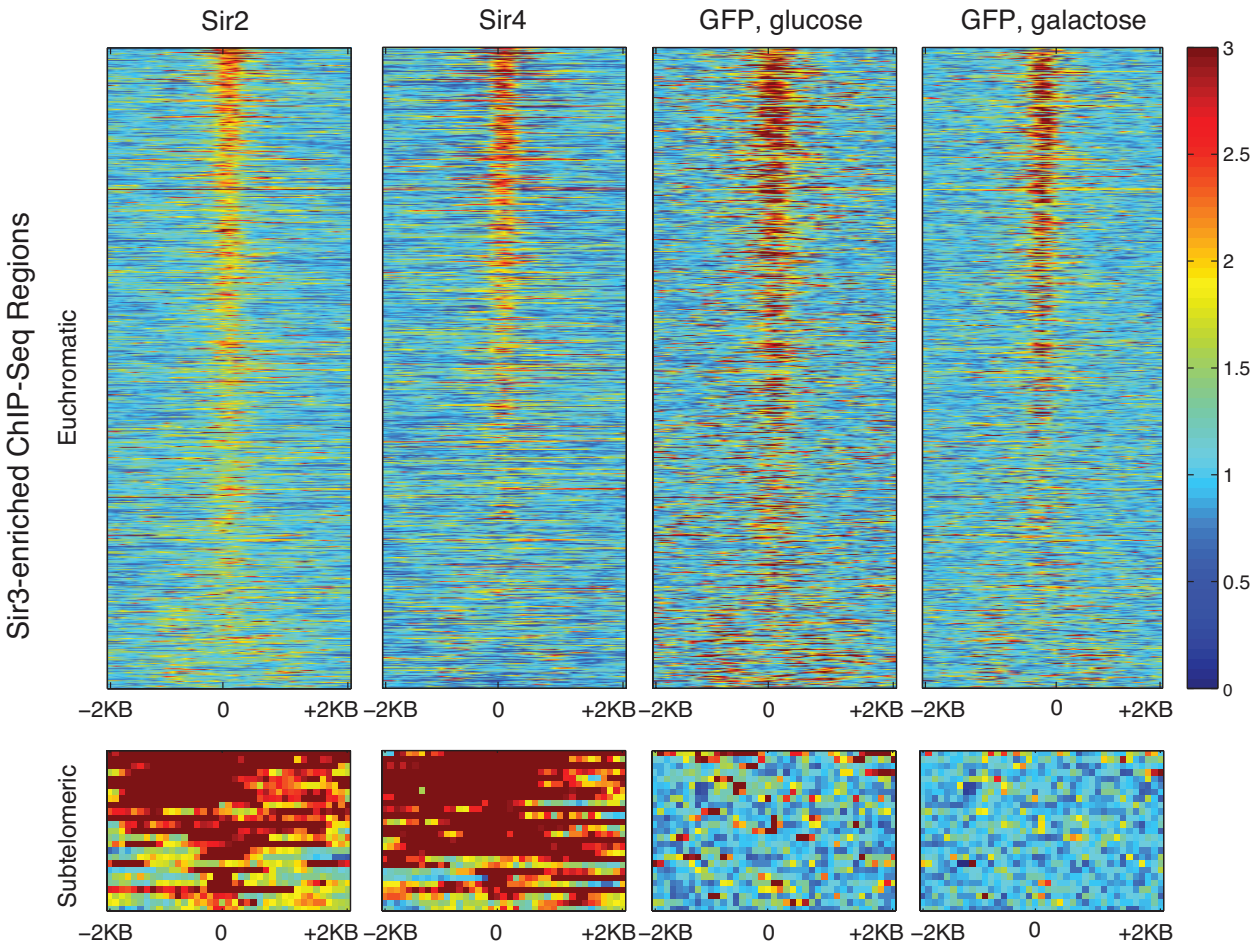

Figure 3.13 GFP and Sir ChIP-Seq levels are correlated only in euchromatin. Heat maps, plotting IP/input ChIP-Seq levels for euchromatic (top) and subtelomeric (bottom) Sir3-enriched regions. On the y-axis, the regions are sorted in descending order of average Sir3 ChIP ratios. On the x-axis, the regions are centered at the Sir3 peak, showing 2KB to the left and right of the Sir3 peak center. The top panels are showing 739 euchromatic regions, 50KB or more from chromosome ends. The lower panels are showing 29 subtelomeric regions within 10KB of chromosome ends.

were filtered out because of high GFP enrichment. Similarly, for Cse4, only 2 out of the 16 centromeric targets (12.5%) had GFP>1.5x, but 61 of the 78 non-centromeric Cse4 targets (78%) had high GFP enrichment (Figure 3.14). These results suggested that it was useful to include a GFP-like ChIP sample as a method for improving the specificity of the ChIP experiments.

3.5 Discussion

Through interrogation of the genome-wide distribution of the yeast Sir-protein silencing complex, Ste12 and Cse4 we found regions that exhibited ChIP enrichment non-specifically. Characterization of these loci revealed that they correlated with regions of high expression. To test whether this enrichment was due to unforeseen biology, we assayed the enrichment of a completely heterologous protein in yeast, GFP, and found that the GFP enrichment paralleled the non-specific signal identified for the 5 endogenous proteins above. Thus, this was a pervasive problem not indicative of new biology, but rather a systematic enrichment across datasets. We term these loci "hyper-ChIPable."

Our results agree with the work of Fan and Struhl, questioning reports of pervasive Mediator complex binding across the yeast genome (Fan and Struhl 2009). The recapitulated hyper-ChIPability of all unrelated proteins that we analyzed, including silencing factors and GFP, make it clear that this spurious signal was not limited to the Mediator, but is a general and underappreciated problem with the ChIP procedure per se.

There are many possible causes of the hyper-ChIPability. The detection of increased enrichment signal in no-tag and no-GFP controls suggests that something is happening during immunoprecipitation specifically, causing chromatin from highly expressed genes to be selectively recovered. The input non-immunoprecipitated samples would of course lack that enrichment, leading to the genesis of biologically artifactual enrichments. It may be that DNA from actively transcribed regions, because of nucleosome depletion, is more exposed and likely to interact with beads or antibodies during the IP through something as simple as electrostatic interactions. Other possibilities include nonspecific interactions between some antibodies and RNA polymerase II and RNA polymerase III.

Regardless of the cause, our findings clearly argue for caution in interpreting ChIP signals in regions that are highly expressed. One way of ascertaining if an enrichment is biologically relevant is to evaluate the underlying expression state of a locus. Genes expressed at the highest levels would be most vulnerable to the artifact described here. This sort of enrichment has already been reported in the literature for Sir proteins. For example, Sir2 was reported to be enriched at *CDC19* by Li et al., a locus we find to be "hyper-ChIPpable," but no biological consequence for this enrichment was found (Li et al. 2013). Additionally, Sir3 was reported to associate with the *GAL1-10* locus specifically upon induction by galactose, which is consistent with our findings that this non-specific enrichment occurs only when genes are highly expressed (Radman-Livaja et al. 2011). By inference, interpreting the enrichment profiles of proteins that cause high-level expression may be especially problematic because the consequence of their function is to set the stage for this artifact. One discriminator of the real signal is that enrichment distributed over a gene body, as shown in the examples here, is indicative of this artifact.

Because input samples do not show the same enrichment as IP, and because no-tag experiments were so variable, obtaining genome-wide ChIP samples for multiple different proteins

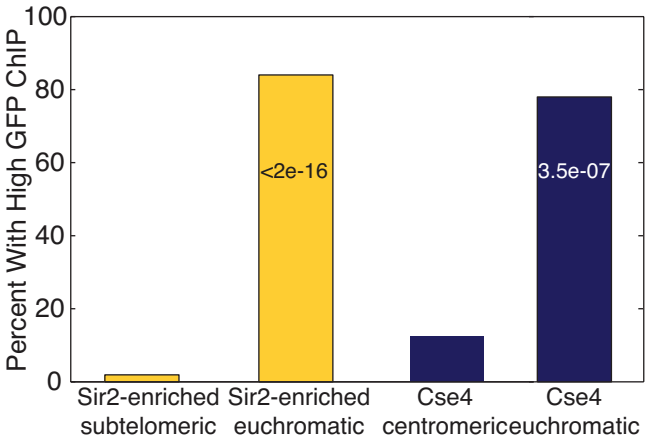

Figure 3.14 Using GFP ChIP-Seq to improve ChIP localization analysis. Percent of Sir- and Cse4-enriched loci with average GFP ChIP ratio>1.5. For Sir proteins, the comparison is between the subtelomeric regions where the Sir proteins are known to localize and the euchromatic loci where the ChIP signal is artifactual. For the Cse4 centromere-binding protein, the comparison is between centromeric and euchromatic/non-centromeric regions. $\chi 2$ p-values are shown within the euchromatic bars.

of different functions would appear to be the safest way to avoid errors of interpretation. A GFP or an endogenous nuclear-localized protein that does not bind to DNA or chromatin, or a protein such as Cse4 known to have just a handful of targets, can serve as a good control to identify biologically meaningless ChIP peaks and to estimate the intrinsic level of hyper-ChIPability of a given locus. More work is necessary to identify the biophysical basis of hyper-ChIPability, but the fundamental biological cause of the artifact is high-level transcription as reported by RNA polymerase ChIP signals, RNA-seq read counts, and directly by the induction-specific appearance of the artifact at the *GAL* genes.

Clearly at highly expressed genes, ChIP can be used successfully to identify proteins critical for the high expression. However, very likely, published reports of ChIP signals at highly expressed genes should be re-analyzed, given the above results. Moreover, given the pervasiveness of this artifact as established here for yeast, it is reasonable to expect that hyper-ChIPability is a general problem of ChIP applications in all organisms. Particularly, the highly expressed HOT regions, where unrelated transcription factors seem to bind without any underlying sequence specificity, may be a consequence of the same hyper-ChIPability. Although there may still be protein- or antibody-specific nuances, a workable normalization standard is needed for each organism and possibly for each tissue type. It would seem that an adequate number of biological repeats of ChIP-Seq analyses of a heterologous protein, such as GFP, to establish the noise level of the hyper-ChIPable peaks would provide a foundation for normalizing ChIP-Seq datasets. The work described here provides such a foundation for yeast studies.

Table 3.3 The 238 Sir-enriched euchromatic loci. Loci are indicated by the chromosome and start and end base pair coordinates using the S288C genome for reference. Each of the values in the Sir2, Sir3, Sir4, Ste12, Cse4 and PolII columns represent the average IP/input value for that region for the indicated protein. The tRNA column indicates if there is a tRNA within the region. The MACS column indicates if the locus was identified by the peak calling program MACS for either the Sir2, Sir3 or Sir4 datasets using the parameters described in the materials and methods.

Chrom	Start	Stop	Sir2	Sir3	Sir4	Ste12	Cse4	Pol II	tRNA	MACS
1	70700	71000	2.38	4.56	2.47	5.64	na	0.13	no	Sir4
1	73100	73500	3.49	3.71	3.04	0.91	4.73	28.23	no	Sir2
1	139200	139300	2.09	2.44	2.04	na	na	na	yes	Sir4
1	143200	143300	2.83	2.46	2.36	na	na	na	no	Sir3,Sir4
2	197400	197800	2.3	3.15	3.19	4.27	2.36	0.19	yes	
2	227000	227100	2.11	2.53	2.7	na	na	na	yes	
2	255300	256800	3.98	5.88	7.81	4.09	2.18	44.65	no	Sir2,Sir3,Sir4
2	266300	266500	2.58	3.35	2.79	5.27	2.36	0.77	yes	
2	347500	347800	3.51	3	3.28	6.18	2.73	0.19	yes	
2	373600	375600	2.81	3.31	3.89	24.55	9.45	55.13	no	Sir2,Sir3,Sir4
2	393000	393700	2.72	3.28	2.81	4.27	3.55	17.06	no	Sir4
2	405900	406000	2.13	2.42	2.51	7.09	1.64	0.31	yes	Sir3
2	477600	479300	3.02	3.62	3.4	na	na	na	no	
2	563400	563500	2.25	2.68	2.51	2.27	2.27	6.02	no	
2	680700	681800	3.17	3.69	4.11	2.55	6.55	75.5	no	
3	66500	68200	2.51	2.74	3.34	1.45	2.82	4.48	no	Sir4
3	78500	78800	2.7	3.47	2.66	2.18	0.36	0.04	no	
3	90800	91100	2.47	3.5	3.04	na	na	na	yes	
3	123500	123700	2.09	2.45	3	3.91	1.27	0.9	yes	
3	127700	127900	2.36	2.55	2.43	5.45	1.64	0.42	yes	
3	142600	142800	2.19	2.36	2.34	na	na	na	yes	
3	199200	200300	2.83	3.38	3.98	na	na	na	no	
3	227000	227300	2.42	3.77	3.64	0.45	0.73	0.33	no	Sir2,Sir4
4	309700	309800	3.28	2.32	2.06	0.82	2.55	19.48	no	
4	331800	331900	2.66	2.44	2.04	na	na	na	no	
4	359600	359800	2.32	3.42	3.36	na	na	na	yes	Sir2,Sir3,Sir4
4	434300	434400	2.17	3.45	2.04	na	na	na	yes	
4	437700	438000	2.11	4.15	2.87	5	3.73	0.23	yes	
4	488800	489000	2.47	3	2.32	4.45	6	8.94	yes	
4	519700	521100	2.75	3.24	2.94	5.91	na	0.31	yes	Sir2
4	555600	555700	2.36	3.58	2.72	na	na	na	no	Sir4
4	568800	569000	2.42	3.22	3.06	11.27	5	0.38	yes	
4	601600	602200	3.13	2.74	3.51	2.27	2.09	10.46	no	
4	619900	620100	2.06	3.23	2.77	5	na	0.48	yes	

4	645200	645400	2.15	3.72	3.34	3.64	1.82	0.17	yes	
4	884300	884600	3.13	5.38	2.72	na	na	na	yes	
4	914400	916300	3.57	3.29	7.15	2.91	4.18	44.42	no	Sir2,Sir3,Sir4
4	981000	981100	2.02	2.69	2.7	na	na	na	yes	
4	1095300	1095400	2.19	3.62	3.34	4.18	3.64	0.9	yes	
4	1150800	1151100	2.53	2.42	3	7.27	5.82	0.69	yes	
4	1236500	1238000	3.57	3.36	2.85	2.27	3.09	27.92	no	Sir2,Sir3,Sir4
4	1257000	1257200	2.89	3.46	3.28	4.55	2.18	0.52	yes	
4	1305600	1305700	2.06	2.08	2.53	2.91	2.82	0.46	yes	
4	1329800	1329900	2.04	2.51	2.81	0.73	2.18	9.83	no	Sir4
4	1402900	1403200	2.55	2.79	2.26	na	na	na	no	
4	1461800	1461900	2.32	3.78	2.53	6.73	na	0.6	yes	
5	61800	62000	2.57	2.87	2.55	na	na	na	yes	
5	79500	79600	2.04	2.96	2.32	0.55	na	9.33	no	
5	86000	86800	5.87	5.44	5.26	9.27	5.55	28.44	yes	
5	100100	100300	2.08	2.88	3.3	3.91	1.91	1.69	yes	Sir2
5	135400	135600	2.74	3.18	2.7	na	na	na	yes	
5	138600	140300	3.26	5.88	3.4	7.45	7.64	32.5	yes	
5	207500	207600	2.45	3.99	2.06	na	na	na	yes	
5	225400	225800	5.64	7.31	15	10.82	0.73	0.13	no	Sir4
5	267500	267700	2.09	2.27	2.26	1.27	3.64	22.69	no	Sir3,Sir4
5	288400	288600	2.09	2.94	2.64	4.45	2.45	0.73	yes	Sir3
5	304400	305600	2.25	2.55	3.09	1.55	6.27	25.46	no	Sir2,Sir3,Sir4
5	322300	322800	2.96	2.85	2.45	1.91	10.91	65.38	no	
5	339800	342000	3.66	3.4	3.49	2.55	1.64	9.54	no	Sir4
5	424800	425100	2.47	3.26	3.38	na	na	na	no	Sir3
5	431100	431500	2.64	2.91	2.72	6.09	3.18	0.85	no	
5	435800	435900	2.43	2.13	2.38	na	na	na	yes	
5	442000	443400	2.75	4.06	4.02	3.55	2.09	0.71	yes	
5	492300	492500	2.64	3.9	2.7	6.36	2.45	2.23	yes	
6	58200	58500	2.64	3.15	2.19	2.36	0.45	0.04	no	Sir4
6	75900	76400	2.26	2.99	3.21	1.27	1.45	5.56	no	Sir4
6	101400	101600	2.42	2.55	2.49	5	2.09	1.15	yes	
6	137400	137500	2.64	2.85	2.7	3.09	3.45	0.27	yes	
6	158000	158100	2.06	3.53	2.55	na	na	na	yes	
6	167500	167700	2.74	4.26	2.6	na	na	na	yes	
6	180900	181200	2.75	3.64	3.51	7.91	na	0.42	yes	
6	191500	191700	2.45	3.53	2.85	2.82	4.55	0.48	yes	
7	73800	74000	2.53	2.76	3.17	na	na	na	yes	
7	115600	115700	2.3	2.69	2.13	2.36	0.73	0.15	yes	
7	145400	145500	2.6	2.24	2.66	na	na	na	no	Sir4

7	205600	205700	2	2.56	2.34	17.18	2.91	0.21	yes	
7	278500	278600	2.38	2.68	2.11	na	na	na	no	
7	311800	311900	2.06	2.79	2.36	2.45	17.27	119.73	no	Sir2,Sir4
7	328500	328800	2.98	3.31	2.79	10.45	5	0.73	yes	
7	365500	365600	2.21	2.95	2.13	na	na	na	no	Sir4
7	412400	412500	2.09	2.27	2.04	3.91	3.82	0.85	yes	
7	423000	423300	2.23	4.27	2.98	na	na	na	yes	
7	440700	441000	2.53	3.71	2.49	na	na	na	yes	Sir2,Sir3
7	476800	477000	2.26	2.21	2.21	1.09	4.73	13.31	no	Sir4
7	479800	482400	3.26	3.15	3.21	1.45	11.55	90.44	no	Sir4
7	531600	531800	3.36	4.91	3.02	3.36	3	0.52	yes	
7	541700	541900	2.7	2.87	2.62	na	na	na	yes	
7	561600	561900	2.43	2.9	2.57	na	na	na	yes	
7	599600	601000	2.28	2.76	2.45	1.18	2.36	17.63	no	Sir2,Sir3,Sir4
7	609400	611600	2.83	3.44	3.68	9	2.73	34.56	no	Sir2, Sir3,Sir4
7	661700	661900	2.26	2.83	2.36	2.82	2.82	0.1	yes	
7	700600	701200	3.21	3.35	3.6	10.18	2.82	2	yes	Sir4
7	731100	731200	2.34	3.46	3.47	na	na	na	yes	
7	774300	774500	2.58	3.18	3.26	9.82	2.91	0.19	yes	
7	779500	779700	2.3	2.69	3.28	8.91	2.73	0.15	yes	
7	785100	785200	2.08	2.27	2.89	na	na	na	no	
7	794300	794600	2.47	3.04	2.47	4.36	5.55	2.88	yes	
7	828700	828800	2.04	3.05	2.7	2.91	na	2.98	yes	
7	846900	847900	2.19	3.37	2.64	1.45	1.82	4.69	no	Sir4
7	876300	876600	4.21	3.6	3.94	na	na	na	yes	Sir4
7	878700	878800	2.09	2.17	2.43	4.27	0.82	0.15	yes	Sir4
7	882500	883300	4.42	4.29	3.19	2.91	10.45	56.54	no	
7	930900	931200	3.4	2.86	3.09	4.55	na	1.42	yes	
7	939500	939600	2.32	3.12	2.09	na	na	na	no	
7	958900	959000	2.02	2.9	2.51	3.64	2	4.13	no	Sir2,Sir3,Sir4
7	961200	961300	2.51	2.97	2.13	2.27	na	59.08	no	
7	1004300	1004400	2.25	2.19	2.79	8.73	na	0.08	yes	
8	85300	85400	2.09	3.04	2.62	na	na	na	yes	
8	119700	121400	2.91	3.86	3	3.82	7.36	16.08	no	
8	133000	134500	2.68	3.54	3.36	1.55	2.45	0.08	yes	
8	237100	238100	2.62	3.12	3.09	1.09	2	2.19	yes	
8	297000	297200	2.47	2.19	2.89	10.82	0.27	0.17	no	Sir4
8	358500	358600	2.68	2.51	2.83	na	na	na	yes	
8	381700	382000	2.89	2.97	2.4	na	na	na	no	Sir2,Sir3,Sir4
8	388900	389100	2.6	2.95	2.66	4.91	2	0.27	yes	
8	452600	452800	2.36	3.09	2.81	0.73	na	49.17	no	Sir4

8	467100	467200	2.43	2.88	2.17	4.45	na	0.98	yes	
8	475600	475900	2.45	4.26	3.83	2.73	4	0.35	yes	
9	175000	175200	2.02	3.09	2.21	7.73	4	2.46	yes	Sir4
9	183400	183500	2.11	2.73	2.51	4.91	2.64	0.21	yes	
9	210700	210800	2	2.74	2.4	2.09	9.09	13.1	yes	
9	300300	300500	2.6	2.85	2.55	na	na	na	yes	
9	336400	336500	2.42	2.56	2.32	5.45	4.09	1.1	yes	
10	116000	116100	2.02	2.05	2	4.09	3.36	0.88	yes	
10	120800	122300	5.89	5.45	5.36	0.91	3.73	34.31	no	Sir2,Sir4
10	139400	140100	3.06	3.41	3.79	na	na	na	no	
10	204600	204800	2.74	2.92	2.49	3.91	2.55	0.29	yes	
10	228000	228300	3.43	2.94	2.53	1.91	7.55	116.81	no	
10	234000	234100	2.25	2.46	2.53	8.45	3.73	5.38	yes	
10	354300	355600	2.51	3.23	2.51	6.36	3.36	0.13	yes	
10	391000	391200	2.13	2.65	2.98	3.27	0.73	0.1	yes	
10	422900	424700	2.34	2.82	2.89	3.91	4.73	3.42	yes	
10	526700	526900	2.23	2.26	3.09	na	na	na	no	Sir4
10	538400	538700	2.45	3.27	2.6	3.36	2.45	0.27	yes	
10	541500	543100	2.51	3.03	2.3	3.09	5	3.35	yes	
10	663900	664000	2.38	2.55	2.98	0.91	2.64	35.02	no	
11	74600	74800	2.09	2.99	2.62	7.36	4.91	3.48	yes	
11	202700	202800	2.06	2.77	3.77	2.45	3.73	1.48	yes	Sir4
11	219500	219700	2.32	2.67	2.6	7.09	3.64	0.77	yes	
11	258900	259400	2.87	2.41	4.21	2.82	3.55	26.4	no	Sir4
11	302500	302700	2.09	2.6	2.45	4	na	0.08	yes	
11	326000	326100	2.77	2.85	2.66	2.73	na	57.83	no	
11	458100	458400	2.58	3.68	2.49	na	na	na	yes	
11	490500	490700	2.74	2.76	2.4	2.82	2.55	0.54	yes	
11	513000	513100	2.62	2.88	2	4.36	1.45	0.88	yes	
11	516200	517800	3.77	3.15	3.15	60.91	1.64	3.33	yes	
11	578500	578700	2.4	2.9	2.81	6.27	1.55	0.96	yes	Sir4
12	86900	87000	3.09	3.38	2.17	7.82	0.45	0.85	no	Sir2,Sir4
12	167900	168100	2.11	2.58	2.45	3.36	2.18	1.06	yes	
12	232300	233200	2.64	3.08	2.94	4.27	8.27	59.46	no	
12	258000	259100	2.53	4.27	3.02	2	1.73	9.19	no	Sir3,Sir4
12	283600	283700	2.36	2.09	2.45	na	na	na	no	
12	369400	370200	5.87	7.91	5.77	6.64	5.27	52.08	no	Sir2,Sir4
12	374400	374500	2.64	2.44	2.85	1.45	2.09	1.27	yes	
12	448600	469000	74.7	6.18	5.32	10.09	5.55	2	yes	Sir2
12	472500	472600	2.66	2.79	2.11	na	na	na	no	Sir4
12	490200	490300	2.98	2.01	2.11	na	na	na	no	

12	540700	541000	2.66	2.97	3.49	2	1.18	3.6	no	
12	605300	605500	2.36	3.12	2.4	2.82	2.91	0.23	yes	
12	638900	639800	2.25	2.69	2.7	1.91	10.36	67.23	no	Sir2,Sir4
12	729400	729600	2.13	2.87	2.62	1.45	3.27	22.63	no	Sir4
12	732100	732300	2.36	2.76	2.36	1	1	0.13	yes	Sir4
12	784300	784500	2.45	2.88	3	9.27	2.18	0.15	yes	
12	794000	794100	2.72	2.67	2.81	7.73	na	1.44	yes	
12	797100	797300	2.51	3.1	2.19	7	3	1.1	yes	
12	806900	807000	2.04	2.19	2.09	1.09	na	39.46	no	
12	818500	818700	2.79	3.23	2.6	10.91	2	4.13	yes	
12	837600	839400	5.19	5.1	4.83	2.73	13	93.63	no	Sir4
12	857200	857300	2	2.01	2.15	2.45	3.55	43	no	
12	875300	875600	2.36	2.62	2.57	10.18	1.91	1.77	yes	
12	962900	963000	3.19	2.85	3.15	4.55	2.27	1.31	yes	
12	976100	976200	2.49	5.38	2	na	na	na	yes	
13	92000	92100	2.04	2.15	2.26	6.09	1	0.21	no	Sir3,Sir4
13	131700	132000	3.4	3.06	2.85	4.27	na	0.17	yes	
13	183800	183900	2.91	2.79	3.49	na	na	na	yes	
13	196000	196100	2.02	2.54	2.19	na	na	na	yes	
13	259200	259300	2.42	2.4	2.53	5.27	5	1.13	yes	
13	297200	298700	7.08	3.56	3.94	5.18	na	64.4	no	Sir4
13	372500	372600	2.13	2.03	2.26	5.09	4.64	2.52	yes	
13	420500	420700	2.6	3.27	3.19	5.18	3.91	0.21	yes	
13	463500	463800	2.15	3.87	2.36	3.64	3.18	0.77	yes	
13	504800	505200	2.36	3.01	3.49	1.36	na	0.04	yes	
13	511700	512000	2.66	4.87	2.85	na	na	na	no	Sir2,Sir4
13	556300	556500	2.57	2.42	2.72	1.36	1.45	4.21	no	
13	572900	573100	2.25	2.38	2.09	1.91	na	1.79	yes	
13	586700	586900	2.47	2.37	2.3	na	na	na	yes	
13	626400	626700	2.74	2.97	2.81	na	na	na	no	
13	652400	652800	2.49	3.54	2.45	2	4.18	73.04	no	Sir3,Sir4
13	747900	748000	2.75	2.28	2.09	na	na	na	yes	
13	774700	775300	3.57	8.78	3.4	4.82	0.73	1.52	no	Sir4
13	808200	808300	2.72	2.42	2.32	na	na	na	yes	
13	837800	838100	2.64	3.88	2.38	4.91	na	0.69	yes	
14	88800	89600	2.94	3	2.45	8.09	12.27	118.77	no	Sir2
14	102600	105000	2.6	2.82	2.66	5.64	3.45	2.1	yes	
14	230100	230400	3.36	2.86	3.38	0.91	na	24.5	no	Sir4
14	500200	500700	3.98	4.63	3.3	na	na	na	no	Sir2
14	568100	568300	2.55	3	2.87	na	na	na	yes	
14	575300	577200	3	3.49	4.6	4.55	4.91	81	no	Sir2,Sir4

14	631700	632000	2.58	3.53	3.09	12.73	5.18	0.17	yes	
15	110300	111200	3.13	4.86	3.36	5.18	2.36	30.46	yes	
15	226600	226700	2.11	2.59	2.45	5.82	2.27	0.48	yes	
15	282100	282300	2.4	2.26	2.77	3.09	3.27	2.08	yes	
15	288200	288300	2.23	3.05	2.77	9.18	5.18	4.27	yes	
15	340200	340400	2.42	2.5	2.85	3	3.64	1.33	yes	
15	438600	438800	2.94	3.55	2.96	6.64	3.27	1.67	yes	
15	445100	446000	2.26	3.04	3.34	0.91	7.45	56.65	no	Sir4
15	464400	464600	2.36	3.45	2.89	4	7.45	0.48	yes	
15	487400	487500	2.25	3.56	2.49	12.36	1.45	0.15	yes	Sir3
15	571900	572200	2.32	2.67	2.94	8.55	2.73	14.5	yes	
15	594300	594500	3.47	3	2.57	3.73	4.36	0.81	yes	
15	620100	620500	2.06	2.83	2.85	1	2.91	37.71	no	Sir2,Sir3,Sir4
15	663900	664000	2.06	2.36	2.66	na	na	na	yes	
15	710100	710300	2.25	3.69	2.6	na	na	na	yes	
15	780100	780900	4.15	6.09	3.96	2.82	10.18	124.44	no	Sir2,Sir3,Sir4
15	832400	832700	2.42	2.69	3.83	3.73	5.45	81.83	no	Sir2,Sir3,Sir4
15	976300	976700	3.19	3.76	2.98	na	na	na	yes	
15	980700	980900	2.34	2.78	2.47	7	3	1.23	yes	
15	1028100	1028200	2.09	2.03	2.3	1	5.18	31.21	no	Sir2,Sir3,Sir4
16	108900	110500	2.19	2.71	2.74	1.18	1.64	10.08	no	Sir2,Sir3,Sir4
16	173600	173700	2.72	3.42	2.36	na	na	na	no	
16	210200	210300	2.68	3.58	2.02	4.45	2.09	1.13	yes	
16	304000	304100	2.26	2.5	2.43	0.82	5.09	46.38	no	
16	339000	339100	2.13	2.53	2.17	2.09	1.36	0.46	yes	Sir4
16	405100	405200	2.62	2.64	2.13	na	na	na	no	
16	435900	436100	2.47	2.71	3.19	4.36	4.82	0.88	yes	
16	560200	560300	2.23	2.87	2.47	na	na	na	yes	
16	572200	572500	2.85	3.17	2.96	7.36	3.82	0.25	yes	Sir2, Sir3,Sir4
16	582100	582200	2.25	2.47	2.02	6.27	na	1.54	yes	
16	643300	643400	3.26	2.37	2.79	2.91	3.45	9.73	no	
16	646000	646400	2.43	2.65	2.72	2.18	15.27	25.46	no	
16	689500	689700	2.43	2.58	2.83	6.73	4.55	0.42	yes	
16	700600	702100	3.58	2.96	3.11	na	na	na	no	
16	744200	744400	2.34	3.24	3.11	na	na	na	yes	
16	789600	790000	16.89	31.4	46.89	28.09	0.55	1.48	no	Sir2,Sir3,Sir4
16	810600	810900	2.11	2.95	2.7	na	na	na	yes	Sir4
16	819400	824400	3.3	4.04	4.13	5.82	5.73	14.5	yes	
16	856900	857000	2.06	2.76	2.3	5.91	3.27	3.19	yes	
16	860300	860400	2.04	2.68	2.81	5.45	1.91	0.46	yes	

Chapter 4: Mutation of a Non-Sirtuin Histone Deacetylase Restores Silencing Independently of Sir2 Catalytic Activity

4.1 Abstract

Sir2's catalytic activity is necessary for silencing and the only known role for this catalytic activity in yeast silencing is to deacetylate H3 and H4 N-terminal tails, creating high-affinity binding sites for the Sir complex. This histone deacetylation model makes the simple prediction that preemptively removing Sir2's H3 and H4 acetyl substrates should restore silencing in the Sir2 catalytic mutant. However, this is not the case. We conducted a forward genetics screen to determine what part of Sir2's catalytic activity has not been accounted for in silencing. We found that mutation of a non-sirtuin histone deacetylase, Rpd3, restored Sir protein based silencing in the absence of Sir2's catalytic activity, yet depended upon the presence of the catalytically inactive Sir2 protein. Interestingly, this restoration of silencing by the Rpd3 mutant was dependent on another sirtuin histone deacetylase, Hst3. Silencing restoration by Rpd3 was independent of known Rpd3 and Hst3 histone substrates, resulting in investigation of changes in protein acetylation dependent on Rpd3 and Hst3. This study implicated the acetylation of a non-histone substrate as potentially important for silencing.

4.2 Introduction

Sir2 is the founding member of the sirtuin enzyme family, which deacetylate acetylated lysines. Unlike other protein deacetylases that catalyze the hydrolysis of acetyl-lysine, sirtuins couple this lysine deacetylation to NAD^+ hydrolysis (Sauve et al. 2006). Utilizing this high-energy cofactor for deacetylation allows sirtuins to be in tune with and potentially regulated by the energy balance and/or redox balance within the cell. Sirtuins are found to regulate diverse processes across all biological kingdoms—ranging from life-span regulation and fat metabolism to chromatin modifications. *S. cerevisiae* have five sirtuins: Sir2 and four *H*omologs of *Sir2*, Hst 1-4, which are involved in cell cycle regulation and chromatin modification and perhaps other functions as well.

Of the five yeast sirtuins, Sir2, the catalytic member of the Sir protein silencing complex, is the most well studied. Sir2's catalytic activity is necessary for silencing as a structurally intact, but catalytically inactive Sir2 allele, *sir2N345A*, cannot support gene silencing (Imai et al. 2000). Multiple studies indicate that the catalytic activity of Sir2 is necessary for the deacetylation of histone H4 N-terminal lysine residue 16 (H4K16) at silent loci. Point mutations changing H4K16 to glutamine, which mimics the hyperacetylated state, disrupt silencing at *HML* (Park and Szostak 1990). This H4K16 to glutamine silencing defect can be suppressed by a point mutation in Sir3, indicating that acetylation of H4K16 likely disrupts the Sir3-nucleosome association (Johnson et al. 1990). More recent structural studies of the Sir3 BAH domain co-crystallized with the nucleosome core confirm this association (Armache et al. 2011; Wang et al. 2013). Additionally, Sir2 shows preference for deacetylation of H4K16 in vitro (Imai et al. 2000) and there is evidence that Sir2 deacetylates H4K16 in vivo. Deletion of the MYST-family histone acetyltransferase, Sas2, results in decreased H4K16-acetyl at the boundaries of silenced loci (Suka et al. 2002; Kimura et al. 2002).

This decreased acetylation is dependent on Sir2, indicating that Sir2 and Sas2 likely have opposing activities on H4K16 acetylation at silenced loci.

This evidence for Sir2 deacetylation of H4K16 combined with other biochemical and genetic studies led to the nucleation and spreading model for yeast silencing: Sir2, Sir3 and Sir4 are recruited to the silent mating loci through interactions with proteins that bind the silencers, Abf1, Rap1 and ORC. Once nucleated to the silencers, Sir2 deacetylates the neighboring nucleosome at H4K16 to allow the Sir complex to bind to the hypoacetylated nucleosome. Iterative rounds of deacetylation result in the spreading of Sir protein complexes across the silenced loci, critical for silencing at *HML* and *HMR* (Rusché et al. 2002; Hoppe et al. 2002). The nucleation and spreading model as described above makes the simple prediction that although Sir2's catalytic activity is necessary, it should be bypassed by removal of the H4K16 acetylation. However, this prediction is not observed. Preemptively removing H4K16-acetyl either by deleting *SAS2*, the histone acetyl transferase that acetylates H4K16, or by expressing H4K16R, mimicking the hypoacetylated state, does not restore the silencing defect of the Sir2 catalytic mutant, *sir2N345A* (Yang and Kirchmaier 2006). This silencing defect is not due to lack of affinity between the Sir complex and H4K16R as Sir proteins associate, as assayed by chromatin immunoprecipitation, but do not silence, in the *sir2N345A* H4K16R mutant. Thus, the model is missing a key role for Sir2's catalytic activity in silencing.

There are several different suggestions as to what role of Sir2's catalytic activity has not been accounted for. For example, Sir2 may be critical for the deacetylation of other histone residues that are not targets of Sas2. Besides the H3 and H4 lysine N-terminal tail residues, a core lysine acetylation, H3K56, has been implicated in silencing (Xu et al. 2007). H3K56 is acetylated in a cell-cycle dependent manner, peaking during S-phase and is important for the deposition of newly synthesized histones into chromatin (Masumoto et al. 2005). It is thought to be deacetylated after deposition into the chromatin by two other sirtuins, Hst3 and Hst4 (Celic et al. 2006). Interestingly, a point mutation in H3K56 disrupts telomeric silencing (Xu et al. 2007; Yang et al. 2008). Additionally, H3K56ac is more abundant at silenced loci when *SIR2* is deleted, suggesting a possible role for deacetylation at this core position in silencing. However, there is contradictory evidence as to whether Sir2 can deacetylate H3K56 in vitro (Xu et al. 2007; Oppikofer et al. 2011). Thus this mark's role in silencing has remained controversial. Another unaccounted role for Sir2 in silencing is that Sir2 may deacetylate a non-histone protein. A recent study reported Sir2-dependent deacetylation of a non-histone protein in yeast, Ifh1 and Pck1 (Downey et al. 2013; Lin et al. 2009). Thus, although Sir2 has been classically defined as a histone deacetylase, there are non-histone protein acetylations regulated by Sir2, and one or more of these could be required for silencing.

The sirtuin catalytic reaction, rather than a specific deacetylation per se, could be necessary for silencing. Sirtuins couple the lysine deacetylation reaction to the hydrolysis of NAD^+, producing a small molecule byproduct, 2-O-Acetyl-ADP-Ribose (OAAR) and nicotinamide (Tanner et al. 2000). One study found that OAAR can promote structural changes in the Sir protein complex as assayed by electron microscopy (Liou et al. 2005). Additionally, as measured by electromobility-shift assays, addition of OAAR increases the affinity for the Sir protein complex for reconstituted chromatin (Martino et al. 2009). These data suggest that OAAR could promote the association and a critical last compaction of chromatin. This possible interaction between the Sir complex and the sirtuin metabolite was suggested to be mediated by a putative OAAR binding pocket in Sir3 (Ehrentraut et al. 2010). However, crystallization of the AAA+ ATPase-like domain of Sir3 revealed

that it would preclude nucleotide binding and mutations in this region of Sir3 have little effect on silencing in vivo (Ehrentraut et al. 2011). Additionally, other studies have shown that that a sirtuin reaction is not necessary for silencing. Tethering of a non-sirtuin histone deacetylase domain to Sir3 bypasses the need for Sir2 in silencing, although not to wild-type levels (Chou et al. 2008). However, in the mammalian X-chromosome inactivation, the histone variant macroH2A binds OAAR generated from the sirtuin SIRT1 with a K_d that is on the same order of magnitude as the concentration of OAAR in a cell (Kustatscher et al. 2005; Lee et al. 2008), providing precedent for this small molecule to be involved in chromatin silencing. Thus, it is unclear as to whether this metabolite is required for silencing in vivo.

Since there are many possible unaccounted roles for Sir2's catalytic activity in silencing, we have conducted a forward genetic screen. Yeast expressing the catalytically inactive allele of Sir2, *sir2N345A* as the only source of Sir2, and in which the H4K16-acetyl has been preemptively removed by deletion of *SAS2*, were mutagenized, recovering five mutants that partially restored silencing in the absence of Sir2 catalytic activity. Two of these mutants contained point mutations of the non-sirtuin histone deacetylase Rpd3. Rpd3 has been previously identified as antagonistic to silencing by restricting the spread of Sir proteins at the boundary of silent chromatin domains (Sun and Hampsey 1999; Zhou et al. 2009). Analysis of the Rpd3 mutants revealed that they were likely loss-of-function mutations that restore Sir dependent silencing. Interestingly, this mutant specifically requires the activity of Hst3 to restore silencing, revealing a role for another sirtuin in silencing. Point mutant analysis indicated that the known histone targets of Rpd3 and Hst3 are not involved in Rpd3's silencing restoration, prompting identification of non-histone acetylations dependent on Rpd3 and Hst3. This study has identified suppressor mutations that are able to silence independently of Sir2's catalytic activity, further elucidating the catalytic role for the highly conserved sirtuin enzymatic group.

4.3 Materials and Methods

Yeast Strains, Plasmids and Culture All yeast strains were derived from the W303 background and genotypes are indicated in Table 4.1. Deletions were constructed through one-step integration of knockout cassettes (Longtine et al. 1998). The *hmr-a1Δ::URA3* reporter was previously described (Zill et al. 2010). All plasmids used are indicated in Table 4.2. Plasmids bearing the histone point mutations were introduced into strains containing a pRS316 plasmid bearing wild-type H3 and H4 (pJR2657). Plasmid swap using 5-FOA counter selection against the pRS316 plasmid was used to recover yeast with only the mutant histone plasmid. To determine silencing phenotype, fivefold serial dilutions of overnight cultures was spotted onto appropriate media at an initial approximate density of $4x10^7$/ml as in (Zill et al. 2010). To test for mating ability, cells of the strain of interest were manually mixed on a YPD plate with an alpha mating tester (JRY2728) or the a-mating tester (JRY2726). These cell mixtures were grown overnight at 30°C. After this incubation the cell mixtures were replica plated onto minimal medium plates (YM), which selects for successful mating events.

EMS mutagenesis EMS mutagenesis was conducted as described (Amberg et al. 2005). Briefly, 10 OD Units (Abs = 600 nm) were pelleted, washed with distilled water and resuspended in 0.1 M sodium phosphate buffer (pH 7). 30µl of ethylmethanesulfonate was added to the sample and

Table 4.1 Yeast strains used in chapter 4

Name	Genotype	Alias
JRY2726	*MAT**a** HIS34-1*	
JRY2728	*MATα HIS34-1*	
JRY9097	*MAT**a**,ADE2, lys2-, sas2Δ::Hyg, hmr-**a**1Δ::URA, Sir2Δ::HIS3, LEU2::Sir2N345A*	DTY22
JRY9567	*MAT**a**,ADE2, lys2-, sas2Δ::Hyg, hmr-**a**1Δ::URA, Sir2Δ::HIS3, LEU2::Sir2N345A, sum1-1* *derived from EMS mutagenesis	DTY47
JRY9568	*MAT**a**,ADE2, lys2-, sas2Δ::Hyg, hmr-**a**1Δ::URA, Sir2Δ::HIS3, LEU2::Sir2N345A, rpd3P264L* *derived from EMS mutagenesis	DTY48
JRY9569	*MAT**a**,ADE2, lys2-, sas2Δ::Hyg, hmr-**a**1Δ::URA, Sir2Δ::HIS3, LEU2::Sir2N345A, rpd3P397H* *derived from EMS mutagenesis	ADY64
JRY9570	*MAT**a**,ADE2, lys2-, sas2Δ::Hyg, hmr-**a**1Δ::URA, Sir2Δ::HIS3, LEU2::Sir2N345A, orc3A333V* *derived from EMS mutagenesis	DTY60
JRY9571	*MAT**a**,ADE2, lys2-, sas2Δ::Hyg, hmr-**a**1Δ::URA, Sir2Δ::HIS3, LEU2::Sir2N345A, ems mutant* *derived from EMS mutagenesis	DTY55
JRY9572	*MATα , ade2-1, LYS, sas2Δ::Hyg, hmr-**a**1Δ::URA, Sir2Δ::HIS3, LEU2::Sir2N345A*	DTY149
JRY9573	*MAT**a**, ADE2, lys2-, sas2Δ::Hyg, hmr-**a**1Δ::URA, Sir2Δ::HIS3, LEU2::Sir2N345A, rpd3Δ::Kan*	DTY164
JRY9574	*MATα , ade2-1, LYS, sas2Δ::Hyg, hmr-**a**1Δ::URA, Sir2Δ::HIS3, LEU2::Sir2N345A, , rpd3Δ::Kan*	DTY165
JRY9575	*MAT**a**, ADE2, lys2-, sas2Δ::Hyg, hmr-**a**1Δ::URA, Sir2Δ::HIS3, LEU2::Sir2N345A, pho23Δ::Nat*	DTY229
JRY9576	*MAT**a**, ADE2, lys2-, sas2Δ::Hyg, hmr-**a**1Δ::URA, Sir2Δ::HIS3, LEU2::Sir2N345A, sap30Δ::Nat*	DTY231
JRY9577	*MAT**a**, ADE2, lys2-, sas2Δ::Hyg, hmr-**a**1Δ::URA, Sir2Δ::HIS3, LEU2::Sir2N345A, eaf3Δ::Nat*	DTY237
JRY9578	*MAT**a**, ADE2, lys2-, sas2Δ::Hyg, hmr-**a**1Δ::URA, Sir2Δ::HIS3, LEU2::Sir2N345A, rco1Δ::Nat*	DTY233
JRY9579	*MAT**a**, ADE2, lys2-, sas2Δ::Hyg, hmr-**a**1Δ::URA, Sir2Δ::HIS3, LEU2::Sir2N345A, sin3Δ::Nat*	DTY235
JRY9580	*MAT**a**,ADE2, lys2-, sas2Δ::Hyg, hmr-**a**1Δ::URA, Sir2Δ::HIS3, LEU2::Sir2N345A, rpd3P264L, sir3Δ::Nat*	DTY223
JRY9581	*MAT**a**,ADE2, lys2-, sas2Δ::Hyg, hmr-**a**1Δ::URA, Sir2Δ::HIS3, LEU2::Sir2N345A, rpd3P264L, sir3Δ::Nat*	DTY224
JRY9582	*MAT**a**, ADE2, lys2-, sas2Δ::Hyg, hmr-**a**1Δ::URA, Sir2Δ::HIS3, LEU2::Sir2N345A, rpd3Δ::Kan, sir3Δ::Nat*	DTY221
JRY9583	*MAT**a**, ADE2, lys2-, sas2Δ::Hyg, hmr-**a**1Δ::URA, Sir2Δ::HIS3, LEU2::Sir2N345A, rpd3Δ::Kan, sir3Δ::Nat*	DTY222
JRY9584	*MAT**a**,ADE2, lys2-, sas2Δ::Hyg, hmr-**a**1Δ::URA, Sir2Δ::HIS3, LEU2::Sir2N345A, rpd3P264L, sir4Δ::Nat*	DTY227
JRY9585	*MAT**a**,ADE2, lys2-, sas2Δ::Hyg, hmr-**a**1Δ::URA, Sir2Δ::HIS3, LEU2::Sir2N345A, rpd3P264L, sir4Δ::Nat*	DTY228
JRY9586	*MAT**a**, ADE2, lys2-, sas2Δ::Hyg, hmr-**a**1Δ::URA, Sir2Δ::HIS3, LEU2::Sir2N345A, rpd3Δ::Kan, sir4Δ::Nat*	DTY225

JRY9587	*MAT**a**, ADE2, lys2-, sas2Δ::Hyg, hmr-**a**1Δ::URA, Sir2Δ::HIS3, LEU2::Sir2N345A, rpd3Δ::Kan, sir4Δ::Nat*	DTY226
JRY9588	*MATα, ADE2, lys2-, sas2Δ::Hyg, hmr-**a**1Δ::URA, sir2Δ::HIS3, leu2-3,112, rpd3Δ::Kan*	DTY199
JRY9589	*MATα, ADE2, lys2- sas2Δ::Hyg, hmr-**a**1Δ::URA, sir2Δ::HIS3, leu2-3,112, rpd3Δ::Kan*	DTY202
JRY9590	*MAT**a**,ADE2, lys2-, sas2Δ::Hyg, hmr-**a**1Δ::URA, Sir2Δ::HIS3, LEU2::Sir2N345A, hst1Δ::Kan*	DTY175
JRY9591	*MAT**a**,ADE2, lys2-, sas2Δ::Hyg, hmr-**a**1Δ::URA, Sir2Δ::HIS3, LEU2::Sir2N345A, hst2Δ::Kan*	DTY354
JRY9592	*MAT**a**,ADE2, lys2-, sas2Δ::Hyg, hmr-**a**1Δ::URA, Sir2Δ::HIS3, LEU2::Sir2N345A, hst3Δ::Kan*	DTY176
JRY9593	*MAT**a**,ADE2, lys2-, sas2Δ::Hyg, hmr-**a**1Δ::URA, Sir2Δ::HIS3, LEU2::Sir2N345A, hst4Δ::Kan*	DTY177
JRY9594	*MAT**a**,ADE2, lys2-, sas2Δ::Hyg, hmr-**a**1Δ::URA, Sir2Δ::HIS3, LEU2::Sir2N345A, rpd3P264L, hst1Δ::Nat*	DTY184
JRY9595	*MAT**a**,ADE2, lys2-, sas2Δ::Hyg, hmr-**a**1Δ::URA, Sir2Δ::HIS3, LEU2::Sir2N345A, rpd3P264L, hst2Δ::Nat*	DTY356
JRY9596	*MAT**a**,ADE2, lys2-, sas2Δ::Hyg, hmr-**a**1Δ::URA, Sir2Δ::HIS3, LEU2::Sir2N345A, rpd3P264L, hst3Δ::Nat*	DTY186
JRY9597	*MAT**a**,ADE2, lys2-, sas2Δ::Hyg, hmr-**a**1Δ::URA, Sir2Δ::HIS3, LEU2::Sir2N345A, rpd3P264L, hst4Δ::Nat*	DTY187
JRY9598	*MAT**a**, ADE2, lys2-, sas2Δ::Hyg, hmr-**a**1Δ::URA, Sir2Δ::HIS3, LEU2::Sir2N345A*	DTY406
JRY9599	*MAT**a**, ADE2, LYS, sas2Δ::Hyg, hmr-**a**1Δ::URA, Sir2Δ::HIS3, LEU2::Sir2N345A*	DTY407
JRY9600	*MAT**a**, ADE2, lys2-, sas2Δ::Hyg, hmr-**a**1Δ::URA, Sir2Δ::HIS3, LEU2::Sir2N345A, rpd3Δ::Kan*	DTY408
JRY9601	*MATα, ADE2, lys2-, sas2Δ::Hyg, hmr-**a**1Δ::URA, Sir2Δ::HIS3, LEU2::Sir2N345A, rpd3Δ::Kan*	DTY409
JRY9602	*MAT**a**, ADE2, lys2-, SAS2, hmr-**a**1Δ::URA, Sir2Δ::HIS3, LEU2::Sir2N345A, rpd3Δ::Kan*	DTY410
JRY9603	*MATα, ADE2, lys2-, SAS2, hmr-**a**1Δ::URA, Sir2Δ::HIS3, LEU2::Sir2N345A, rpd3Δ::Kan*	DTY411
JRY9604	*MATα, ADE2, LYS, sas2Δ::Hyg, hmr-**a**1Δ::URA, sir2Δ::HIS3, leu2-3,112, hht1-hhf1Δ::Hyg, hht2-hhf2Δ::Nat, pJR3212 [H3K56R-H4]*	DTY312
JRY9605	*MATα, ADE2, LYS, sas2Δ::Hyg, hmr-**a**1Δ::URA, sir2Δ::HIS3, leu2-3,112, hht1-hhf1Δ::Hyg, hht2-hhf2Δ::Nat, pJR3213[H3K56Q-H4]*	DTY313
JRY9606	*MATα, ADE2, LYS, sas2Δ::Hyg, hmr-**a**1Δ::URA, sir2Δ::HIS3, leu2-3,112, hht1-hhf1Δ::Hyg, hht2-hhf2Δ::Nat, pJR2759[H3-H4]*	DTY314
JRY9607	*MATα, ADE2, LYS, sas2Δ::Hyg, hmr-**a**1Δ::URA, sir2Δ::HIS3, leu2-3,112, hht1-hhf1Δ::Hyg, hht2-hhf2Δ::Nat, pJR2760[H3-H4K5,8,12R]*	DTY315
JRY9608	*MATα, ADE2, LYS, sas2Δ::Hyg, hmr-**a**1Δ::URA, sir2Δ::HIS3, leu2-3,112, hht1-hhf1Δ::Hyg, hht2-hhf2Δ::Nat, pJR2761[H3-H4K5,8,12,16R]*	DTY316
JRY9609	*MATα, ADE2, LYS, sas2Δ::Hyg, hmr-**a**1Δ::URA, sir2Δ::HIS3, leu2-3,112, hht1-hhf1Δ::Hyg, hht2-hhf2Δ::Nat, rpd3Δ::Kan, pJR3212 [H3K56R-H4]*	DTY302

JRY9610	*MATα, ADE2, LYS, sas2Δ::Hyg, hmr-**a**1Δ::URA, sir2Δ::HIS3, leu2-3,112, hht1-hhf1Δ::Hyg, hht2-hhf2Δ::Nat, rpd3Δ::Kan, pJR3213[H3K56Q-H4]*	DTY303
JRY9611	*MATα, ADE2, LYS, sas2Δ::Hyg, hmr-**a**1Δ::URA, sir2Δ::HIS3, leu2-3,112, hht1-hhf1Δ::Hyg, hht2-hhf2Δ::Nat, rpd3Δ::Kan, pJR2759[H3-H4]*	DTY304
JRY9612	*MATα, ADE2, LYS, sas2Δ::Hyg, hmr-**a**1Δ::URA, sir2Δ::HIS3, leu2-3,112, hht1-hhf1Δ::Hyg, hht2-hhf2Δ::Nat, rpd3Δ::Kan, pJR2760[H3-H4K5,8,12R]*	DTY305
JRY9613	*MATα, ADE2, LYS, sas2Δ::Hyg, hmr-**a**1Δ::URA, sir2Δ::HIS3, leu2-3,112, hht1-hhf1Δ::Hyg, hht2-hhf2Δ::Nat, rpd3Δ::Kan, pJR2761[H3-H4K5,8,12,16R]*	DTY306
JRY9614	*MATα,ADE2, lys2-, sas2Δ::Hyg, hmr-**a**1Δ::URA, Sir2Δ::HIS3, LEU2::Sir2N345A, sum1-1* *double backcrossed	DTY127
JRY9615	*MAT**a**,ADE2, lys2-, sas2Δ::Hyg, hmr-**a**1Δ::URA, Sir2Δ::HIS3, LEU2::Sir2N345A, sum1-1* *double backcrossed	DTY128
JRY9616	*MAT**a**,ADE2, lys2-, sas2Δ::Hyg, hmr-**a**1Δ::URA, Sir2Δ::HIS3, LEU2::Sir2N345A, sum1-1* *double backcrossed	DTY129
JRY9617	*MATα/ MAT**a**, ADE/ade2-1, LYS/lys2-, sas2Δ::Hyg/sas2Δ::Hyg, hmr-**a**1Δ::URA/ hmr-**a**1Δ::URA, sir2Δ::HIS33/sir2Δ::HIS3, Leu2::Sir2N345A/Leu2::Sir2N345A, orc3A333V/ORC3*	DTY171
JRY9618	*MATα/ MAT**a**, ADE/ade2-1, LYS/lys2-, sas2Δ::Hyg/sas2Δ::Hyg, hmr-**a**1Δ::URA/ hmr-**a**1Δ::URA, sir2Δ::HIS33/sir2Δ::HIS3, Leu2::Sir2N345A/Leu2::Sir2N345A, orc3A333V/ORC3*	DTY258
JRY9619	*MAT**a**, ADE2, lys2-, sas2Δ::Hyg, hmr-**a**1Δ::URA, Sir2Δ::HIS3, LEU2::Sir2N345A, lys1Δ::Nat*	DTY344
JRY9620	*MAT**a**, ADE2, lys2-, sas2Δ::Hyg, hmr-**a**1Δ::URA, Sir2Δ::HIS3, LEU2::Sir2N345A, lys1Δ::Nat, rpd3Δ::kan*	DTY346
JRY9621	*MAT**a**, ADE2, lys2-, sas2Δ::Hyg, hmr-**a**1Δ::URA, Sir2Δ::HIS3, LEU2::Sir2N345A, lys1Δ::Nat, rpd3Δ::kan, hst3Δ::kan*	DTY348
JRY9622	*MAT**a**, ADE2, lys2-, sas2Δ::Hyg, hmr-**a**1Δ::URA, Sir2Δ::HIS3, LEU2::Sir2N345A, lys1Δ::Nat, rpd3Δ::kan, hst3Δ::kan*	DTY351

Table 4.2 Plasmids used in chapter 4

Plasmid	Backbone	Yeast Selection	Bacterial Resistance	Insert	Source
pJR2657	pRS316	*URA3*	AMP	*HHT2-HHF2*	
pJR2759	pRS314	*TRP1*	AMP	*HHT2-HHF2*	
pJR3212	pRS314	*TRP1*	AMP	*hht2(K56R)-HHF2*	R. Zunder
pJR3213	pRS314	*TRP1*	AMP	*hht2(K56Q)-HHF2*	R. Zunder
pJR2760	pRS314	*TRP1*	AMP	*HHT2-hhf2(K,5,8,12R)*	
pJR2761	pRS314	*TRP1*	AMP	*HHT2-hhf2(K,5,8,12Q)*	
Pooled Genomic Library	pLEJ009	*TRP1, Kan*	AMP	*Sau3*A1 Genomic Fragments	(Jauert, Jensen, & Kirkpatrick, 2005)

incubated at 30˚C for 1 hour. Cells were washed with 5% sodium thiosulfate and resuspended in PBS and plated on YPD. Plates were grown overnight on YPD, then replica plated to 5-FOA. After mutagenesis, yeast were grown at room temperature.

Whole Genome Sequencing Library Preparation and Data Analysis DNA for whole genome sequencing analysis was isolated following the yeast DNA extraction protocol for a Southern blot as in (Hoffman and Winston 1987). For the JRY9567 libraries, three double-backcrossed segregants exhibiting the mutant phenotype were grown to saturation in a liquid culture and DNA extracted as described. The three segregants, JRY9609, JRY9610 and JRY9611, were barcoded separately and sequenced with the unmutagenized parent, JRY9097, and the original mutant, JRY9567. For the JRY9570 and JRY9569 libraries, bulk segregant analysis as in (Birkeland et al. 2010) was performed to determine causative mutations. Briefly, segregants from JRY9612 and JRY9613 were assayed for their silencing phenotype. 10 segregants with a silencing restoration phenotype and 10 segregants with a non-silencing phenotype were grown overnight to saturation. These liquid cultures were pooled equally according to the OD_{600} of each culture. DNA was then isolated from these pooled cultures as described. 4µg of DNA was sheared with the S220 Focused-ultrasonicator (Covaris Woburn, MA) and the libraries were constructed using the Illumina Tru-Seq library preparation kit. Samples were indexed and sequenced in two lanes on the Illumina HiSeq 2000 as 50 base-single-end reads. Reads were mapped using BWA (Li and Durbin 2009) to a modified the Sac Cer 2 genome. SNPs were detected using VCFtools (Danecek et al. 2011) and visualized on IGV (Thorvaldsdóttir et al. 2013). Number of reads mapped for each sample is recorded in Table 4.3.

RNA Isolation and Analysis RNA was prepared as in (Ozaydin and Rine 2010). cDNA was synthesized using Superscript III First-Strand Synthesis from Invitrogen, utilizing oligo(dt) primers. Quantitative PCR (qPCR) analysis was conducted on the MX3000P machine from Stratagene using DyNAmo HS SYBR Green qPCR kit (Thermo Scientific). All primers sequences for RNA analysis are listed in Table 4.4. Amplification values for all primer sets were normalized to *ACT1* cDNA amplification values for that sample. RNA analysis was performed on three independent RNA preparations and error bars represent standard deviation of the values obtained from the three preparations.

SILAC Analysis to Enrich for Acetyl-lysine Peptides and Mass Spectrometry The appropriate strains were grown in media containing "light" lysine (L-Lysine $^{12}C_6$, $^{14}N_2$) or "heavy" lysine (L-Lysine $^{13}C_6$, $^{15}N_2$) (Cambridge Isotope Labs) to an OD_{600} of .4-.5 and 80 OD_{600} units were pelleted and stored at -80˚C. Strains had *LYS1* deleted to ensure appropriate incorporation of labeled lysine (Table 4.1). Pellets were resuspended in Urea buffer (.1 M Tris-HCL pH 8.0, 8M Urea, .15 M NaCl, Roche protease inhibitor mini tablet without EDTA, 10 mM Sodium Butyrate, 10 mM Nicotinamide) and cells disrupted utilizing BioSpec Mini-beadbeater 14 times for 1.5 min with 1.5 min of rest in between. The extracts were spun two times for 10 min at 17xG. The supernatant, the protein smaple, was then quantitated using BCA protein assay kit (Thermo Scientific) and 20 mgs from each "heavy" and "light" samples were combined. The Disulphide bonds in the combined protein samples were reduced in 4mM TCEP (Sigma C4706) for 30 min at room temperature and free lysines alkylated in 10 mM iodoacetamide (Sigma L1149) for 30 min at

Table 4.3 Number of reads mapped for each experiment in chapter 4

Sample	Number of Mapped Reads
JRY9097	24324128
JRY9567	31451777
JRY9614	23313738
JRY9615	29407529
JRY9616	22330041
JRY9569 Mutant Pool	7714958
JRY9569 Wildtype Pool	8405843
JRY9570 Mutant Pool	12837055
JRY9570 Wildtype Pool	10454114

Table 4.4 Primers used for qPCR in chapter 4

Name	Sequence
ACT1 F	TGT CCT TGT ACT CTT CCG GT
ACT1 R	CCG GCC AAA TCG ATT CTC AA
α2 F	TCC ACA AAT CAC AGA TGA GT
α2 R	GTT GGC CCT AGA TAA GAA TCC
a1 F	TGG ATG ATA TTT GTA GTA TGG CGG A
a1 R	TCC CTT TGG GCT CTT CTC TT
URA3 F	CTT CCA AGG GTT CTC TAG CAC ACG
URA3 R	CTG TAC TGC TGA CCC AAT GCA TCG

room temperature in the dark. The protein samples were then digested with 200 ug Trypsin (Pierce) and incubated at room temperature overnight. These digested protein samples were dissolved in IP buffer (.1M tris, pH 8.0, 50 mM NaCl with protease inhibitors) and immunoprecipitated with 25 µl acetyl lysine agarose beads (Immunechem) and incubated at 4˚C for 2 hours. Samples were washed twice each with cold IP buffer and with deionized and double distilled water. The peptides were eluted from the acetyl-lysine agarose beads with .15 % V/V Trifluoroacetic acid. Samples were analyzed on a Thermo Scientific LTQ Orbitrap Elite MS system. Peptides were then separated by an organic gradient from 5% to 30% ACN in 0.1% formic acid over 112 minutes at a flow rate of 300 nl/min. The MS continuously collected spectra in a data-dependent fashion over the entire gradient. Analysis of data was performed with MaxQuant Software (Cox and Mann 2008).

4.4 Results

4.4.1 A Screen Identified Five Supressors able to Silence Independently of Sir2 Catalytic Activity

To investigate what function of Sir2's catalytic activity is not accounted for in the current silencing model (Rusché et al. 2002; Hoppe et al. 2002), we conducted a forward genetics screen. *SAS2* was deleted in a haploid strain with the catalytically dead, but structurally intact, *SIR2* allele, *sir2N345A* (Imai et al. 2000). To report on silencing at *HMR*, the **a**1 open reading frame was replaced with *URA3*. Cells expressing *URA3* are sensitive to the drug 5-fluoroorotic acid (5-FOA), allowing for easy selection of those cells that have silenced *URA3* at *HMR* by their ability to grow on 5-FOA (Boeke et al. 1984) (Figure 4.1a). This *sir2N345A sas2Δ* strain was mutagenized with ethyl methanesulfonate (EMS) and mutants were identified by growth on 5-FOA. To ensure that the mutants' growth was not due to mutation of the *URA3* reporter gene at *HMR*, silencing was also scored by restoration of mating ability. The *sir2N345A sas2Δ* unmutagenized parent is unable to mate due to expression of the α genes from *HML*, and the **a** genes from *MAT*, resulting in a pseudodiploid cell identity. Mutants of interest were those now able to mate due to silencing of *HML* (Figure 4.1a). Thus this two-step selection-then-screen for mating ability recovered mutants that restore silencing independently of Sir2 catalytic activity.

From the initial selection of mutagenized cells that were able to grow on 5-FOA, about 3000 individual colonies were screened for mating ability. Five mutants were recovered that both grew on 5-FOA as well as exhibited some restoration of mating ability (Figure 4.1B). All mutants recovered were able to grow both on media lacking uracil and on medium with uracil and 5-FOA, indicating that silencing was only partially restored. Silencing was also not restored to wild-type levels at *HML* as judged by the low levels of mating of the mutants (Figure 4.1B). Interestingly, one mutant, JRY9571, mated as both an **a** and α, possibly indicating interesting regulation of the cell-type specific genes in addition to a silencing phenotype. Mutants were mated to a strain isogenic to the parent but of the opposite mating type, to determine if the silencing phenotype, as judged by 5-FOA resistance, was dominant or recessive. For all mutants identified, the diploids were no longer resistant to 5-FOA indicating that the silencing phenotype was recessive (data not shown).

Different strategies were taken to identify the causative restoration-of-silencing mutation for each mutant. Due to the incompleteness of the silencing phenotype, it was difficult to identify the mutation by traditional cloning-by-complementation methods. However, by taking advantage of a

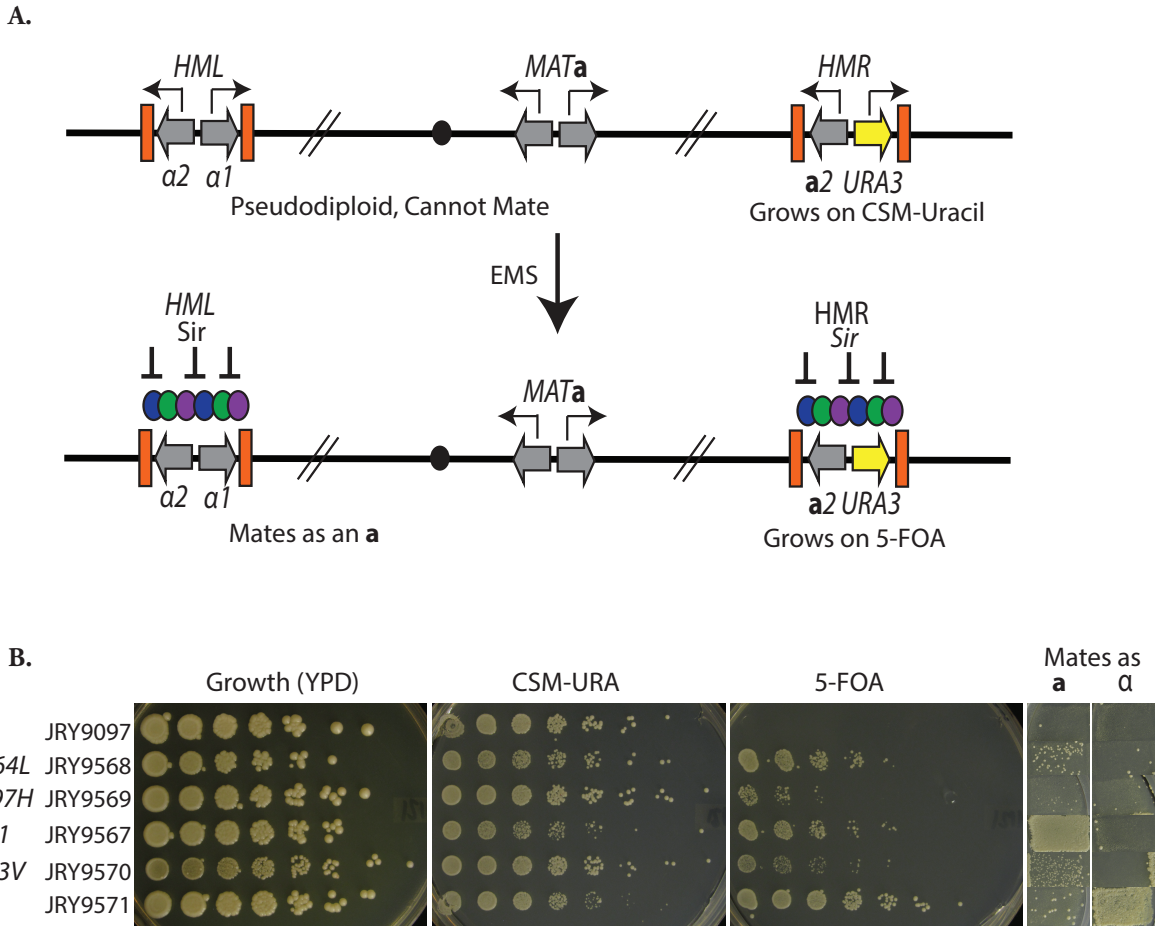

Figure 4.1 A forward genetics screen identified suppressors of Sir2's catalytic activity. (A) Schematic of the screen to identify mutations that restored silencing in the absence of Sir2 catalytic activity. A *sir2N345A sas2Δ* strain had the *URA3* reporter integrated in place of the **a**1 open reading frame at *HMR*. Expression of the *URA3* gene resulted in cells that grow on CSM-URA but are sensitive to 5-FOA. Expression of the α genes from *HML* and **a** genes from *MAT* resulted in a pseudodiploid cell identity that cannot mate. This strain was mutagenized with EMS and mutants that reestablished silencing as assayed by resistance to 5-FOA and the ability to mate were isolated. (B) The phenotypes of the parent strain (JRY9097) and the five mutants that were isolated from the suppressor screen. Five-fold serial dilutions assayed for growth phenotypes on the indicated medias. Growth in the patches on the right indicates successful matings as either an a or α cell identity.

subtle colony-morphology phenotype linked to the silencing phenotype exhibited of JRY9568 (data not shown) this secondary phenotype was amenable to cloning by complementation from a plasmid library. Rpd3, a non-sirtuin histone deacetylase was able to complement both the silencing and colony morphology phenotype. Sanger sequencing of this region in JRY9568 identified a transition mutation that caused a proline to leucine coding change at amino acid 264 in Rpd3.

Three of the other suppressor mutants were identified through two different whole genome sequencing methods. First, JRY9567 was backcrossed twice. Three individual segregants of the second JRY9567 backcross were barcoded and sequenced using next generation sequencing technology. The causative mutation was determined as the Single Nucleotide Polymorphisms (SNPs) that all of the backcrossed segregants with the restoration-of-mating phenotype shared in common but was not present in the unmutagenized parent strain. This identified a point mutation in the gene encoding the repressor Sum1. This identical change in the *SUM1* gene, *sum1-1*, was previously isolated in a screen to identify mutations that can restore silencing in the absence of Sir proteins (Chi and Shore 1996; Klar et al. 1985). Two other mutations were identified through pooled linkage analysis (Birkeland et al. 2010). This analysis identified another independent mutation in Rpd3 (JRY9569), indicating that a limited number of genes could mutate to give the phenotype of interest. Additionally, an alanine to valine mutation at amino acid 333 in Orc3 was also recovered, which was responsible for the restoration of mating phenotype in another mutant (JRY9570). The causal mutation in the last mutant, JRY9571, was not determined as the diploids made with this strain failed to sporulate, precluding the backcross or pooled linkage analysis.

4.4.2 Mutation of *RPD3* Restored Sir Silencing

Two different mutants identified in the screen were in the non-sirtuin histone deacetylase Rpd3. Rpd3 has been implicated in silencing previously, as mutation of Rpd3 suppressed the silencing defect of an *HMR-E* silencer with a defective Rap1 binding site (Vannier et al. 1996). Additionally, mutants in the *Drosophila* Rpd3 homolog and deletion of the yeast *RPD3* show increase Position-Effect Variagation and Telomere Position Effect, respectively (De Rubertis et al. 1996). Thus, Rpd3 has been identified as antagonistic to silencing previously in multiple species. To determine if the deletion of Rpd3 could also restore silencing, or whether the point mutants had some novel property, *RPD3* was deleted in the original *sir2N345A sas2Δ* parent strain. As with the point mutants, the deletion also suppressed the silencing defect of the *sir2N345A* mutation, indicating that the point mutations are likely loss of function mutations (Figure 4.2). Interestingly, as judged by resistance to 5-FOA, silencing at *HMR* is slightly better in the *rpd3P264L* mutant than the *rpd3Δ* (Figure 4.2a). However, this point mutant is derived from the original EMS mutagenesis, so we cannot rule out background mutations improving silencing.

Rpd3 is a histone deacetylase found in two distinct complexes: the Rpd3 Large complex (Rpd3L) and Rpd3 small complex (Rpd3S). The small complex deacetylates coding regions of actively transcribed genes to prevent intragenic transcription (Carrozza et al. 2005). The large complex is involved in general transcriptional repression of many genes (Kasten et al. 1997). To determine if Rpd3L or Rpd3S was specifically involved in the restoration of silencing, we deleted components specific to the Small complex, *EAF3* and *RCO1*, or the Large Complex, *PHO23* and *SAP30*, in the *sir2N345A sas2Δ* strain to determine, if as in the *rpd3Δ*, these deletions could also restore silencing. Neither the deletions specifically in the small complex or the large complex restored

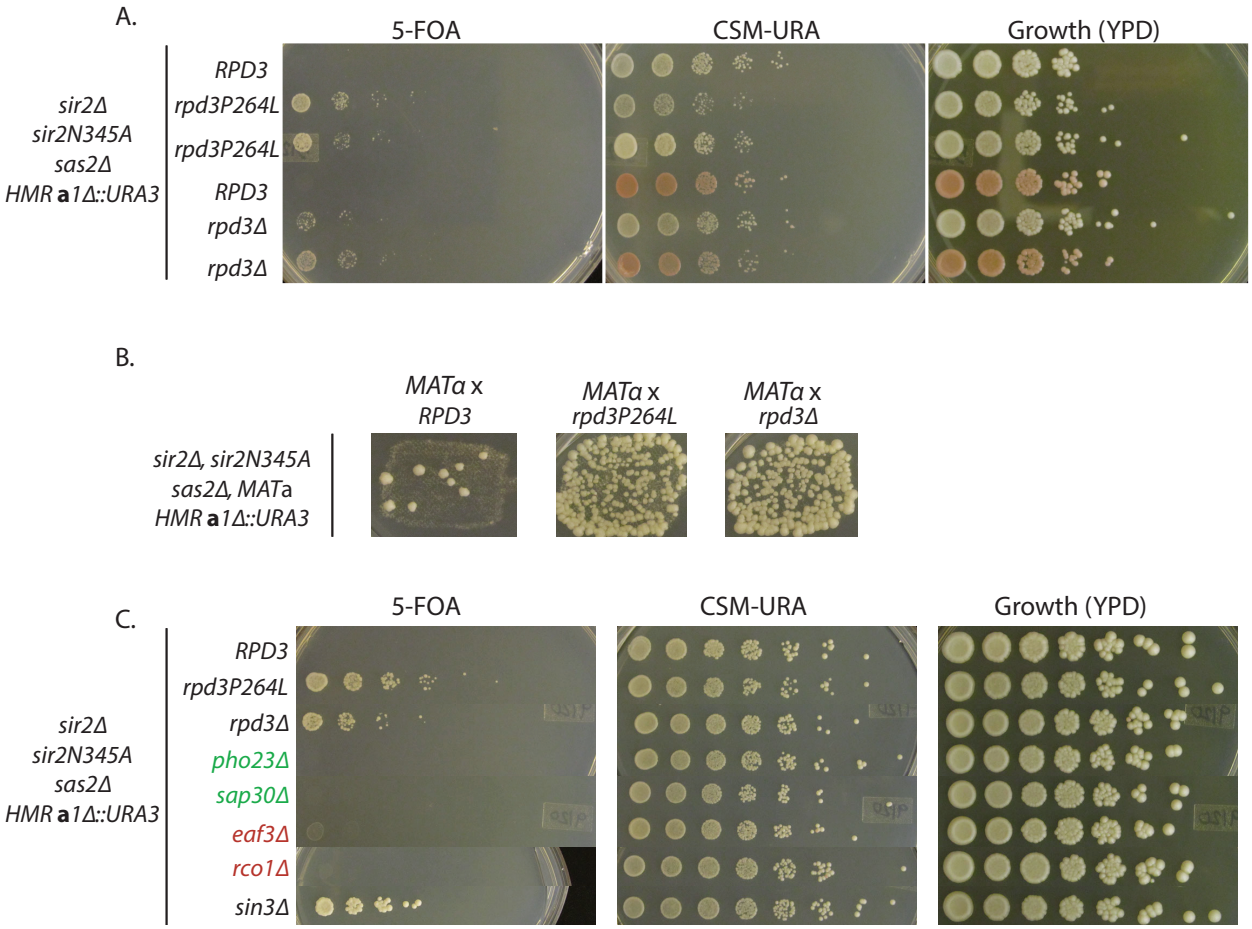

Figure 4.2 Mutation of *RPD3* and *SIN3* Restored Silencing. (A) Five-fold serial dilutions of yeast were spotted on plates to determine their growth phenotype. Growth on 5-FOA indicates silencing of the *HMR-**a**1Δ::URA3* reporter. All strains are in the *sir2N345A sas2Δ* background. The first row is the unmutagenized, *RPD3* parent. The next two rows are replicates of JRY9568, the *rpdP264L* isolated point mutant. The fourth row is isogenic to the unmutagenized parent except of the opposite mating type *MATα* and *ade2-1*. The last two rows are *rpd3Δ* deleted from the parent and the isogenic *MATα* strain. (B) Mating tests of the parent JRY9097, JRY9568, and the *rpd3Δ*. Growth on the media indicates mating. (C) The Rpd3 subunit indicated was deleted in JRY9097 to determine if deletion of that subunit could also restore silencing. Green labels indicate Rpd3L subunits and red labels indicate Rpd3S subunits.

silencing in the absence of Sir2 catalytic activity (Figure 4.2c). However, deletion of *SIN3*, the scaffolding platform for both the small and large Rpd3 complexes, phenocopied the *rpd3Δ*. Thus, it is likely that to be able to restore silencing independent of Sir2 catalytic activity, Rpd3 function must be completely compromised.

Rpd3 is known to be involved in general transcriptional repression (Kurdistani et al. 2004; Chen et al. 2012; Carrozza et al. 2005). Therefore, it was unlikely that the restoration of silencing was due to a direct down regulation of the **a** and α alleles due to the absence of a general repressor. However, the down regulation of the **a** and α alleles by the *rpd3* mutation was formally possible if the *rpd3* mutant caused derepression of some other repressor that down-regulated the **a** and α alleles and not due to a restoration of silencing specifically at *HML* and *HMR*. To test this hypothesis, we measured RNA expression from the original unmutagenized parent strain (*RPD3*) and *rpd3P264L* point mutant and compared the expression from the *MAT* locus to the expression from *HML* and *HMR*. If the restoration of silencing due to general down regulation of the **a**1 promoter than both the **a**1 gene at *MAT* and the *URA3* gene at *HMR* would show decreased expression in the mutant. However, if the apparent suppression of the *sir2N345A* is due to promoter-independent silencing restoration then the decrease in expression will be specific to *HMR* and not apparent at the *MAT* locus. Consistent with a silencing-specific phenotype rather than a transcriptional down-regulation, decreased expression was observed only at *HML* and *HMR* and not the *MAT* locus (Figure 4.3a).

Previous screens have been conducted that identify mutants that silence independently of the Sir proteins (Chi and Shore 1996). One of these previous mutations, *sum1-1*, was re-recovered in this very screen, exhibiting that silencing can be restored in this *sir2N345A sas2Δ* background independent of Sir proteins. Since we were interested in understanding unaccounted roles for Sir2's catalytic activity in silencing, we tested whether the *rpd3* mutants restored silencing by involving the Sir complex, or whether they functioned by some independent means like *sum1-1*. To determine if silencing restoration by the *rpd3* mutant is dependent on Sir proteins, we tested whether the *rpd3Δ* and *rpd3P264L* mutant could still restore silencing in *sir3Δ* and *sir4Δ*. Restoration of silencing by Rpd3 required both Sir3 and Sir4, indicating that Sir protein-dependent silencing has been restored (Figure 4.3b). Additionally, we tested whether the restoration of silencing requires the Sir2 structural component. As with the *sir3Δ* and *sir4Δ*, *sir2N345A* was also required to restore silencing by *rpd3Δ* (Figure 4.3b). Thus the entire Sir protein structural complex was required for the *rpd3Δ* silencing restoration, but Sir2's catalytic activity was not.

4.4.3 Wild-type Sas2 Prevented *rpd3Δ* silencing restoration

Silencing restoration by the *rpd3* mutant was observed in a *sas2Δ* deletion in anticipation of the impact caused by the lack of Sir2's known catalytic activity (Suka et al. 2002; Kimura et al. 2002). However, even though the mutation was isolated in this *sas2Δ*, it was formally possible that *sas2Δ* was not required for silencing restoration by *rpd3Δ*. To test if deletion of *SAS2* and thus presumably H4K16 hypoacetylation was necessary for silencing restoration by *rpd3Δ*, we tested if the *rpd3Δ* can silence in a *SAS2* wildtype background. Wild-type *SAS2* prevented the silencing restoration by *rpd3Δ* (Figure 4.4), indicating that the *rpd3Δ* appeared unable to compensate for the loss of Sir2 catalytic activity if H4K16 was acetylated. Thus the mechanism of silencing restoration by *rpd3Δ* likely reveals a new, unaccounted function for Sir2's catalytic activity in silencing.

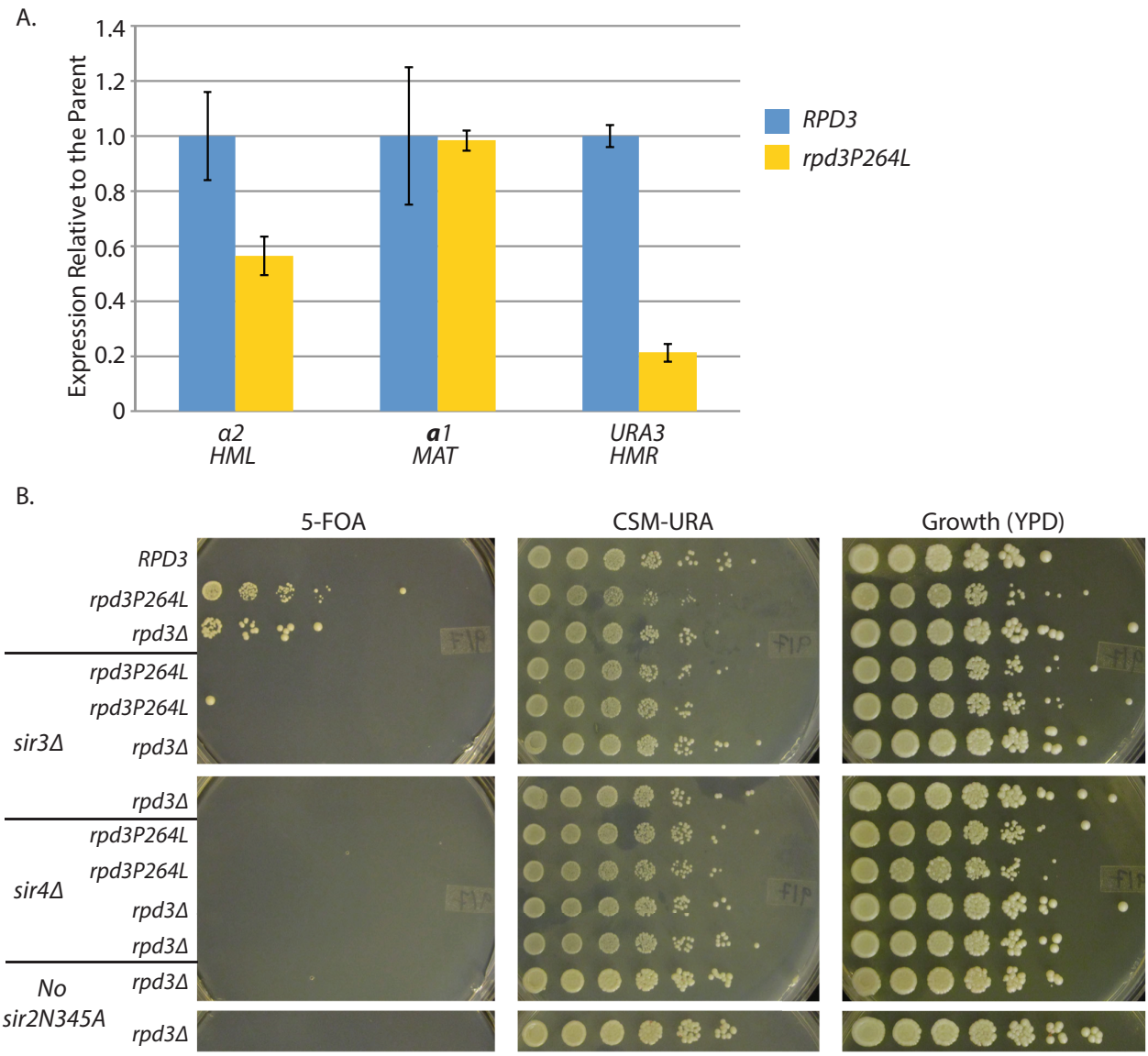

Figure 4.3 The *rpd3* mutant restored Sir-based silencing. (A) *α2*, **a***1* and *URA3* transcripts were measured to determine expression levels at *HML*, *MAT* and *HMR*, respectively. RNA was normalized to *ACT1* for each sample and reported as relative to the *RPD3* sample. Error bars are the standard deviation of 3 biological replicates. (B) Five-fold serial dilutions of the indicated genotypes were spotted to determine the growth phenotype. All strains are *sir2Δ, sas2Δ, HMR-***a***1Δ::URA3* and all but the bottom two rows also express *sir2N345A*. *SIR3* and *SIR4* were deleted as indicated. The replicates represent individual transformants for the knockouts or individual spores from the same tetrad dissection.

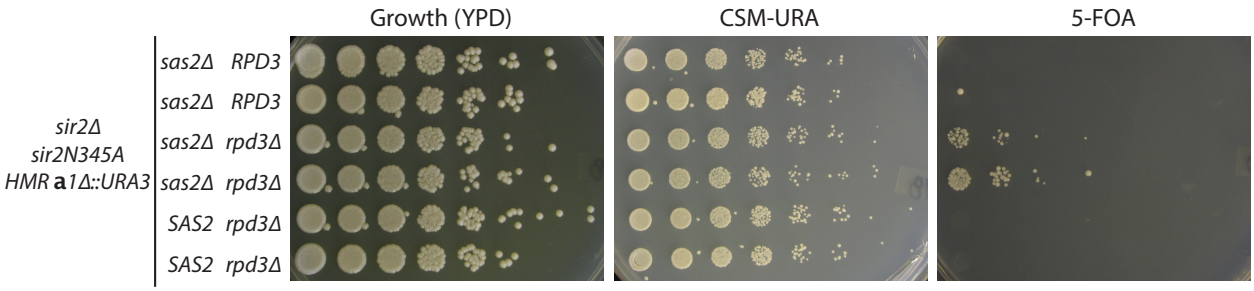

Figure 4.4 Restoration of silencing by *rpd3Δ* is dependent on *sas2Δ*. Restoration of silencing at *HMR* by *rpd3Δ* was tested in a *SAS2* wildtype strain. 5-fold serial dilutions were plated on the indicated medias to determine growth phenotype. All strains only express the catalytically dead sir2 allele, *sir2N345A*, and have the *HMR*-**a***1Δ::URA3* reporter. Duplicates represent individual spores from the same tetrad dissection.

4.4.4 Restoration of Silencing by *rpd3* was Dependent on the Sirtuin Hst3

Silencing is lost when yeast are grown in the presence of the sirtuin inhibitor nicotinamide (NAM), a competitive inhibitor of probably most or all sirtuins (Landry et al. 2000; Bitterman et al. 2002). This silencing loss has been attributed to inhibiting Sir2, resulting in a loss of silencing. However, nicotinamide inhibits the four yeast HSTs in addition to Sir2. More recently, Hst3 and Hst4 have been implicated in silencing (Yang et al. 2008), suggesting the possibility that NAM's effect on silencing could be due to more than just inhibition of Sir2. Silencing in the *rpd3* mutant provides a unique opportunity to determine if any of the other yeast sirtuins contribute to the NAM-sensitive silencing sensitivity since silencing in this mutant is independent of Sir2 activity. Thus, to determine if any other sirtuins contribute to silencing, we tested silencing restoration by the *rpd3P264L* mutant in the presence of NAM. Surprisingly, silencing restoration by *rpd3P264L* was sensitive to NAM, thus implicating another sirtuin in silencing (data not shown). To determine which sirtuin was important for silencing in the *rpd3* mutant, we deleted *HST1-4* in the *rpd3* mutant and assayed silencing by the *HMR-**a**1Δ::URA3* reporter. The *rpd3* mutant depended specifically on *HST3*, accounting for the silencing restoration's sensitivity to nicotinamide (Figure 4.5). *HST3* mutants show a much more severe phenotype than *HST4* mutants, even though they are thought to deacetylate the same substrate (Celic et al. 2006). Thus, Hst4 may still be important for the *rpd3P264L* silencing restoration, but to a lesser degree than Hst3. However, when comparing the *rpd3P264L* silencing restoration in an *hst4Δ* to a wild-type *HST4* background, silencing restoration, as judged by ability to grow on 5-FOA, was not even marginally compromised in the *hst4Δ* (Figure 4.5). This result identifies a specific role for Hst3 in *HMR* silencing independent of Hst1,2 and 4.

4.4.5 Silencing Restoration by Rpd3 Mutant is Independent of known Histone Substrates

Rpd3 deacetylates histone H4 K5-ac and K12-ac (Suka et al. 2001). Point mutational analysis of H4K5 and H4K12 to alanine, arginine or glycine show slight silencing defects, but to a lesser degree than the H4K16 point mutations (Park and Szostak 1990; Johnson et al. 1990). Hst3 deacetylates Histone H3K56 (Celic et al. 2006). Since these are the known chromatin substrates for Rpd3 and Hst3 in yeast, we tested if the restoration of silencing by the *rpd3Δ* is dependent on H4K5, H4K12 and H3K56 acetylations. To test this hypothesis, we constructed strains in which the endogenous copies of histones H3 and H4 were deleted and either wild type or mutant H3 and H4 were expressed from a single copy plasmid. Silencing was assayed at *HMR* by the ability of cells of various genotypes to mate with a *MATα* strain as measured by growth on selective media for diploids. *rpd3Δ* restored silencing of the *sir2N345A sas2Δ* when H3 and H4 were expressed from a plasmid, altering histone dosage (Figure 4.6). Neither the hyperacetylated (Q) or hypoacetylated (R) H3K56 mimics restored silencing in the *sir2N345A sas2Δ* mutant (Figure 4.6). This result was consistent with a previous study that showed that loss of H3K56 acetylation could not rescue the silencing defect caused by *sir2N345A* (Yang et al. 2008). Additionally, neither H3K56 acetylation state mimic interfered with the silencing restoration provided by the *rpd3Δ*. This indicated that the inability of the *rpd3* mutant to restore silencing in an *hst3Δ*, was not likely due to elevated H3K56-

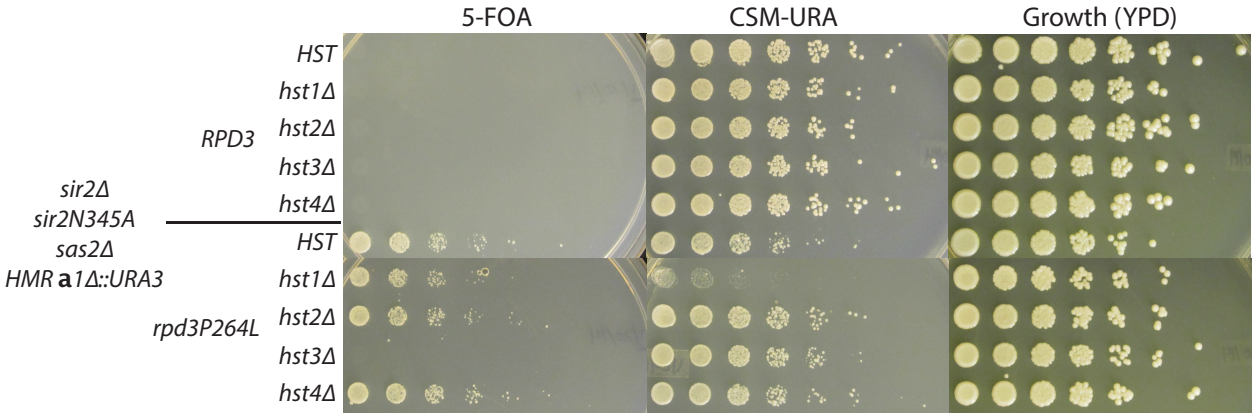

Figure 4.5 Silencing by the *rpd3* mutant was dependent on Hst3. Five-fold serial dilutions were spotted on the indicated media to determine growth phenotype. All strains are *sir2Δ, sir2N345A*, and have the *HMR-***a***1Δ::URA3* reporter to measure silencing as growth on 5-FOA. *RPD3* and *HST* genotypes are as indicated.

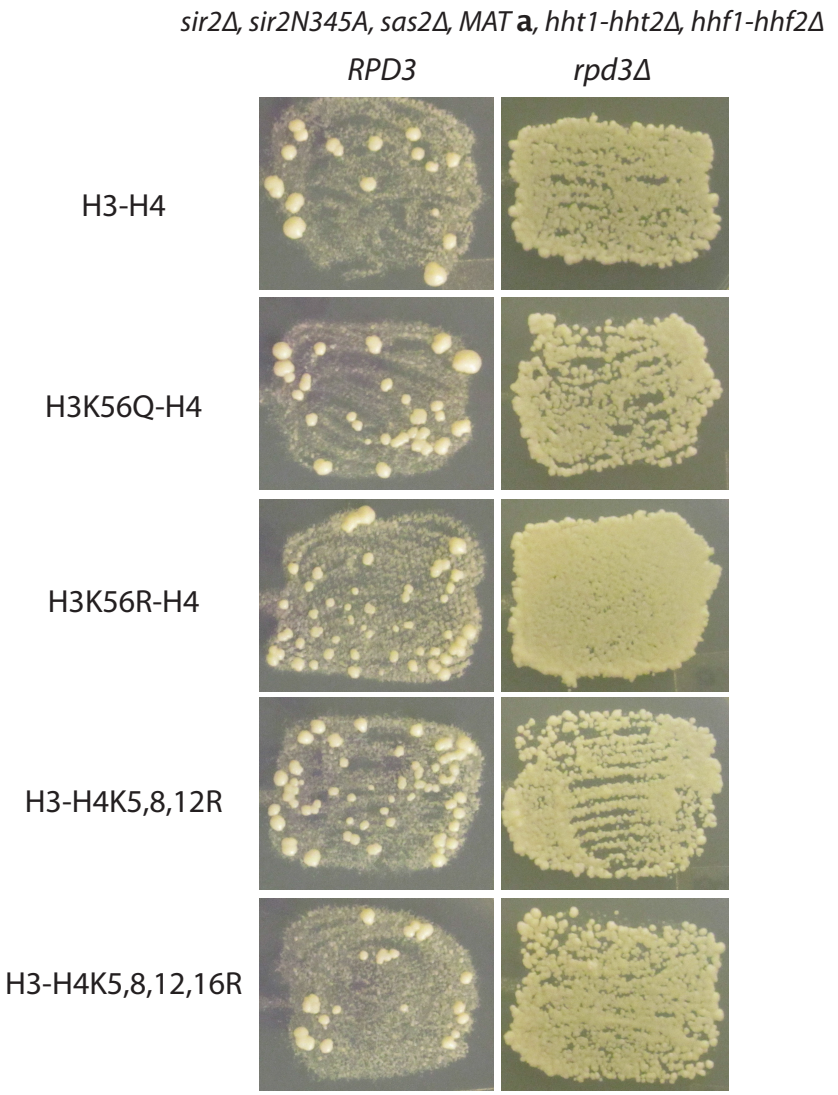

Figure 4.6 Silencing by *rpd3Δ* was independent of known histone acetylations. Endogenous copies of H3 and H4 were deleted and wild-type or mutant H3 and H4 were expressed from a CEN-ARS plasmid. Silencing was tested by mating to a *MATα* tester strain (JRY2728) and replica plated to minimal media. Growth indicates successful mating.

ac. By implication, there appeared to be another substrate of Hst3 whose acetylation promoted silencing in the absence of *SIR2* and *RPD3* catalytic function.

As is suggested by models invoking a role for OAAR, both the histone deacetylation reaction and the hypoacetylation resulting from the catalysis, may be necessary together for silencing. Consistent with this model, previous studies have suggested Rpd3's antagonistic activity towards silencing is due to preemptive removal of the sirtuin histone substrate by Rpd3, thus limiting the local production of OAAR (Ehrentraut et al. 2010). Although the restoration of silencing observed by the *rpd3Δ* was independent of Sir2 catalytic activity, this silencing restoration was still dependent on a sirtuin, Hst3. Hence these data allowed the possibility that OAAR production may still be important for silencing. To test if the act of deacetylating histones was important for silencing, I tested the ability of the *rpd3Δ* to restore silencing in cells expressing the H4 tail mutants at the previously identified Rpd3 substrates, H4K5,12 as well as H4K16. H4K8 was also mutated in these plasmids as its acetylation state largely correlated with H4K5 and K12 (Kurdistani et al. 2004; Dion et al. 2005). In no case did the H4 tail mutants mimicking hypoacetylated histones prevent silencing restoration by *rpd3Δ* (Figure 4.6). Thus local production of OAAR by the deacetylation of H4 tail residues was not important for the silencing restoration.

4.4.6 Many Non-Histone Acetylations were Dependent on Rpd3 and Hst3

Rpd3 was originally identified as a histone deacetylase, however recent studies have shown that Rpd3 also deacetylates some nonhistone proteins (Kaluarachchi Duffy et al. 2012; Henriksen et al. 2012). Since the known histone substrates for Rpd3 were not important for the restoration of silencing (Figure 4.6), I thought it possible that Rpd3 deacetylation of a non-histone protein may contribute to the silencing restoration phenotype. To determine what deacetylations are directly dependent on Rpd3, or what acetylations occur indirectly due to loss of Rpd3, in collaboration with Mike Downey in the Toczyski lab, we performed SILAC, enriching for acetyl-lysine peptides. The *sir2N345A sas2Δ rpd3Δ* strain was grown in the presence of heavy lysine while *sir2N345A sas2Δ RPD3* was grown in the presence of light lysine. The heavy and light lysine protein samples from each culture were combined and immunoprecipitated against an acetyl-lysine antibody to enrich for acetylated peptides. Mass spectrometry was then performed allowing for the relative quantitation of heavy labeled acetyl-peptides or light acetyl peptides. 12 different peptides exhibited a 2-fold or greater intensity of the heavy-labeled lysine over the light lysine (H/L>2), indicating that they may be direct targets of Rpd3 as they are more acetylated in the *rpd3Δ* (Table 4.5, green values). Interestingly, H3K56-acetyl may be a target of Rpd3 deacetylation. 51 different proteins show a greater amount of acetylation in the *RPD3* sample, which is indicative of an indirect change in acetylation in response to *RPD3* genotype (Table 4.5, red values). Of these proteins that have increased acetylation when Rpd3 is present, many are involved in chromatin complexes such as members of the Rpd3L complex, Pho23 and Sds3, as well as members of the NuA4 complex and Htz1.

Since the restoration of silencing by the *rpd3Δ* was dependent on Hst3, but was independent of H3K56 acetylation, we wanted to determine other deacetylations besides H3K56 that are dependent on Hst3. Therefore we also performed the same SILAC analysis as described above comparing *HST3* to *hst3Δ*. This SILAC analysis of Hst3-dependent deacetylations was performed in both an *RPD3* and *rpd3Δ* to determine if the Rpd3 genotype affected Hst3-dependent

Table 4.5 Acetylations dependent on Rpd3. SILAC was performed on an *RPD3* strain (labeled with light lysine) and an *rpd3Δ* (labeled with heavy lysine). Acetylated peptides showing a 2-fold or more difference between the samples are shown. Those peptides that were more abundant in the light sample (H/L < .5) are shown in red and those peptides that were more abundant in the heavy sample (H/L > 2) are shown in green. Modified peptide sequences appearing twice indicates that those peptides had a 2-fold or greater difference in enrichment in both technical replicates.

Gene Names	Modified sequence	Ratio H/L	Intensity L (*RPD3*)	Intensity H (*rpd3Δ*)
ADH1	_EK(ac)DIVGAVLK_	0.047851	90424000	3401300
ADH1	_EK(ac)DIVGAVLK_	0.047975	106030000	3953800
HSP12	_EYITDK(ac)ADK_	0.067747	2152800	86496
HSP12	_EYITDK(ac)ADK_	0.072453	2124400	175970
HSP12	_ASEALK(ac)PDSQK_	0.081195	1389000	96477
HSP12	_ASEALK(ac)PDSQK_	0.083352	1878600	149900
PHO23	_SSQALK(ac)SESR_	0.11397	1656800	130560
PHO23	_SSQALK(ac)SESR_	0.12939	1025100	93734
HSP12	_SYAEQGKEYITDK(ac)ADK_	0.16359	1492500	112650
SDS3	_VSNK(ac)DLSR_	0.16968	1663500	240140
CTT1	_GDSQYTAEQCPFK(ac)AVNFQR_	0.17599	4950300	596380
CTT1	_GDSQYTAEQCPFK(ac)AVNFQR_	0.18242	3190800	449050
RPS17A;RPS17B	_NK(ac)IAGYTTHLMK_	0.19216	5120900	902030
RPS17A;RPS17B	_NK(ac)IAGYTTHLMK_	0.26569	5361000	1097800
RPS6A;RPS6B	_K(ac)FFGLSK_	0.27039	9061200	1916300
RPS6A;RPS6B	_K(ac)FFGLSK_	0.28507	10747000	2476600
RNT1	_TLLK(ac)GNLK_	0.29391	420920	198450
RPS7B;RPS7A	_LESFQAVYNK(ac)LTGK_	0.29459	1872900	543090
RPL28	_FVSK(ac)LAEEK_	0.2964	2173600	548000
YBL028C	_GVFQK(ac)AVDAR_	0.31292	764190	107990
ESA1	_SHDGK(ac)EEPGIAK(ac)K_	0.31844	401960	114310
PMA1	_SLK(ac)QYPK_	0.32051	1201600	264900
YNG2	_TSK(ac)LQNEIDVSSR_	0.36387	10884000	3285400
RPS17A;RPS17B	_RASK(ac)ALIER_	0.36692	4018000	1239100
EPL1	_SAHDDGLDSFSK(ac)GDSGAGASAGSSNSR_	0.36764	10329000	3305500
NOG1	_HLFSGK(ac)R_	0.36802	856950	238690
RPL3	_AFTK(ac)YSAK_	0.36819	1560200	532330

RPL28	_FVSK(ac)LAEEK_	0.37565	2273700	611570
YNG2	_TSK(ac)LQNEIDVSSR_	0.37666	10252000	3131100
SMT3	_RQGK(ac)EMDSLR_	0.37818	3171600	642590
RPL29	_TYK(ac)YPSLK_	0.3827	26557000	8781500
SMT3	_RQGK(ac)EMDSLR_	0.38362	1236200	400190
RPL29	_TYK(ac)YPSLK_	0.38607	26260000	8184000
SMT3	_QGK(ac)EM(ox)DSLR_	0.38628	1051300	288660
RPS17A;RPS17B	_RASK(ac)ALIER_	0.38758	6479400	2030200
RPL3	_AFTK(ac)YSAK_	0.39097	1576200	493400
RPL42A;RPL42B	_VTQYK(ac)AGK_	0.39545	451710	189620
SEC18	_GK(ac)AVSTVFDQDELAK_	0.39818	959110	263670
RPS17A;RPS17B	_ASK(ac)ALIER_	0.39901	51869000	16287000
SMT3	_QGK(ac)EMDSLR_	0.40226	8655400	2833400
RPS17A;RPS17B	_ASK(ac)ALIER_	0.40444	54329000	17427000
SMT3	_QGK(ac)EMDSLR_	0.40852	9130100	2921500
TAF12	_K(ac)WNPSQNYNQK_	0.41283	305090	110370
ESF2	_ISSK(ac)DDIFSK_	0.41446	3210900	1062300
RPL13B;RPL13A	_NLPILK(ac)NHFR_	0.41999	3419700	1231200
RPS24A;RPS24B	_DKK(ac)IFGTGK_	0.42181	897250	288890
BDF1	_SK(ac)DIYPYESK_	0.42268	1230400	427690
SMT3	_RQGK(ac)EMDSLR_	0.42619	3492600	1254700
EPL1	_SAHDDGLDSFSK(ac)GDSGAGASAGSSNSR_	0.42993	10966000	3305500
HTZ1	_(ac)SGK(ac)AHGGK(ac)GK_	0.43592	1917600	563090
HTZ1	_(ac)SGK(ac)AHGGK(ac)GK_	0.44112	2220000	601560
RPL43A;RPL43B	_K(ac)LEIQQHAR_	0.44243	233500	68376
RPL3	_DLDRPGSK(ac)FHK_	0.44519	403840	147300
SMT3	_RQGK(ac)EMDSLR_	0.44784	857070	218510
ESF2	_ISSK(ac)DDIFSK_	0.44805	3493800	1244200
YDJ1	_GGK(ac)K(ac)GAVK_	0.44825	1249900	550000
SPT5	_MNPEIISK(ac)MGPPSSK_	0.45504	652750	256630
ILV3	_LNK(ac)YSYIITEPK_	0.45924	672990	291440
RPL43A;RPL43	_K(ac)LEIQQHAR_	0.461	605560	170190

B				
MET17	_LASGVTK(ac)DLIR_	0.46145	372500	174280
RPS17A;RPS17B	_IAGYTTHLMK(ac)R_	0.4672	3478700	1291600
LYS21;LYS20	_QYSHGK(ac)DMNYIAK_	0.46989	2344200	822980
RPL43A;RPL43B	_K(ac)LEIQQHAR_	0.47192	2488700	1139000
RPL43A;RPL43B	_K(ac)LEIQQHAR_	0.47869	2169200	947220
SNF2;STH1	_VIQAGK(ac)FDNK_	0.4815	1228500	475670
RPL42A;RPL42B	_VTQYK(ac)AGK_	0.48345	463760	183250
RPL29	_NHK(ac)HALHGTAK_	0.48386	26273	9742.6
RPL29	_NHK(ac)HALHGTAK_	0.48843	1638100	714650
RPS24A;RPS24B	_IFGTGK(ac)R_	0.49285	1202500	424720
RPL37A	_FK(ac)NGFQTGSASK_	0.49386	389400	153320
RPL29	_NHK(ac)HALHGTAK_	0.49601	3203700	1362600
RPL34B;RPL34A	_THK(ac)TVSR_	0.49726	2516400	1378100
BDF1	_SK(ac)DIYPYESK_	0.49742	1203500	486180
YNL134C	_DK(ac)LPEGPVK_	2.1094	2961400	4478600
HHT1	_KQLASK(ac)AAR_	2.1517	12617000	16130000
YCR102C	_KHEK(ac)LLK_	2.1541	212820	455370
HHT1	_K(ac)STGGK(ac)APR_	2.1588	65055000	115110000
YNL134C	_DK(ac)LPEGPVK_	2.1959	3124900	5916500
HHT1	_K(ac)SAPSTGGVK_	2.2306	7436400	13454000
CAR1	_GPK(ac)YMLK_	2.2653	278520	511970
HHT1	_K(ac)SAPSTGGVK_	2.3302	7932500	14773000
SSB1;SSB2	_NTVFDAK(ac)R_	2.3439	1741300	2165100
HHT1	_K(ac)STGGK(ac)APR_	2.4128	342120	693240
PFK2	_SAIFK(ac)GCR_	3.6746	457930	2364400
INO1	_CTYK(ac)DNELLTK_	4.1939	1167800	3855400
INO1	_CTYK(ac)DNELLTK_	4.5538	1072400	4244100
TEF4	_K(ac)DVDACFVK_	5.2	108150	609080

Table 4.5 Acetylations dependent on Hst3. SILAC was performed on an *HST3* strain and *hst3Δ* in an *rpd3Δ* or *RDP3Δ* background. Acetylated peptides showing a 2-fold or more difference between the samples are shown. Modified peptide sequences appearing twice indicates that those peptides had a 2-fold or greater difference in enrichment in both technical replicates.

Gene Names	Modified sequence	Ratio H/L normalized	Intensity L	Intensity H	Heavy Labeled	Light Labled
BUD23	_DSK(ac)FTGR_	0.11578	535850	76241	*HST3 rpd3Δ*	*hst3Δ rpd3Δ*
ENO1	_AAGHDGK(ac)IK_	0.16232	3079100	268470	*HST3 rpd3Δ*	*hst3Δ rpd3Δ*
RPS22B;RPS22A	_LNK(ac)CGVISPR_	0.26695	491530	214320	*HST3 rpd3Δ*	*hst3Δ rpd3Δ*
IFH1	_K(ac)SK(ac)LIQR_	0.34005	2311300	765210	*HST3 rpd3Δ*	*hst3Δ rpd3Δ*
HHT1	_RFQK(ac)STELLIR_	0.34206	13783000	4642300	*HST3 rpd3Δ*	*hst3Δ rpd3Δ*
IFH1	_K(ac)SK(ac)LIQR_	0.37551	2092400	708310	*HST3 rpd3Δ*	*hst3Δ rpd3Δ*
TY1	_TEECEK(ac)ASTK_	0.41292	1434100	654740	*HST3 rpd3Δ*	*hst3Δ rpd3Δ*
HHT1	_FQK(ac)STELLIR_	0.43031	34368000	14843000	*HST3 rpd3Δ*	*hst3Δ rpd3Δ*
HHT1	_RFQK(ac)STELLIR_	0.43582	884630	447670	*HST3 rpd3Δ*	*hst3Δ rpd3Δ*
HHT1	_RFQK(ac)STELLIR_	0.44185	25421000	11786000	*HST3 rpd3Δ*	*hst3Δ rpd3Δ*
TY1	_GLSGEYK(ac)FLR_	0.45367	1885400	678780	*HST3 rpd3Δ*	*hst3Δ rpd3Δ*
TOP2	_ENTPEQDDVATK(ac)K_	0.46673	193990	101040	*HST3 rpd3Δ*	*hst3Δ rpd3Δ*
TY1	_TEECEK(ac)ASTK_	0.47334	1271200	601180	*HST3 rpd3Δ*	*hst3Δ rpd3Δ*
HHT1	_FQK(ac)STELLIR_	0.47428	619410000	310390000	*HST3 rpd3Δ*	*hst3Δ rpd3Δ*
SNF6	_LFSEK(ac)TIR_	0.47657	873170	930620	*HST3 rpd3Δ*	*hst3Δ rpd3Δ*
IFH1	_EVNGSGTTTTQQALSFK(ac)FK_	0.48686	593460	151050	*HST3 rpd3Δ*	*hst3Δ rpd3Δ*
TY1	_GLSGEYK(ac)FLR_	0.49187	1281800	913100	*HST3 rpd3Δ*	*hst3Δ rpd3Δ*
HHT1	_FQK(ac)STELLIR_	0.49475	567560000	294030000	*HST3 rpd3Δ*	*hst3Δ rpd3Δ*

IFH1	_EVNGSGTTTTQQALSFK(ac)FK_	0.49537	2671400	1358100	*HST3 rpd3Δ*	*hst3Δ rpd3Δ*
SHM2	_AVEFAQQVQQSLPK(ac)DACR_	2.0035	1683400	3447900	*HST3 rpd3Δ*	*hst3Δ rpd3Δ*
RHR2;HOR2	_GCDIIVK(ac)NHESIR_	2.0396	77740	170640	*HST3 rpd3Δ*	*hst3Δ rpd3Δ*
MSY1	_DIK(ac)MLDFLADFGR_	3.5589	146550	1252900	*HST3 rpd3Δ*	*hst3Δ rpd3Δ*
MSY1	_DIK(ac)MLDFLADFGR_	3.6644	219390	825220	*HST3 rpd3Δ*	*hst3Δ rpd3Δ*
MET17	_LASGVTK(ac)DLIR_	4.2141	170910	309930	*HST3 rpd3Δ*	*hst3Δ rpd3Δ*
ENO1	_AAGHDGK(ac)IK_	0.11629	1688100	106060	*hst3Δ RPD3*	*HST3 RPD3*
ADE1	_CKDYAK(ac)EK_	0.27518	440000	129830	*hst3Δ RPD3*	*HST3 RPD3*
ADE1	_CKDYAK(ac)EK_	0.30659	1315900	499620	*hst3Δ RPD3*	*HST3 RPD3*
SHM2	_ALK(ac)AFHVTPDK_	0.33757	1564100	411760	*hst3Δ RPD3*	*HST3 RPD3*
ADE1	_CKDYAK(ac)EK_	0.3633	770710	271690	*hst3Δ RPD3*	*HST3 RPD3*
SHM2	_ALK(ac)AFHVTPDK_	0.37873	1346000	507520	*hst3Δ RPD3*	*HST3 RPD3*
RPS18A;RPS18B	_YSNLVCK(ac)K_	0.40305	873130	345460	*hst3Δ RPD3*	*HST3 RPD3*
SHM2	_AVEFAQQVQQSLPK(ac)DACR_	0.40338	5685500	2220100	*hst3Δ RPD3*	*HST3 RPD3*
SHM2	_ALK(ac)AFHVTPDK_	0.42043	7596400	3286300	*hst3Δ RPD3*	*HST3 RPD3*
PMA1	_SLK(ac)QYPK_	0.4318	874410	398360	*hst3Δ RPD3*	*HST3 RPD3*
SHM2	_LKDFK(ac)AK_	0.43991	3122700	1286300	*hst3Δ RPD3*	*HST3 RPD3*
RPL42A;RPL42B	_HTQHK(ac)VTQYK_	0.45163	737520	295380	*hst3Δ RPD3*	*HST3 RPD3*
SHM2	_LKDFK(ac)AK_	0.45197	1604900	681890	*hst3Δ RPD3*	*HST3 RPD3*
SHM2	_ALK(ac)AFHVTPDK_	0.46279	6820900	3132700	*hst3Δ RPD3*	*HST3 RPD3*
HEM1	_TIDK(ac)YGCGAGGTR_	0.46409	349240	302590	*hst3Δ RPD3*	*HST3 RPD3*
SHM2	_LKDFK(ac)AK_	0.46482	1904600	844460	*hst3Δ*	*HST3*

					RPD3	*RPD3*
CDC8	_LLK(ac)FPER_	0.4694	1551600	509640	*hst3Δ RPD3*	*HST3 RPD3*
SHM2	_VDEGSDVLNTWK(ac)K_	0.47308	499440	307110	*hst3Δ RPD3*	*HST3 RPD3*
ADE4	_DLKPGEAVIIPK(ac)NCSK_	0.48791	1006400	584270	*hst3Δ RPD3*	*HST3 RPD3*
SHM2	_LKDFK(ac)AK_	0.49701	3514800	1614600	*hst3Δ RPD3*	*HST3 RPD3*
RPL11A;RPL11B	_GTVGNSHK(ac)TTK_	0.49865	114700	81312	*hst3Δ RPD3*	*HST3 RPD3*
HHT1	_RFQK(ac)STELLIR_	2.1418	299770	515740	*hst3Δ RPD3*	*HST3 RPD3*
YKR070W	_SLVNK(ac)YSR_	2.2014	285320	450960	*hst3Δ RPD3*	*HST3 RPD3*
HHT1	_FQK(ac)STELLIR_	2.3703	260680000	624640000	*hst3Δ RPD3*	*HST3 RPD3*
HHT1	_RFQK(ac)STELLIR_	2.3861	337510	717770	*hst3Δ RPD3*	*HST3 RPD3*
HHT1	_FQK(ac)STELLIR_	2.442	215150000	524520000	*hst3Δ RPD3*	*HST3 RPD3*
HHT1	_RFQK(ac)STELLIR_	2.4609	6299500	15583000	*hst3Δ RPD3*	*HST3 RPD3*
HHT1	_FQK(ac)STELLIR_	2.4732	55662	135560	*hst3Δ RPD3*	*HST3 RPD3*
HHT1	_RFQK(ac)STELLIR_	2.5294	16303000	45574000	*hst3Δ RPD3*	*HST3 RPD3*
HHT1	_FQK(ac)STELLIR_	2.606	275330	693200	*hst3Δ RPD3*	*HST3 RPD3*
PFK2	_SAIFK(ac)GCR_	2.9054	428240	1685900	*hst3Δ RPD3*	*HST3 RPD3*
TKL1	_APEVFK(ac)FFGFTPEGVAER_	3.0146	392880	1516400	*hst3Δ RPD3*	*HST3 RPD3*
PFK2	_SAIFK(ac)GCR_	3.4332	559660	2102300	*hst3Δ RPD3*	*HST3 RPD3*

deacetylations. As demonstrated previously, H3K56 is more acetylated in the *hst3Δ*, confirming the validity of this method (Table 4.6). Interestingly, in either the *RPD3* or *rpd3Δ* background there are fewer substrates whose deacetylation is dependent on Hst3 than on Rpd3 (comparing the results from Tables 4.5 and 4.6), possibly indicating that Rpd3 is a more global regulator of acetylation than Hst3. In the *rpd3Δ* background, the chromatin interacting protein Snf6 exhibits Hst3 dependent deacetylation, indicating a possible link of non-histone deacetylations to chromatin modification. Overall, both the changes in acetylation dependent on Rpd3 and Hst3 highlight the many non-histone possible substrates for these protein deacetylases.

4.5 Discussion

We performed a forward genetic screen to identify what role of Sir2's catalytic activity has not been accounted for in the contemporary understanding of silencing. We isolated five different mutations that restore silencing in a strain with a catalytically inactive allele of Sir2 and a *sas2Δ*. Two of the mutations were in the non-sirtuin histone deacetylase, Rpd3. Restoration of silencing in this mutant was dependent on the *sas2Δ*, likely indicating that the H4K16-acetyl would prevent the *rpd3* mutations ability to restore silencing. Surprisingly, restoration of silencing by the *rpd3Δ* was dependent on another sirtuin histone deacetylase, Hst3. Further analyses revealed that this restoration of silencing was independent of all known histone substrates for both Rpd3 and Hst3, prompting the identification of novel, non-histone acetylation changes associated with Rpd3 and Hst3.

4.5.1 The Role of Rpd3 in Silencing

Rpd3 has been implicated previously as antagonistic to silencing (De Rubertis et al. 1996; Sun and Hampsey 1999). The work reported here ssupports those findings as deletion of *RPD3* results in silencing restoration independently of Sir2's catalytic activity. Many studies have suggested Rpd3 as important for boundary function restricting the spreading of Sir proteins (Donze et al. 1999; Zhou et al. 2009; Ehrentraut et al. 2010). The work reported here clearly shows an antagonistic role for Rpd3 in the establishment of silencing in addition to this boundary function. A previous study suggested that Rpd3 antagonizes Sir2's function by competing for Sir2's histone substrate (Ehrentraut et al. 2010). Ehrentraut and colleagues suggested that removal of Sir2's histone substrate prevents Sir proteins from spreading because Sir2 cannot generate OAAR, hypothesized to be necessary for silencing. However, we show that competition for histone substrates cannot account for Rpd3's anti-silencing activity since the *rpd3Δ* silencing restoration still occurs when expressing the hypoacetylated histone point mutants. However, it is curious that deletion of a non-sirtuin deacetylase restores silencing and that this silencing restoration is dependent on sirtuin deacetylase, possibly leaving open a role for OAAR, generated from a non-histone sirtuin substrate.

4.5.2 Hst3 Has a Unique Role in Silencing

Previous studies have implicated two other sirtuins, Hst3 and Hst4 as important for silencing at telomeres (Yang et al. 2008). The work reported here clearly highlights an Hst3 specific role for silencing at *HML* and *HMR* that is independent of Hst4. This result is consistent with an Hst3-

specific role in the stability of silencing at *HML* (A. Dodson, personal communication). The previously known role for Hst3 and Hst4 has been to deacetylate H3K56 following its incorporation into chromatin during replication (Celic et al. 2006). However, at least in silencing restoration by *rpd3Δ*, Hst3's role is independent of this core histone lysine acetylation as the restoration of silencing by *rpd3Δ* was dependent on Hst3, but independent of H3K56 acetylation status. By inference Hst3 may have another acetyl-lysine substrate in silencing. Alternatively, the point mutation arginine and glutamine "mimics" of the hypoacetylated and hyperacetylated states, respectively, may fail to mimic with sufficient fidelity. Thus follow-up studies mutating the histone acetyltransferase that acetylates H3K56, Rtt109, are needed to definitively test the H3K56 acetylation state on the *rpd3* mutant's silencing restoration. The SILAC analysis conducted suggests possible other targets for Hst3 besides H3K56. Deleting these putative substrates in the *rpd3Δ* to see if the affect the silencing phenotype will be important follow-up studies.

4.5.3 The Importance of Non-Histone Acetylation Substrates

Many lysine deacetylases have classically been identified as histone deacetylases. Although it is true that these proteins deacetylate histones, they do not only deacetylate histones as many non-histone protein acetylation states are influenced by both Rpd3 and Hst3 genotypes (Table 4.5 and Table 4.6). A previous study of Rpd3-dependent deacetylations also identified by SILAC (Henriksen et al. 2012), had little overlap between the proteins identified in our study reported here. One possible reason for the difference between the datasets could be due to the different backgrounds the deacetylations were assayed in. We conducted the SILAC study in the s*ir2N345A sas2Δ* background. In contrast the other study was performed on a wild type W303 strain merely lacking *RPD3*. The mutation of a deacetylase, Sir2, and an acetyltransferase, Sas2, may have altered the landscape of lysine acetylations assayed, accounting for the differences between the studies. Additionally, other studies have utilized a genetic approach to identifying novel, non-histone Rpd3 substrates (Kaluarachchi Duffy et al. 2012). This study explored deacetylations through synthetic dosage lethality: a library overexpressing all yeast genes performed in an *rpd3Δ*. If overexpression of a gene and the *rpd3Δ* show lethality or sickness, this indicates a possible Rpd3 substrate. Here there was some overlap identified, such as the NuA4 complex member Yng2. All these studies, including ours, highlight the importance of non-histone substrates of deacetylases.

4.5.4 Silencing Independent of Sir2 Catalytic Activity

The forward genetic screen for silencing mutants identified five mutants in four different genes that restore silencing independent of Sir2's catalytic activity. Although the screen has not yet been saturated, there are indications that there are few genes in which mutations can restore silencing independent of Sir2's catalytic activity. Recovery of the *sum1-1* allele as one of the few mutants isolated is strong evidence of the very few ways to bypass Sir2's catalytic activity in silencing. This mutation was previously isolated in a screen to suppress the silencing defect of all three sir protein complex members (Klar et al. 1985). The silencing restoration observed by *sum1-1* in the *sir2N345A sas2Δ* background is dependent on Hst1 (data not shown), indicating that it is restoring silencing through the same previously described mechanism (Rusché and Rine 2001). An additional indication that the screen is nearing saturation was the isolation of two different mutations in *RPD3*.

One surprising mutation recovered from the screen is the *orc3A333V* mutant. The ORC complex binds to all four silencers at *HMR* and *HML* to recruit the Sir2, Sir3, Sir4 complex through interactions bridged by Sir1 (Triolo and Sternglanz 1996; Zhang et al. 2002; Hou et al. 2005). Mutations have been previously isolated in Orc2 and Orc5 that effect silencing (Foss et al. 1993; Loo et al. 1995; Micklem et al. 1993). However, all previous mutations isolated have weakened silencing, where the *ORC3* mutation isolated in this screen improved silencing. Additionally, a study found that deleting *SAS2* exacerbates the silencing defect of the *orc5-1* mutant (Zou and Bi 2008). Although this makes the isolation of the *orc3A333V* mutation even more surprising, it does suggest an interaction between Sas2 and ORC that may be important for the silencing restoration by the *orc3A333V* mutant. Future studies determining if the *sas2Δ* is necessary for silencing restoration of this *orc3* mutant would help to determine if the ORC *SAS2* interaction is important for restoration of silencing independent of Sir2 catalytic activity. Crosslinking studies have identified that the Orc3 subunit is adjacent to Orc2 and interacts with DNA (Chen et al. 2008) and one mutation in Orc3 has been identified in a screen to identify factors involved in gross chromosomal rearrangements (Huang and Koshland 2003). Further investigation is necessary to understand how the Orc3 mutation isolated overcomes the Sir2 silencing defect, possibly by investigating interactions between the *orc3A333V* allele and Sir proteins. Additionally, isolation of a mutation in an essential gene underscores that the screen was performed exhaustively as there is a smaller chance of recovering mutations in essential genes that restore the phenotype of interest, but do not result in cell death.

One mutation's identity has yet to be determined. Due to this mutant's unusual bi-mating phenotype and its sporulation defect, it was likely that this mutation was distinct from those already isolated. The bi-mating phenotype exhibited, may indicate that the mutation effects the mating type regulation of the cell. Further RNA analysis of the expression of genes from *MAT, HMR, HML* and other cell-type specific genes could help to elucidate the mechanism of silencing restoration in by this mutant.

References

Amberg, D. C., Burke, D. J., & Strathern, J. N. (2005). *Methods in Yeast Genetics: A Cold Spring Harbor Laboratory Course Manual, 2005 Edition*. *A Cold Spring Harbor Laboratory Course Manual* (p. 205).

Aparicio, O., Geisberg, J. V, Sekinger, E., Yang, A., Moqtaderi, Z., & Struhl, K. (2005). Chromatin immunoprecipitation for determining the association of proteins with specific genomic sequences in vivo. *Current Protocols in Molecular Biology / Edited by Frederick M. Ausubel ... [et Al.]*, *Chapter 21*, Unit 21.3. doi:10.1002/0471142727.mb2103s69

Aparicio, O. M., Billington, B. L., & Gottschling, D. E. (1991). Modifiers of position effect are shared between telomeric and silent mating-type loci in S. cerevisiae. *Cell*, *66*(6), 1279–87.

Armache, K.-J., Garlick, J. D., Canzio, D., Narlikar, G. J., & Kingston, R. E. (2011). Structural basis of silencing: Sir3 BAH domain in complex with a nucleosome at 3.0 Å resolution. *Science (New York, N.Y.)*, *334*(6058), 977–82. doi:10.1126/science.1210915

Babiarz, J. E., Halley, J. E., & Rine, J. (2006). Telomeric heterochromatin boundaries require NuA4-dependent acetylation of histone variant H2A.Z in *Saccharomyces cerevisiae*, *5*, 700–710. doi:10.1101/gad.1386306.some

Bantignies, F., Roure, V., Comet, I., Leblanc, B., Schuettengruber, B., Bonnet, J., Tixier, V., Mas, A., & Cavalli, G. (2011). Polycomb-dependent regulatory contacts between distant Hox loci in *Drosophila*. *Cell*, *144*(2), 214–26. doi:10.1016/j.cell.2010.12.026

Barton, A. B., & Kaback, D. B. (2006). Telomeric silencing of an open reading frame in Saccharomyces cerevisiae. *Genetics*, *173*(2), 1169–73. doi:10.1534/genetics.106.058420

Beisel, C., & Paro, R. (2011). Silencing chromatin: comparing modes and mechanisms. *Nature Reviews. Genetics*, *12*(2), 123–35. doi:10.1038/nrg2932

Bi, X., Braunstein, M., Shei, G. J., & Broach, J. R. (1999). The yeast *HML I* silencer defines a heterochromatin domain boundary by directional establishment of silencing. *Proceedings of the National Academy of Sciences of the United States of America*, *96*(21), 11934–9.

Birkeland, S. R., Jin, N., Ozdemir, A. C., Lyons, R. H., Weisman, L. S., & Wilson, T. E. (2010). Discovery of mutations in Saccharomyces cerevisiae by pooled linkage analysis and whole-genome sequencing. *Genetics*, *186*(4), 1127–37. doi:10.1534/genetics.110.123232

Bitterman, K. J., Anderson, R. M., Cohen, H. Y., Latorre-Esteves, M., & Sinclair, D. a. (2002). Inhibition of silencing and accelerated aging by nicotinamide, a putative negative regulator of yeast sir2 and human SIRT1. *The Journal of Biological Chemistry*, *277*(47), 45099–107. doi:10.1074/jbc.M205670200

Boeke, J. D., LaCroute, F., & Fink, G. R. (1984). A positive selection for mutants lacking orotidine-5'-phosphate decarboxylase activity in yeast: 5-fluoro-orotic acid resistance. *Molecular & General Genetics : MGG*, *197*(2), 345–6.

Brand, a H., Breeden, L., Abraham, J., Sternglanz, R., & Nasmyth, K. (1985). Characterization of a "silencer" in yeast: a DNA sequence with properties opposite to those of a transcriptional enhancer. *Cell*, *41*(1), 41–8.

Braunstein, M., Rose, a B., Holmes, S. G., Allis, C. D., & Broach, J. R. (1993). Transcriptional silencing in yeast is associated with reduced nucleosome acetylation. *Genes & Development*, *7*(4), 592–604. doi:10.1101/gad.7.4.592

Carrozza, M. J., Li, B., Florens, L., Suganuma, T., Swanson, S. K., Lee, K. K., Shia, W., Anderson, S., Yates, J., Washburn, M. P., & Workman, J. L. (2005). Histone H3 methylation by Set2 directs deacetylation of coding regions by Rpd3S to suppress spurious intragenic transcription. *Cell*, *123*(4), 581–92. doi:10.1016/j.cell.2005.10.023

Celic, I., Masumoto, H., Griffith, W. P., Meluh, P., Cotter, R. J., Boeke, J. D., & Verreault, A. (2006). The sirtuins Hst3p and Hst4p preserve genome integrity by controlling histone h3 lysine 56 deacetylation. *Current Biology : CB*, *16*(13), 1280–9. doi:10.1016/j.cub.2006.06.023

Chen, L., & Widom, J. (2005). Mechanism of transcriptional silencing in yeast. *Cell*, *120*(1), 37–48. doi:10.1016/j.cell.2004.11.030

Chen, X.-F., Kuryan, B., Kitada, T., Tran, N., Li, J.-Y., Kurdistani, S., … Carey, M. (2012). The Rpd3 core complex is a chromatin stabilization module. *Current Biology : CB*, *22*(1), 56–63. doi:10.1016/j.cub.2011.11.042

Chen, Y., Negre, N., Li, Q., Mieczkowska, J. O., Slattery, M., Liu, T., Zhang, Y., Tae-Kyung, K., Housheng, H. H., Zieba, J. Yijun, R., Bickel, P. J., Myers, R. M., Wold, B. J., White, K. P., Lieb, J. D. & Liu, X. S. (2012). Systematic evaluation of factors influencing ChIP-seq fidelity. *Nature Methods*, *9*(6), 609–14. doi:10.1038/nmeth.1985

Chen, Y., Rai, R., Zhou, Z.-R., Kanoh, J., Ribeyre, C., Yang, Y., Zheng, H., Damay, P., Wang, F., Tsujii, H., Hiraoka, Y., Shore, D., Hu, H., Chang, S., & Lei, M. (2011). A conserved motif within RAP1 has diversified roles in telomere protection and regulation in different organisms. *Nature Structural & Molecular Biology*, *18*(2), 213–21. doi:10.1038/nsmb.1974

Chen, Z., Speck, C., Wendel, P., Tang, C., Stillman, B., & Li, H. (2008). The architecture of the DNA replication origin recognition complex in *Saccharomyces cerevisiae*. *Proceedings of the National Academy of Sciences of the United States of America*, *105*(30), 10326–31. doi:10.1073/pnas.0803829105

Cheng, T. H., & Gartenberg, M. R. (2000). Yeast heterochromatin is a dynamic structure that requires silencers continuously. *Genes & Development*, *14*(4), 452–63. doi:10.1101/gad.14.4.452

Chi, M. H., & Shore, D. (1996). SUM1-1, a dominant suppressor of SIR mutations in Saccharomyces cerevisiae, increases transcriptional silencing at telomeres and HM mating-type loci and decreases chromosome stability. *Molecular and Cellular Biology*, *16*(8), 4281–94.

Chou, C.-C., Li, Y.-C., & Gartenberg, M. R. (2008). Bypassing Sir2 and O-acetyl-ADP-ribose in transcriptional silencing. *Molecular Cell*, *31*(5), 650–9. doi:10.1016/j.molcel.2008.06.020

Conrad, T., & Akhtar, A. (2011). Dosage compensation in *Drosophila melanogaster*: epigenetic fine-tuning of chromosome-wide transcription. *Nature Reviews. Genetics*, *13*(2), 123–34. doi:10.1038/nrg3124

Cox, J., & Mann, M. (2008). MaxQuant enables high peptide identification rates, individualized p.p.b.-range mass accuracies and proteome-wide protein quantification. *Nature Biotechnology*, *26*(12), 1367–72. doi:10.1038/nbt.1511

Danecek, P., Auton, A., Abecasis, G., Albers, C. A., Banks, E., DePristo, M. A, Handsaker, R. E., Lunter, G., Marth, G. T., Sherry, S. T., McVean, G., Durbin, R. & 1000 Genomes Project (2011). The variant call format and VCFtools. *Bioinformatics (Oxford, England)*, *27*(15), 2156–8. doi:10.1093/bioinformatics/btr330

De Rubertis, F., Kadosh, D., Henchoz, S., Pauli, D., Reuter, G., Struhl, K., & Spierer, P. (1996). The histone deacetylase RPD3 counteracts genomic silencing in Drosophila and yeast. *Nature*, *384*(6609), 589–91. doi:10.1038/384589a0

Dekker, J., Rippe, K., Dekker, M., & Kleckner, N. (2002). Capturing chromosome conformation. *Science (New York, N.Y.)*, *295*(5558), 1306–11. doi:10.1126/science.1067799

Dieci, G., & Sentenac, A. (1996). Facilitated recycling pathway for RNA polymerase III. *Cell*, *84*(2), 245–52.

Dillin, A., & Rine, J. (1997). Separable functions of ORC5 in replication initiation and silencing in *Saccharomyces cerevisiae*. *Genetics*, *147*(3), 1053–62.

Dion, M. F., Altschuler, S. J., Wu, L. F., & Rando, O. J. (2005). Genomic characterization reveals a simple histone H4 acetylation code. *Proceedings of the National Academy of Sciences of the United States of America*, *102*(15), 5501–6. doi:10.1073/pnas.0500136102

Donze, D., Adams, C. R., Rine, J., & Kamakaka, R. T. (1999). The boundaries of the silenced *HMR* domain in *Saccharomyces cerevisiae*. *Genes & Development*, *13*(6), 698–708.

Donze, D., & Kamakaka, R. T. (2001). RNA polymerase III and RNA polymerase II promoter complexes are heterochromatin barriers in *Saccharomyces cerevisiae*. *The EMBO Journal*, *20*(3), 520–31. doi:10.1093/emboj/20.3.520

Downey, M., Knight, B., Vashisht, A. a, Seller, C. a, Wohlschlegel, J. a, Shore, D., & Toczyski, D. P. (2013). Gcn5 and sirtuins regulate acetylation of the ribosomal protein transcription factor Ifh1. *Current Biology : CB*, *23*(17), 1638–48. doi:10.1016/j.cub.2013.06.050

Ehrenhofer-Murray, A. E., Rivier, D. H., & Rine, J. (1997). The role of Sas2, an acetyltransferase homologue of *Saccharomyces cerevisiae*, in silencing and ORC function. *Genetics*, *145*(4), 923–34.

Ehrentraut, S., Hassler, M., Oppikofer, M., Kueng, S., Weber, J. M., Mueller, J. W., Gasser, S., Ladurner, A. G., & Ehrenhofer-Murray, A. E. (2011). Structural basis for the role of the Sir3 AAA+ domain in silencing: interaction with Sir4 and unmethylated histone H3K79. *Genes & Development*, *25*(17), 1835–46. doi:10.1101/gad.17175111

Ehrentraut, S., Weber, J. M., Dybowski, J. N., Hoffmann, D., & Ehrenhofer-Murray, A. E. (2010). Rpd3-dependent boundary formation at telomeres by removal of Sir2 substrate. *Proceedings of the National Academy of Sciences of the United States of America*, *107*(12), 5522–7. doi:10.1073/pnas.0909169107

Fan, X., & Struhl, K. (2009). Where does mediator bind in vivo? *PloS One*, *4*(4), e5029. doi:10.1371/journal.pone.0005029

Fillingham, J., Recht, J., Silva, A. C., Suter, B., Emili, A., Stagljar, I., Krogan, N., Allis, D., Keogh, M. C., & Greenblatt, J. F. (2008). Chaperone control of the activity and specificity of the histone H3 acetyltransferase Rtt109. *Molecular and Cellular Biology*, *28*(13), 4342–53. doi:10.1128/MCB.00182-08

Flores, O., & Orozco, M. (2011). nucleR: a package for non-parametric nucleosome positioning. *Bioinformatics (Oxford, England)*, *27*(15), 2149–50. doi:10.1093/bioinformatics/btr345

Foss, M., McNally, F. J., Laurenson, P., & Rine, J. (1993). Origin recognition complex (ORC) in transcriptional silencing and DNA replication in *S. cerevisiae*. *Science (New York, N.Y.)*, *262*(5141), 1838–44.

Fourel, G., Revardel, E., Koering, C. E., & Gilson, E. (1999). Cohabitation of insulators and silencing elements in yeast subtelomeric regions. *The EMBO Journal*, *18*(9), 2522–37. doi:10.1093/emboj/18.9.2522

Fox, C. a., Ehrenhofer-Murray, A. E., Loo, S., & Rine, J. (1997). The origin recognition complex, SIR1, and the S phase requirement for silencing. *Science (New York, N.Y.)*, *276*(5318), 1547–51. doi:10.1126/science.276.5318.1547

Furey, T. S. (2012). ChIP-seq and beyond: new and improved methodologies to detect and characterize protein-DNA interactions. *Nature Reviews. Genetics*, *13*(12), 840–52. doi:10.1038/nrg3306

Furuyama, S., & Biggins, S. (2007). Centromere identity is specified by a single centromeric nucleosome in budding yeast. *Proceedings of the National Academy of Sciences of the United States of America*, *104*(37), 14706–11. doi:10.1073/pnas.0706985104

Gao, L., & Gross, D. S. (2008). Sir2 silences gene transcription by targeting the transition between RNA polymerase II initiation and elongation. *Molecular and Cellular Biology*, *28*(12), 3979–94. doi:10.1128/MCB.00019-08

Ghidelli, S., Donze, D., Dhillon, N., & Kamakaka, R. T. (2001). Sir2p exists in two nucleosome-binding complexes with distinct deacetylase activities. *The EMBO Journal*, *20*(16), 4522–35. doi:10.1093/emboj/20.16.4522

Gottschling, D. E., Aparicio, O. M., Billington, B. L., & Zakian, V. A. (1990). Position effect at *S. cerevisiae* telomeres: reversible repression of Pol II transcription. *Cell*, *63*(4), 751–62.

Grunstein, M., & Gasser, S. M. (2013). Epigenetics in *Saccharomyces cerevisiae*. *Cold Spring Harbor Perspectives in Biology*, *5*(7), 1–28. doi:10.1101/cshperspect.a017491

Haber, J. E. (2012). Mating-type genes and MAT switching in Saccharomyces cerevisiae. *Genetics*, *191*(1), 33–64. doi:10.1534/genetics.111.134577

Hanlon, S. E., & Lieb, J. D. (2004). Progress and challenges in profiling the dynamics of chromatin and transcription factor binding with DNA microarrays. *Current Opinion in Genetics & Development*, *14*(6), 697–705. doi:10.1016/j.gde.2004.09.008

Hecht, A., Strahl-Bolsinger, S., & Grunstein, M. (1996). Spreading of transcriptional repressor SIR3 from telomeric heterochromatin. *Nature*, *383*(6595), 92–6. doi:10.1038/383092a0

Henikoff, J. G., Belsky, J. A., Krassovsky, K., MacAlpine, D. M., & Henikoff, S. (2011). Epigenome characterization at single base-pair resolution. *Proceedings of the National Academy of Sciences of the United States of America*, *108*(45), 18318–23. doi:10.1073/pnas.1110731108

Henriksen, P., Wagner, S. a, Weinert, B. T., Sharma, S., Bacinskaja, G., Rehman, M., Juffers, H. J., Walther, T. C., Walther, Lisby, M., & Choudhary, C. (2012). Proteome-wide analysis of lysine acetylation suggests its broad regulatory scope in *Saccharomyces cerevisiae*. *Molecular & Cellular Proteomics : MCP*, *11*(11), 1510–22. doi:10.1074/mcp.M112.017251

Herskowitz, I. (1988). Life cycle of the budding yeast *Saccharomyces cerevisiae*. *Microbiological Reviews*, *52*(4), 536–53.

Hicks, J., Strathern, J. N., & Klar, A. J. (1979). Transposable mating type genes in *Saccharomyces cerevisiae*. *Nature*, *282*(5738), 478–3.

Ho, J. W. K., Bishop, E., Karchenko, P. V, Nègre, N., White, K. P., & Park, P. J. (2011). ChIP-chip versus ChIP-seq: lessons for experimental design and data analysis. *BMC Genomics*, *12*(1), 134. doi:10.1186/1471-2164-12-134

Hoffman, C. S., & Winston, F. (1987). A ten-minute DNA preparation from yeast efficiently releases autonomous plasmids for transformation of *Escherichia coli*. *Gene*, *57*(2-3), 267–72.

Hoppe, G. J., Tanny, J. C., Rudner, A. D., Gerber, S. A., Danaie, S., Gygi, S. P., & Moazed, D. (2002). Steps in assembly of silent chromatin in yeast: Sir3-independent binding of a Sir2/Sir4 complex to silencers and role for Sir2-dependent deacetylation. *Molecular and Cellular Biology*, *22*(12), 4167–80. doi:10.1128/MCB.22.12.4167

Hou, Z., Bernstein, D. a, Fox, C. a., & Keck, J. L. (2005). Structural basis of the Sir1-origin recognition complex interaction in transcriptional silencing. *Proceedings of the National Academy of Sciences of the United States of America*, *102*(24), 8489–94. doi:10.1073/pnas.0503525102

Huang, D., & Koshland, D. (2003). Chromosome integrity in *Saccharomyces cerevisiae*: the interplay of DNA replication initiation factors, elongation factors, and origins. *Genes & Development*, *17*(14), 1741–54. doi:10.1101/gad.1089203

Imai, S., Armstrong, C. M., Kaeberlein, M., & Guarente, L. (2000). Transcriptional silencing and longevity protein Sir2 is an NAD-dependent histone deacetylase. *Nature*, *403*(6771), 795–800. doi:10.1038/35001622

Jauert, P. a, Jensen, L. E., & Kirkpatrick, D. T. (2005). A novel yeast genomic DNA library on a geneticin-resistance vector. *Yeast (Chichester, England)*, *22*(8), 653–7. doi:10.1002/yea.1250

Jeon, Y., Sarma, K., & Lee, J. T. (2012). New and Xisting regulatory mechanisms of X chromosome inactivation. *Current Opinion in Genetics & Development*, *22*(2), 62–71. doi:10.1016/j.gde.2012.02.007

Johnson, A., Li, G., Sikorski, T. W., Buratowski, S., Woodcock, C. L., & Moazed, D. (2009). Reconstitution of heterochromatin-dependent transcriptional gene silencing. *Molecular Cell*, *35*(6), 769–81. doi:10.1016/j.molcel.2009.07.030

Johnson, L. M., Kayne, P. S., Kahn, E. S., & Grunstein, M. (1990). Genetic evidence for an interaction between SIR3 and histone H4 in the repression of the silent mating loci in *Saccharomyces cerevisiae*. *Proceedings of the National Academy of Sciences of the United States of America*, *87*(16), 6286–90.

Kaluarachchi Duffy, S., Friesen, H., Baryshnikova, A., Lambert, J.-P., Chong, Y. T., Figeys, D., & Andrews, B. (2012). Exploring the yeast acetylome using functional genomics. *Cell*, *149*(4), 936–48. doi:10.1016/j.cell.2012.02.064

Kasten, M. M., Dorland, S., & Stillman, D. J. (1997). A large protein complex containing the yeast Sin3p and Rpd3p transcriptional regulators. *Molecular and Cellular Biology*, *17*(8), 4852–8.

Kidder, B. L., Hu, G., & Zhao, K. (2011). ChIP-Seq: technical considerations for obtaining high-quality data. *Nature Immunology*, *12*(10), 918–22. doi:10.1038/ni.2117

Kimura, A., Umehara, T., & Horikoshi, M. (2002). Chromosomal gradient of histone acetylation established by Sas2p and Sir2p functions as a shield against gene silencing. *Nature Genetics*, *32*(3), 370–7. doi:10.1038/ng993

Klar, a J., Kakar, S. N., Ivy, J. M., Hicks, J. B., Livi, G. P., & Miglio, L. M. (1985). SUM1, an apparent positive regulator of the cryptic mating-type loci in Saccharomyces cerevisiae. *Genetics*, *111*(4), 745–58.

Kueng, S., Oppikofer, M., & Gasser, S. M. (2013). SIR proteins and the assembly of silent chromatin in budding yeast. *Annual Review of Genetics*, *47*, 275–306. doi:10.1146/annurev-genet-021313-173730

Kurdistani, S., Tavazoie, S., & Grunstein, M. (2004). Mapping global histone acetylation patterns to gene expression. *Cell*, *117*(6), 721–33. doi:10.1016/j.cell.2004.05.023

Kustatscher, G., Hothorn, M., Pugieux, C., Scheffzek, K., & Ladurner, A. G. (2005). Splicing regulates NAD metabolite binding to histone macroH2A. *Nature Structural & Molecular Biology*, *12*(7), 624–5. doi:10.1038/nsmb956

Landry, J., Sutton, a, Tafrov, S. T., Heller, R. C., Stebbins, J., Pillus, L., & Sternglanz, R. (2000). The silencing protein SIR2 and its homologs are NAD-dependent protein deacetylases. *Proceedings of the National Academy of Sciences of the United States of America*, *97*(11), 5807–11. doi:10.1073/pnas.110148297

Lazarus, A. G., & Holmes, S. G. (2011). A cis-acting tRNA gene imposes the cell cycle progression requirement for establishing silencing at the *HMR* locus in yeast. *Genetics*, *187*(2), 425–39. doi:10.1534/genetics.110.124099

Lee, S., Tong, L., & Denu, J. M. (2008). Quantification of endogenous sirtuin metabolite O -acetyl-ADP-ribose. *Analytical Biochemistry*, *383*(2), 174–179. doi:10.1016/j.ab.2008.08.033

Lefrançois, P., Euskirchen, G. M., Auerbach, R. K., Rozowsky, J., Gibson, T., Yellman, C. M., Gerstein, M., & Snyder, M. (2009). Efficient yeast ChIP-Seq using multiplex short-read DNA sequencing. *BMC Genomics*, *10*, 37. doi:10.1186/1471-2164-10-37

Li, H., & Durbin, R. (2009). Fast and accurate short read alignment with Burrows-Wheeler transform. *Bioinformatics (Oxford, England)*, *25*(14), 1754–60. doi:10.1093/bioinformatics/btp324

Li, H., Handsaker, B., Wysoker, A., Fennell, T., Ruan, J., Homer, N., … Durbin, R. (2009). The Sequence Alignment/Map format and SAMtools. *Bioinformatics (Oxford, England)*, *25*(16), 2078–9. doi:10.1093/bioinformatics/btp352

Li, H., Ruan, J., & Durbin, R. (2008). Mapping short DNA sequencing reads and calling variants using mapping quality scores. *Genome Research*, *18*(11), 1851–8. doi:10.1101/gr.078212.108

Li, M., Valsakumar, V., Poorey, K., Bekiranov, S., & Smith, J. S. (2013). Genome-wide analysis of functional sirtuin chromatin targets in yeast. *Genome Biology*, *14*(5), R48. doi:10.1186/gb-2013-14-5-r48

Lieb, J. D., Liu, X., Botstein, D., & Brown, P. O. (2001). Promoter-specific binding of Rap1 revealed by genome-wide maps of protein-DNA association. *Nature Genetics*, *28*(4), 327–34. doi:10.1038/ng569

Lin, Y., Lu, J., Zhang, J., Walter, W., Dang, W., Wan, J., … Zhu, H. (2009). Protein acetylation microarray reveals that NuA4 controls key metabolic target regulating gluconeogenesis. *Cell*, *136*(6), 1073–84. doi:10.1016/j.cell.2009.01.033

Liou, G., Tanny, J. C., Kruger, R. G., Walz, T., & Moazed, D. (2005). Assembly of the SIR complex and its regulation by O-acetyl-ADP-ribose, a product of NAD-dependent histone deacetylation. *Cell*, *121*(4), 515–27. doi:10.1016/j.cell.2005.03.035

Liou, G.-G., Tanny, J. C., Kruger, R. G., Walz, T., & Moazed, D. (2005). Assembly of the SIR complex and its regulation by O-acetyl-ADP-ribose, a product of NAD-dependent histone deacetylation. *Cell*, *121*(4), 515–27. doi:10.1016/j.cell.2005.03.035

Loney, E. R., Inglis, P. W., Sharp, S., Pryde, F. E., Kent, N. a, Mellor, J., & Louis, E. J. (2009). Repressive and non-repressive chromatin at native telomeres in *Saccharomyces cerevisiae*. *Epigenetics & Chromatin*, *2*(1), 18. doi:10.1186/1756-8935-2-18

Longtine, M. S., McKenzie, A., Demarini, D. J., Shah, N. G., Wach, A., Brachat, A., … Pringle, J. R. (1998). Additional modules for versatile and economical PCR-based gene deletion and modification in Saccharomyces cerevisiae. *Yeast (Chichester, England)*, *14*(10), 953–61. doi:10.1002/(SICI)1097-0061(199807)14:10<953::AID-YEA293>3.0.CO;2-U

Loo, S., Fox, C. a, Rine, J., Kobayashi, R., Stillman, B., & Bell, S. (1995). The origin recognition complex in silencing, cell cycle progression, and DNA replication. *Molecular Biology of the Cell*, *6*(6), 741–56.

Loo, S., & Rine, J. (1994). Silencers and domains of generalized repression. *Science (New York, N.Y.)*, *264*(5166), 1768–71.

Louis, E. J. (1995). The chromosome ends of *Saccharomyces cerevisiae*. *Yeast (Chichester, England)*, *11*(16), 1553–73. doi:10.1002/yea.320111604

Lynch, P. J., & Rusché, L. N. (2009). A silencer promotes the assembly of silenced chromatin independently of recruitment. *Molecular and Cellular Biology*, *29*(1), 43–56. doi:10.1128/MCB.00983-08

Mahoney, D. J., & Broach, J. R. (1989). The *HML* mating-type cassette of *Saccharomyces cerevisiae* is regulated by two separate but functionally equivalent silencers. *Molecular and Cellular Biology*, *9*(11), 4621–30.

Marchfelder, U., Rateitschak, K., & Ehrenhofer-Murray, A. E. (2003). SIR-dependent repression of non-telomeric genes in *Saccharomyces cerevisiae*? *Yeast (Chichester, England)*, *20*(9), 797–801. doi:10.1002/yea.1001

Martino, F., Kueng, S., Robinson, P., Tsai-Pflugfelder, M., van Leeuwen, F., Ziegler, M., … Gasser, S. M. (2009). Reconstitution of yeast silent chromatin: multiple contact sites and O-AADPR binding load SIR complexes onto nucleosomes in vitro. *Molecular Cell*, *33*(3), 323–34. doi:10.1016/j.molcel.2009.01.009

Masumoto, H., Hawke, D., Kobayashi, R., & Verreault, A. (2005). A role for cell-cycle-regulated histone H3 lysine 56 acetylation in the DNA damage response. *Nature*, *436*(7048), 294–8. doi:10.1038/nature03714

Meyer, B. J. (2010). Targeting X chromosomes for repression. *Current Opinion in Genetics & Development*, *20*(2), 179–89. doi:10.1016/j.gde.2010.03.008

Micklem, G., Rowley, A., Harwood, J., Nasmyth, K., & Diffley, J. F. (1993). Yeast origin recognition complex is involved in DNA replication and transcriptional silencing. *Nature*, *366*(6450), 87–9. doi:10.1038/366087a0

Moazed, D., Kistler, A., Axelrod, A., Rine, J., & Johnson, A. D. (1997). Silent information regulator protein complexes in *Saccharomyces cerevisiae*: a SIR2/SIR4 complex and evidence for a regulatory domain in SIR4 that inhibits its interaction with SIR3. *Proceedings of the National Academy of Sciences of the United States of America*, *94*(6), 2186–91.

Moqtaderi, Z., & Struhl, K. (2004). Genome-wide occupancy profile of the RNA polymerase III machinery in Saccharomyces cerevisiae reveals loci with incomplete transcription complexes. *Molecular and Cellular Biology*, *24*(10), 4118–27. doi:10.1128/MCB.24.10.4118

Nasmyth, K. A., & Tatchell, K. (1980). The structure of transposable yeast mating type loci. *Cell*, *19*(3), 753–64.

Norris, A., & Boeke, J. D. (2010). Silent information regulator 3: the Goldilocks of the silencing complex. *Genes & Development*, *24*(2), 115–22. doi:10.1101/gad.1865510

Oki, M., & Kamakaka, R. T. (2005). Barrier function at HMR. *Molecular Cell*, *19*(5), 707–16. doi:10.1016/j.molcel.2005.07.022

Oppikofer, M., Kueng, S., Martino, F., Soeroes, S., Hancock, S. M., Chin, J. W., … Gasser, S. M. (2011). A dual role of H4K16 acetylation in the establishment of yeast silent chromatin. *The EMBO Journal*, *30*(13), 2610–21. doi:10.1038/emboj.2011.170

Ozaydin, B., & Rine, J. (2010). Expanded roles of the origin recognition complex in the architecture and function of silenced chromatin in *Saccharomyces cerevisiae*. *Molecular and Cellular Biology*, *30*(3), 626–39. doi:10.1128/MCB.00614-09

Park, E. C., & Szostak, J. W. (1990). Point mutations in the yeast histone H4 gene prevent silencing of the silent mating type locus *HML*. *Molecular and Cellular Biology*, *10*(9), 4932–4.

Park, P. J. (2009). ChIP-seq: advantages and challenges of a maturing technology. *Nature Reviews. Genetics*, *10*(10), 669–80. doi:10.1038/nrg2641

Phillips-Cremins, J. E., Sauria, M. E. G., Sanyal, A., Gerasimova, T. I., Lajoie, B. R., Bell, J. S. K., Ong, C. T., Hookway, T. A., Guo, C., Sun, Y., Bland, M. J., Wagstaff, W., Dalton, S., McDevitt, T. C., Sen, R., Dekker, J., Taylor, J.,& Corces, V. G. (2013). Architectural protein subclasses shape 3D organization of genomes during lineage commitment. *Cell*, *153*(6), 1281–95. doi:10.1016/j.cell.2013.04.053

Pillus, L., & Rine, J. (1989). Epigenetic inheritance of transcriptional states in S. cerevisiae. *Cell*, *59*(4), 637–47.

Pryde, F. E., & Louis, E. J. (1999). Limitations of silencing at native yeast telomeres. *The EMBO Journal*, *18*(9), 2538–50. doi:10.1093/emboj/18.9.2538

Radman-Livaja, M., Ruben, G., Weiner, A., Friedman, N., Kamakaka, R., & Rando, O. J. (2011). Dynamics of Sir3 spreading in budding yeast: secondary recruitment sites and euchromatic localization. *The EMBO Journal*, *30*(6), 1012–26. doi:10.1038/emboj.2011.30

Ravindra, a, Weiss, K., & Simpson, R. T. (1999). High-resolution structural analysis of chromatin at specific loci: *Saccharomyces cerevisiae* silent mating-type locus *HMRa*. *Molecular and Cellular Biology*, *19*(12), 7944–50.

Recht, J., Tsubota, T., Tanny, J. C., Diaz, R. L., Berger, J. M., Zhang, X., … Allis, C. D. (2006). Histone chaperone Asf1 is required for histone H3 lysine 56 acetylation, a modification associated with S phase in mitosis and meiosis. *Proceedings of the National Academy of Sciences of the United States of America*, *103*(18), 6988–93. doi:10.1073/pnas.0601676103

Reifnyder, C., Lowell, J., Clarke, A., & Pillus, L. (1997). Yeast SAS silencing genes and human genes associated with AML and HIV-1 Tat interactions are homologous with acetyltransferases. *Nature Genetics*, *16*(1), 109. doi:10.1038/ng0597-106

Rine, J., & Herskowitz, I. (1987). Four genes responsible for a position effect on expression from *HML* and *HMR* in *Saccharomyces cerevisiae*. *Genetics*, *116*(1), 9–22.

Rine, J., Strathern, J. N., Hicks, J. B., & Herskowitz, I. (1979). A suppressor of mating-type locus mutations in *Saccharomyces cerevisiae*: evidence for and identification of cryptic mating-type loci. *Genetics*, *93*(4), 877–901.

Ringrose, L., & Paro, R. (2004). Epigenetic regulation of cellular memory by the Polycomb and Trithorax group proteins. *Annual Review of Genetics*, *38*, 413–43. doi:10.1146/annurev.genet.38.072902.091907

Rivier, D. H., Ekena, J. L., & Rine, J. (1999). *HMR-I* is an origin of replication and a silencer in *Saccharomyces cerevisiae*. *Genetics*, *151*(2), 521–9.

Rivier, D. H., & Rine, J. (1992). An origin of DNA replication and a transcription silencer require a common element. *Science (New York, N.Y.)*, *256*(5057), 659–63.

Roberts, D. N., Stewart, A. J., Huff, J. T., & Cairns, B. R. (2003). The RNA polymerase III transcriptome revealed by genome-wide localization and activity-occupancy relationships. *Proceedings of the National Academy of Sciences of the United States of America*, *100*(25), 14695–700. doi:10.1073/pnas.2435566100

Roy, R., Meier, B., McAinsh, A. D., Feldmann, H. M., & Jackson, S. P. (2004). Separation-of-function mutants of yeast Ku80 reveal a Yku80p-Sir4p interaction involved in telomeric silencing. *The Journal of Biological Chemistry*, *279*(1), 86–94. doi:10.1074/jbc.M306841200

Rusché, L. N., Kirchmaier, A. L., & Rine, J. (2002). Ordered Nucleation and Spreading of Silenced Chromatin in *Saccharomyces cerevisiae*. *Molecular Biology of the Cell*, *13*(July), 2207–2222. doi:10.1091/mbc.E02

Rusché, L. N., Kirchmaier, A. L., & Rine, J. (2003). The establishment, inheritance, and function of silenced chromatin in *Saccharomyces cerevisiae*. *Annual Review of Biochemistry*, *72*, 481–516. doi:10.1146/annurev.biochem.72.121801.161547

Rusché, L. N., & Rine, J. (2001). Conversion of a gene-specific repressor to a regional silencer. *Genes & Development*, *15*(8), 955–67. doi:10.1101/gad.873601

Sauve, A. a, Wolberger, C., Schramm, V. L., & Boeke, J. D. (2006). The biochemistry of sirtuins. *Annual Review of Biochemistry*, *75*, 435–65. doi:10.1146/annurev.biochem.74.082803.133500

Simon, J. a, & Kingston, R. E. (2009). Mechanisms of polycomb gene silencing: knowns and unknowns. *Nature Reviews. Molecular Cell Biology*, *10*(10), 697–708. doi:10.1038/nrm2763

Singh, J., & Klar, a J. (1992). Active genes in budding yeast display enhanced in vivo accessibility to foreign DNA methylases: a novel in vivo probe for chromatin structure of yeast. *Genes & Development*, *6*(2), 186–196. doi:10.1101/gad.6.2.186

Smith, J. S., Brachmann, C. B., Celic, I., Kenna, M. a, Muhammad, S., Starai, V. J., Avalos, J. L., Escalante-Semerena, J. C., Grubmeyer, C., Wolberger, C., & Boeke, J. D. (2000). A phylogenetically conserved NAD+-dependent protein deacetylase activity in the Sir2 protein family. *Proceedings of the National Academy of Sciences of the United States of America*, *97*(12), 6658–63.

Sperling, A. S., & Grunstein, M. (2009). Histone H3 N-terminus regulates higher order structure of yeast heterochromatin. *Proceedings of the National Academy of Sciences of the United States of America*, *106*(32), 13153–9. doi:10.1073/pnas.0906866106

Strathern, J. N., Klar, A. J., Hicks, J. B., Abraham, J. A., Ivy, J. M., Nasmyth, K., & McGill, C. (1982). Homothallic switching of yeast mating type cassettes is initiated by a double-stranded cut in the MAT locus. *Cell*, *31*(1), 183–92.

Suka, N., Luo, K., & Grunstein, M. (2002). Sir2p and Sas2p opposingly regulate acetylation of yeast histone H4 lysine16 and spreading of heterochromatin. *Nature Genetics*, *32*(3), 378–83. doi:10.1038/ng1017

Suka, N., Suka, Y., Carmen, A. A., Wu, J., & Grunstein, M. (2001). Highly specific antibodies determine histone acetylation site usage in yeast heterochromatin and euchromatin. *Molecular Cell*, *8*(2), 473–9.

Sun, Z. W., & Hampsey, M. (1999). A general requirement for the Sin3-Rpd3 histone deacetylase complex in regulating silencing in *Saccharomyces cerevisiae*. *Genetics*, *152*(3), 921–32.

Takahashi, Y.-H., Schulze, J. M., Jackson, J., Hentrich, T., Seidel, C., Jaspersen, S. L., Kobor, M. S., & Shilatifard, A. (2011). Dot1 and histone H3K79 methylation in natural telomeric and HM silencing. *Molecular Cell*, *42*(1), 118–26. doi:10.1016/j.molcel.2011.03.006

Tanner, K. G., Landry, J., Sternglanz, R., & Denu, J. M. (2000). Silent information regulator 2 family of NAD- dependent histone/protein deacetylases generates a unique product, 1-O-acetyl-ADP-ribose. *Proceedings of the National Academy of Sciences of the United States of America*, *97*(26), 14178–82. doi:10.1073/pnas.250422697

Tanny, J. C., Dowd, G. J., Huang, J., Hilz, H., & Moazed, D. (1999). An enzymatic activity in the yeast Sir2 protein that is essential for gene silencing. *Cell*, *99*(7), 735–45.

Teytelman, L., Osborne Nishimura, E. a, Özaydin, B., Eisen, M. B., & Rine, J. (2012). The enigmatic conservation of a Rap1 binding site in the *Saccharomyces cerevisiae HMR-E* silencer. *G3 (Bethesda, Md.)*, *2*(12), 1555–62. doi:10.1534/g3.112.004077

Teytelman, L., Ozaydin, B., Zill, O., Lefrançois, P., Snyder, M., Rine, J., & Eisen, M. B. (2009). Impact of chromatin structures on DNA processing for genomic analyses. *PloS One*, *4*(8), e6700. doi:10.1371/journal.pone.0006700

Teytelman, L., Thurtle, D. M., Rine, J., & van Oudenaarden, A. (2013). Highly expressed loci are vulnerable to misleading ChIP localization of multiple unrelated proteins. *Proceedings of the National Academy of Sciences of the United States of America*, *110*(46), 18602–7. doi:10.1073/pnas.1316064110

Thorvaldsdóttir, H., Robinson, J. T., & Mesirov, J. P. (2013). Integrative Genomics Viewer (IGV): high-performance genomics data visualization and exploration. *Briefings in Bioinformatics*, *14*(2), 178–92. doi:10.1093/bib/bbs017

Triolo, T., & Sternglanz, R. (1996). Role of interactions between the origin recognition complex and SIR1 in transcriptional silencing. *Nature*, *381*(6579), 251–3. doi:10.1038/381251a0

Valenzuela, L., Dhillon, N., Dubey, R. N., Gartenberg, M. R., & Kamakaka, R. T. (2008). Long-range communication between the silencers of HMR. *Molecular and Cellular Biology*, *28*(6), 1924–35. doi:10.1128/MCB.01647-07

Vannier, D., Balderes, D., & Shore, D. (1996). Evidence that the transcriptional regulators SIN3 and RPD3, and a novel gene (SDS3) with similar functions, are involved in transcriptional silencing in S. cerevisiae. *Genetics*, *144*(4), 1343–53.

Vega-Palas, M. a, Martín-Figueroa, E., & Florencio, F. J. (2000). Telomeric silencing of a natural subtelomeric gene. *Molecular & General Genetics : MGG*, *263*(2), 287–91.

Wang, F., Li, G., Altaf, M., Lu, C., Currie, M. a, Johnson, A., & Moazed, D. (2013). Heterochromatin protein Sir3 induces contacts between the amino terminus of histone H4 and nucleosomal DNA. *Proceedings of the National Academy of Sciences of the United States of America*, *110*(21), 8495–500. doi:10.1073/pnas.1300126110

Weiss, K., & Simpson, R. T. (1998). High-resolution structural analysis of chromatin at specific loci: *Saccharomyces cerevisiae* silent mating type locus *HMLalpha*. *Molecular and Cellular Biology*, *18*(9), 5392–403.

Wu, C.-S., Chen, Y.-F., & Gartenberg, M. R. (2011). Targeted sister chromatid cohesion by Sir2. *PLoS Genetics*, *7*(2), e1002000. doi:10.1371/journal.pgen.1002000

Wyrick, J. J., Holstege, F. C., Jennings, E. G., Causton, H. C., Shore, D., Grunstein, M., Lander, E. S., & Young, R. A. (1999). Chromosomal landscape of nucleosome-dependent gene expression and silencing in yeast. *Nature*, *402*(6760), 418–21. doi:10.1038/46567

Xu, E. Y., Zawadzki, K. a, & Broach, J. R. (2006). Single-cell observations reveal intermediate transcriptional silencing states. *Molecular Cell*, *23*(2), 219–29. doi:10.1016/j.molcel.2006.05.035

Xu, F., Zhang, Q., Zhang, K., Xie, W., & Grunstein, M. (2007). Sir2 deacetylates histone H3 lysine 56 to regulate telomeric heterochromatin structure in yeast. *Molecular Cell*, *27*(6), 890–900. doi:10.1016/j.molcel.2007.07.021

Yang, B., & Kirchmaier, A. L. (2006). Bypassing the catalytic activity of SIR2 for SIR protein spreading in Saccharomyces cerevisiae. *Molecular Biology of the Cell*, *17*(12), 5287–97. doi:10.1091/mbc.E06-08-0669

Yang, B., Miller, A., & Kirchmaier, A. L. (2008). HST3/HST4-dependent deacetylation of lysine 56 of histone H3 in silent chromatin. *Molecular Biology of the Cell*, *19*(11), 4993–5005. doi:10.1091/mbc.E08-05-0524

Yu, Q., Olsen, L., Zhang, X., Boeke, J. D., & Bi, X. (2011). Differential contributions of histone H3 and H4 residues to heterochromatin structure. *Genetics*, *188*(2), 291–308. doi:10.1534/genetics.111.127886

Zhang, Y., Liu, T., Meyer, C. a, Eeckhoute, J., Johnson, D. S., Bernstein, B. E., Nussbaum, C., Myers, R. M., Brown, M., Li, W., & Liu, X. S. (2008). Model-based analysis of ChIP-Seq (MACS). *Genome Biology*, *9*(9), R137. doi:10.1186/gb-2008-9-9-r137

Zhang, Z., Hayashi, M. K., Merkel, O., Stillman, B., & Xu, R.-M. (2002). Structure and function of the BAH-containing domain of Orc1p in epigenetic silencing. *The EMBO Journal*, *21*(17), 4600–11.

Zhou, J., Zhou, B. O., Lenzmeier, B. a, & Zhou, J.-Q. (2009). Histone deacetylase Rpd3 antagonizes Sir2-dependent silent chromatin propagation. *Nucleic Acids Research*, *37*(11), 3699–713. doi:10.1093/nar/gkp233

Zhu, X., & Gustafsson, C. M. (2009). Distinct differences in chromatin structure at subtelomeric X and Y' elements in budding yeast. *PloS One*, *4*(7), e6363. doi:10.1371/journal.pone.0006363

Zill, O., Scannell, D., Teytelman, L., & Rine, J. (2010). Co-evolution of transcriptional silencing proteins and the DNA elements specifying their assembly. *PLoS Biology*, *8*(11), e1000550. doi:10.1371/journal.pbio.1000550

Zou, Y., & Bi, X. (2008). Positive roles of SAS2 in DNA replication and transcriptional silencing in yeast. *Nucleic Acids Research*, *36*(16), 5189–200. doi:10.1093/nar/gkn465